ECOLOGICAL DYNAMICS OF *VIBRIO VULNIFICUS* AND *VIBRIO PARAHAEMOLYTICUS*: DISTRIBUTION, MOLECULAR TOOLS, AND HARMFUL ALGAL BLOOM INTERACTIONS

By

Trupti Vilas Potdukhe

B.S., Benedictine University, 2019

A thesis submitted to the Department of Biology
Hal Marcus College of Science and Engineering
The University of West Florida
In partial fulfillment of the requirements for the degree of Master of Science

2021

THESIS CERTIFICATION

Trupti Vilas Potdukhe defended this thesis on 18 October 2021. The members of the thesis committee were:

Lisa A. Waidner, Ph.D.	Committee Chair
Jane M. Caffrey, Ph.D.	Committee Member
Wade H. Jeffrey, Ph.D.	Committee Member

Accepted for the Department:

Peter Cavnar, Ph.D.	Chair	Department of Biology

The University of West Florida Graduate School verifies the names of the committee members and certifies that the thesis has been approved in accordance with university requirements.

Dr. Kuiyan Li, Dean, Graduate School

Acknowledgements

"Being chosen is the greatest gift you could give to another human being." – Trevor Noah

I owe my deepest gratitude to my genius advisor: Dr. Lisa Waidner, for choosing me – for taking me under her wing without a moment's hesitation, and having the absolute courage to envision (and somehow bring about) the potential of a wide-eyed, college graduate. For accepting me purely and completely, even when I could not do so myself. For putting aside her own wants, needs, and hard-earned free time to be radically present for her students. For teaching me how to teach. For showing me how to grow. For exuding bravery in vulnerability. For being my first friend at UWF. Thank you, Dr. Waidner. You will be missed like no other.

A brilliant group of faculty provided a support system and steadfast foundation as I developed my research skills. A huge thank you to my two committee members: Dr. Jane Caffrey, among the most accomplished experts in her field with as much knowledge and wisdom as she has humility, and who had the bottomless supply of patience to walk me through my own writing; and Dr. Wade Jeffrey, who helped me maintain a critical eye when examining my own work, while also showing me how to smile during the hard times. Next, I would like to thank Ms. Barbara Albrecht, a shining gem in the rough, for her strong moral compass, her dedication to her work, and for being an inspiration to all; I would also like to thank Dr. Christopher Pomory, a scientist by discipline, but a statistician at heart, who provided me with an exceptional understanding of biostatistics; Dr. Michael Murrell, who engaged in several fruitful discussions and showed me the value of scientific discourse during my first semester at UWF. A special thank you to the Mote REGS fellowship for granting me the invaluable opportunity of working at their state-of-the-art Marine Aquaculture Park, including my mentor, Dr. Andrea Tarnecki, the brilliant mind behind the *Vibrio-Karenia* project, who always treated mistakes as learning

opportunities, and to Luke Matvey, a diligent undergraduate and kind friend who helped me wash at least a thousand cuvettes and extraneous pieces of glassware over the summer of 2021.

I express my sincerest appreciation for my fellow labmates at UWF, who generously took out time from their own work to help me with mine: first, to Carrie Daniel, a warmhearted soul who kindly took me under her wing to help me assimilate, and a confidant I am beyond fortunate to have in my close circle, whose recent growth and strides in academia have inspired me to look up to her. Another big thank you to Kelsey Hope, whom I had the pleasure of getting to know this year, and was generous with her time to help me with DNA extractions from the sediment samples. Thank you to Mackenzie Rothfus, for her much-needed humor and hard work in helping us knock out sample processing. Nine Henriksson and DJ Johnson, the perfect pair of boat captains, without whose brains and brawn we would not have been able to get through long sampling days. I would also like to thank students Gina Rodriguez, Lacey Bowman, Jo O'Bar, Mark Prousalis, and now Ph.D. student Erika Headrick for their unwavering help and support.

It takes a village to raise a child, but it takes a family to keep her up. There are not enough words to express my appreciation for my loving mother and sister, Manjusha and Tanvi Potdukhe. There would be no road to be paved without the consistent encouragement I have received from both of you my entire life. Thank you for getting me through tough times – I love you guys.

Last, but certainly not least, a big thank you to Steve Celestial and Tanya Streeter for their hard work in keeping CEDB running and thriving, and for a good laugh at any given time; and to Jim Hammond for his engineering-minded solutions and the comedic relief when I needed it most.

Thank you again, and warm hugs to you all.

Table of Contents

Acknowledgements iv

Table of Contents vi

List of Tables vii

List of Figures viii

Abstract ix

Chapter I 1

Vibrio: at a Glance 2
Published patterns and predictors 3
Aims of this work 5

Chapter II 7

Materials and Methods 13
Results 17
Discussion 34

Chapter III 44

Methods 48
Results 54
Discussion 61

Chapter IV 66

Methods 68
Results 72
Discussion 77

Conclusions 80

References 82

Appendices 98

Appendix A 99
Appendix B 101
Appendix C 103
Appendix D 105

List of Tables

1. Means ± standard deviations of physical and chemical water parameters 19
2. Means ± standard deviations of parameters of bottom water and sediment 22
3. Abundances of culturable *Vv* in sediments and surface waters 24
4. Abundances of culturable *Vp* in sediments and surface waters 24
5. Numbers of *Vv* and *Vp* present in biofilms on invertebrates 27
6. Correlations between *Vibrio* abundances and environmental parameters 29
7. ANOVA for factors significant at $p < 0.05$ among the seven basins..... 31
8. ANOVA for factors significant at $p < 0.05$ between open and enclosed basins..... 32
9. Overview of salinity zone, stratification and oxygen levels in all waterbodies examined 33
10. Descriptions of *Vibrio* spp. hemolysin gene families of interest and each corresponding mechanism of pathogenesis 45
11. Number key used to refer to primer pairs used in PCR reactions..... 49
12. Gel electrophoresis results from all primers pairs used in end-point PCR reactions..... 53

List of Figures

1. Locations and dates of sampling 12

2. Boxplots of surface water salinity and temperature 21

3. Boxplots of surface water *Vibrio* abundances 23

4. Boxplots of *Vibrio* abundances in sediments 26

5. Surface water *Vv* and *Vp* with respect to salinity, delineated by basin and water column depths 28

6. Boxplots of dissolved inorganic nitrogen, phosphorus, and total Kjeldahl nitrogen 35

7. Sediment DNA quality assessed by PCR amplification of the SSU 16S rRNA gene 52

8. Gel electrophoresis of all PCR products targeting SSU 16S rDNA using primer pairs BACT1369F / PROK1492R as previously described (DeLong 1992; Suzuki et al 2000) .. 54

9. Gel electrophoresis results showing PCR products of primer pairs targeting *vvhA* in *Vv* ... 56

10. Gel electrophoresis results showing PCR products of primer pairs targeting *tdh* in *Vp* 57

11. Gel electrophoresis results showing PCR products of primer pairs targeting *trh* in *Vp* 58

12. Gel electrophoresis results showing PCR products of newly designed primer pair #4 targeting *tdh* in *Vv*, target amplicon size 179 bp 59

13. Gel electrophoresis results showing PCR products of newly designed primer pairs targeting *tdh* in *Vv* subjected to PCR at 57˚C (left) and 60˚C (right) annealing temperatures 59

14. Gel electrophoresis results showing PCR products of previously published (Bauer and Rørvik 2007) primer pair targeting *ToxR* in *Vp* with a target amplicon size of 297 bp 60

15. The 48-well microassay design as previously described (Bramucci et al 2015) 70

16. Set-up of 48-well co-culture assay apparatus 71

17. Concentration (OD_{600}) of *Vp* over 12 hours 72

18. Growth of *Kb* (circle, control; diamond, co-culture) and *Vv* (circle and solid line, control; square, co-culture) from trial 1 (top panel) and trial 2 (bottom panel) 75

19. Growth of *Kb* (circle, control; diamond, co-culture) and *Vp* (circle and solid line, control; square, co-culture) from trial 1 (top panel) and trial 2 (bottom panel) 76

20. Cell sizes of various microorganisms and their corresponding average abundances in typical aquatic ecosystems [adapted from (Kirchman 2018)] 79

Abstract

With the rising threat of anthropogenic climate change, human pathogens *Vibrio vulnificus* (*Vv*) and *parahaemolyticus* (*Vp*) may become more problematic to world health. The aims of this study were to i) report baseline *Vv* and *Vp* abundances, ii) develop new oligonucleotide primer sets for detection of *Vv* and *Vp* pathogens, and iii) explore interactions with other waterborne nuisances. We sampled surface waters, sediments, and invertebrate biofilms from 43 locations in two estuarine systems over seven dates in winter 2020. Culturable *Vv* was present in most water and sediment samples, but *Vp* only in about half of the surface waters. Surface *Vv* covaried with bottom water pH and tidal coefficient. *Vp* surface concentrations correlated negatively with surface salinity, and positively with total surface nitrogen. Both species correlated with wind, suggesting resuspension was important. These regionally-novel winter baseline *Vibrio* abundances will aid in predicting risk factors in each waterbody of interest. In-house databases were constructed to design better primer pairs for virulence genes. End-point PCR was used to verify new *trh* and *tdh* primers for more accurate detection of *Vv* and *Vp* type strains. A novel *Vv tdh* gene pair showed promise, whereas the *vvhA* pair was no better than published primers. These *in silico* and preliminary end-point PCR data will inform future efforts in quantifying *Vibrio* with quantitative PCR. Finally, an exploratory study showed that *Karenia brevis* (*Kb*), a toxic dinoflagellate rampant in southwest Florida waterways, inhibited *Vv* growth by 150-fold, and *Kb* had little to no effect on *Vp* growth.

Chapter I

HUMAN PATHOGENIC VIBRIO VULNIFICUS AND PARAHAEMOLYTICUS AS RISKS TO ECOSYSTEM FUNCTION AND HUMAN HEALTH

Bacteria are the most diverse and abundant organisms on the planet (Oren 2004). It is often the composition of bacterial communities that drives the functioning of the ecosystem they inhabit – whether that be scavenging the floors of the deepest oceans, or outnumbering their own host in the human gut microbiome. In fact, total bacterial numbers in a "typical" sample of seawater are, on average, 1 million cells mL^{-1}, but this average widely varies, along with the variation in the average bacterial cell size (Kirchman 2018). The ability of many types of heterotrophic bacteria to quickly adapt and respond to changes in their environment is prehistoric, and since unprecedented. For example, the vast range of microbial metabolisms is an excellent example of this advantage, those which, depending on the environment, can vary. Many known human pathogens are strict heterotrophs, such as pathogenic species and strains in the *Vibrio* genus.

Some bacteria in the *Vibrio* genus cause over 80,000 illnesses and 100 deaths in the United States every year (CDC 2019). Even more, cases of vibriosis are predicted to rise in the coming decade, especially in concordance with anthropogenic climate change (Esteves et al 2015; Froelich et al 2019; Malham et al 2014;). The two major species of rising problematic *Vibrio* pathogens, *vulnificus* and *parahaemolyticus*, were responsible for 83 confirmed cases since 2019 in the state of Florida, 16 of which were fatalities (Florida Department of Health 2021). Citizens of northwest Florida living near and/or frequenting neighboring bodies of water that may contain high concentrations (>100 cells mL^{-1}) of pathogenic *Vibrio* may be at greater risk of contracting vibriosis (Johnson et al 2010).

Vibrio: at a Glance

Vibrio are Gram-negative, flagellar bacteria that typically live in marine to estuarine waters (Coia and Cubie 1995). As facultative anaerobes, their metabolic demands can be met even in suboxic waters (Drake et al 2007). *Vibrio vulnificus* (*Vv*) can enter open cuts or wounds *via* exposure to contaminated seawater and may cause necrotizing fasciitis (infamously known as "flesh-eating disease"). Systemic cases often necessitate surgery or peripheral amputations, and in rare cases, result in death (Baker-Austin and Oliver 2020). *Vv* can also cause gastrointestinal disease through ingestion of raw or undercooked shellfish and is the leading cause of reported gastroenteritis and septicemia cases due to foodborne illness (Panicker et al 2004).

V. parahaemolyticus (*Vp*) is transmitted through the consumption of raw or undercooked shellfish, especially oysters. The classic nomenclature for *Vp* strains comes from the properties of its somatic (O) and capsular (K) antigens. Both antigenic properties depend on the environment from which that particular strain originated. In 1996, the first pandemic strain of *Vp* emerged in Calcutta, India, classified as the O3:K6 serovar. A decade later, the same strain broke out in Chile, causing one of the worst diarrheal outbreaks in the world. Since then, the O3:K6 serovar has diverged into several "serovariants" that have made their way to other Asian, American, African, and European countries (Nair et al 2007). An increase in the number of variants is because of increased diversity (i.e., increased genetic differences) among strains. Genetic variation among important functional genes, such as those that confer pathogenicity to humans, is particularly important to recognize in design of molecular tools for detection of *Vibrio* in environmental samples. Fortunately, the global occurrence of large outbreaks has since decreased, but the rate of reported *Vp* cases is rising in the United States (Newton et al 2012; Park et al 2018; Pazhani et al 2014;).

There are currently three confirmed biotypes of potentially harmful *Vv*. Biotype 1 is accountable for most shellfish and wound infections; this is vibriosis in the most traditional sense. Biotype 2 appears in farm-raised eels, but rarely affects humans. A third biotype emerged after a *Vv* wound outbreak in 1996 that originated in an Israeli fish market. Biotype 1, unlike the latter two, can be further separated into two genotypes: clinical and environmental, in which the pathogenicity of the latter is often unknown. Those isolated from diseased humans are considered "clinical" or pathogenic; and their gene sequences in the NCBI database are delineated by "source," (i.e. wound, blood, etc.) Both *Vv* and *Vp* possess specialized genes that contribute to pathogen virulence by promoting phenotypes such as increased epithelial (intestinal) cell adhesion or erythrocyte (red blood cell) lysis (i.e., hemolysis). The strains containing these genes can be quantified using microbiological and/or molecular techniques, providing insights into the dynamics of pathogenic *Vibrio* spp. in aquatic habitats, with regards to climate events, community composition, diversity, and other environmental parameters.

Published patterns and predictors

Several water quality parameters may have strong influence on pathogenic *Vibrio* dynamics, partly due to their known optimal ranges. Temperature and salinity are often reported drivers of *Vibrio* populations, regardless of geographical location of the waterbody. For example, water temperature positively correlated with virulent strains of *Vv* and *Vp* in water, sediment, and oyster shells in a coastal ecosystem near Baton Rouge, LA, USA (Johnson 2015). Increases in water temperature could also induce pathogen growth and decrease water quality. It should be noted, however, that total bacteria abundances are often predicted to increase with temperature, but most aquatic bacteria are non-pathogenic (Kirchman 2018). Many studies of environmental samples, however, point to temperature and salinity as primary considerations in *Vibrio* ecology.

For example, offshore of Galveston, TX in subtropical surface waters in the northern Gulf of Mexico (GoM) contained the highest abundances of culturable *Vv* of waters with salinities 7-16% when water temperatures were between 30˚C and 37˚C (Kelly 1982). However, factors other than temperature and salinity may be responsible for *Vibrio* dynamics. Although droughts in certain cases can promote distribution and abundance of pathogenic bacteria, some droughts relatively do not seem to have much of an effect. For example, abundance of *Vv* in North Carolina estuaries was in fact reduced during a drought season compared to an above-average freshwater inflow event (Wetz and Yoskowitz 2013). Similarly, in a subtropical estuary in Charlotte Harbor of southwest Florida, there were no significant relationships between the presence of *Vv* and pH, salinity, turbidity, dissolved nutrients, or estuarine bacteria, an outlier from other studies (Lipp et al 2001b). Likewise, a decadal study in the Neuse River Estuary found that an increase in *Vibrio* concentrations did not correlate with shifts in the three most commonly reported factors that may predict estuarine *Vibrio* abundance: salinity, temperature, and dissolved oxygen (Froelich and Noble 2014).

Vibrio abundances are hypothesized to be driven by salinity, with an optimal range of about 15 to 25 PSU (Letchumanan et al 2014). However, in South Carolina, USA, *Vibrio* species were found in salinities as low as 5 PSU in standing water caused by hurricane-induced flooding (Frank et al 2021). Another study found high abundances of *Vv* and *Vp* in different areas of a tropical monsoonal estuary located on the southwest coast of India, a system that bears an abundant amount of freshwater influence (Krishna et al 2021). However, the primary finding of this study was that regression tree analysis was a better predictive model for *Vibrio* dynamics than a simple multiple-regression model. This suggests that complex, nonlinear interactions may drive *Vibrio* species within particular regions and even within a region, in distinct waterbodies.

In general, freshening events occur with environmental perturbances due to global climate change – increasing sea surface temperatures lead to the melting of polar ice caps, and freshwater enters the oceans, altering the salinity stratification, temperature, and sea levels, and ultimately ecosystem functioning, worldwide. Pathogenic *Vibrio* well-adapted to harsher conditions (e.g., viable outside optimal ranges, able to withstand natural disasters, etc.) are more likely to proliferate at a faster rate despite this adversity and can quickly begin to dominate the bacterial assemblage. High *Vibrio* abundances have also been found within the sediments, especially in warmer water temperatures (Blackwell and Oliver 2008; Johnson et al 2012; Johnson 2015). Significant storm and/or hurricane events promote water column mixing with benthic sediments and associated biota, thereby significantly increasing abundance of *Vibrio* within the water column (Fries et al 2008; Hughes et al 2013). *Vibrio* diversity could also be spatially influenced. In the Dongshon Bay, *Vibrio* diversity with increased distance from fish-farming sites (Xu et al 2020). This could likely be attributed to the increased levels of human-loaded eutrophication near the aquaculture areas. These findings suggest *Vibrio* diversity and distribution is driven not by a single factor; rather, a collection of parameters associated with seasonality as a whole drives diversity in coastal ecosystems (Kirchman et al 2005). Conducting more multiyear and/or longitudinal studies could help move toward a more holistic understanding of basin-wise *Vibrio* dynamics.

Aims of this work

In this body of work, I examined the distribution of *Vv* and *Vp* in seven basins surrounding the Pensacola, FL area (**Chapter II**); this work is now published (Potdukhe et al 2021). In Chapter III, I describe existing molecular methods for enumerating *Vv* and *Vp* in environmental samples, as well as the description of development and preliminary testing of new

pairs of primers to be used in quantitative PCR (qPCR). In Chapter IV, I describe potential interactions between *Vv* and *Vp* with a toxic dinoflagellate, one that is particularly problematic in Florida. I performed controlled experiments at Mote Marine Laboratory in Sarasota, combining known loads of pathogenic *Vv* and *Vp* with naturally-relevant concentrations of the harmful algal bloom species, *Karenia brevis*.

Chapter II

VIBRIO ABUNDANCE IN SURFACE WATERS, SEDIMENTS, AND INVERTEBRATE BIOFILMS WITHIN THE PENSACOLA AND PERDIDO BAYS IN RELATION TO ENVIRONMENTAL AND PHYSICO-CHEMICAL PARAMETERS

Warm and salty or brackish waters in Florida and other nearby coastal states are currently subject to increased temperatures and frequency of storm events, changing heterotrophic bacterial communities (Lønborg et al 2019). The success of specific groups of bacteria in subtropical estuaries and coasts are affected by many factors including eutrophication, sea-level rise, warming temperatures, and changes in trophic states (Krishna et al 2021; Li et al 2020; Montánchez et al 2019). One major concern associated with these factors is increased *Vibrio* abundances: in the water column, in and on invertebrates, and in the sediments (Hughes et al 2013). *Vibrio vulnificus* (*Vv*) and *V. parahaemolyticus* (*Vp*) are two species that are potentially harmful to humans and the marine life on which local economies depend. Although *Vp* infections are more common in recent years (Lovell 2017), serious *Vv* infections are concurrently increasing in frequency (Baker-Austin and Oliver 2018). These increased pathogenic loads can be attributed to a variety of factors.

Temperature is considered to be a driving factor of *Vibrio* abundances (Johnson 2013; Wetz et al 2014) and may even affect the relative severity of vibriosis (Hernández-Cabanyero et al 2020). However, temperature was not a major factor in this study. In fact, our findings suggest other factors may also be responsible for higher abundances of culturable *Vibrio*. Water column *Vibrio* abundances may increase after storm events, possibly from sediment bacteria resuspension (Fries et al 2008). Increased nutrient loads, often associated with anthropogenic- and climatic-influenced eutrophication, will likely promote higher concentrations of human pathogens such as *Vibrio* species (Malham et al 2014). Higher turbidity has been previously related to *Vp* in subtropical estuaries near coastal northern Gulf of Mexico (GoM). Because

Vibrio may be associated with diatoms and zooplankton, their abundances are likely positively related to increased turbidity, typically measured as concentrations of total suspended solids (TSS). Similarly, a positive relationship is often observed between *Vibrio* abundance and phytoplankton biomass, typically measured by chlorophyll *a* (chl *a*) (Martinez-Urtaza et al 2012). Therefore, the combination of terrestrial inputs of nutrients from rain and storm events, sediment resuspension from high wind speeds, and the quite evident rise in global water temperatures may provide optimal environmental conditions for the success of human pathogens such as *Vv* and *Vp* (Davis et al 2004; Deeb et al 2018; Froelich et al 2019).

Invertebrate filter-feeders (such as oysters or barnacles) are also susceptible to minor changes in water and sediment quality, making them common carriers of pathogenic *Vp* (Aagesen et al 2013). Oysters in the Pensacola Bay System (PBS), including in polluted waterbodies within, such as Bayou Chico, are common (Oliver 2003). Barnacles were abundant invertebrates settling on artificial reefs in the nearby GoM shelf in a recent study (Babcock et al 2020). Often, biofilms on invertebrate shells are considered anoxic, a key consideration in our evaluation of *Vibrio* on invertebrates. *Vv* and *Vp* are aerobes, with some strains functioning as facultative anaerobes (Drake et al 2007). Biofilms on oyster or barnacle shells are often oxic (Ray et al 2019), which could promote success of *Vv*, *Vp*, and other aerobes in shell biofilms. In fact, desiccation or regular air exposure of oysters from nearby northern GoM bays promotes *Vibrio* growth (Grodeska et al 2019; Pruente et al 2020).

In water and sediments or on invertebrates of Florida subtropical estuaries, there is currently little data with respect to *Vv* or *Vp* abundances, except in Apalachicola Bay, FL (Lipp et al 2001a; Williams and LaRock 1985), formerly home to one of the largest oyster fisheries in the United States. It is estimated that warming water temperatures due to climate change may

have a more significant effect in temperate waters (Froelich and Daines 2020). However, abundances in subtropical estuaries are important to assess, not only considering the potentially pathogenic nature of *Vv* and *Vp*, but also because of increasing water and sediment temperatures anticipated with climate change (Thomas 2016). Furthermore, estuaries may be fragile ecosystems, especially so in the current threat of climate change in subtropical regimes. Extreme climate events (droughts, floods, tropical cyclones, heat waves, etc.) have increased in frequency and intensity, coinciding with climate model predictions due to anthropogenic causes. Consequences of warming waters combined with increased intensity or frequency of such extreme events impact a wide range of trophic levels. Terrestrial-derived nutrient influxes into fresh and estuarine systems promote a chain of succession in both primary and secondary producers, leading to changes in the types of heterotrophs. Warming waters expected with global climate change combined with increased terrestrial organic matter inputs exacerbates these changes, in both temperate (Paczkowska et al 2019) and subtropical (Williams and Quigg 2019) regions. Clearly, there is cause for investigating the effects of these changes locally in relation to potentially pathogenic *Vibrio* loads.

To determine baseline presumptive *Vv* and *Vp* loads in winter, we surveyed seven major basins in the Pensacola, FL area (Fig. 1). Locations for this survey were chosen within the PBS and the Perdido Bay, located in northwest Florida. The PBS is an excellent model system to examine the responses of subtropical microbial responses to anthropogenically-driven changes in temperature, freshwater flow, and other parameters (Murrell et al 2018). The PBS is the fourth largest estuary in Florida and is unique in that it is microtidal, nutrient inputs are relatively low (Caffrey and Murrell 2016), and heterotrophs are substrate-limited (Murrell 2003). Flow from the Escambia River provides approximately 70% of the freshwater to Escambia Bay, which is

part of the PBS (Caffrey and Murrell 2016). While light availability, nutrient fluxes, primary productivity, and chl *a* are influenced by riverine nutrient inputs (Caffrey and Murrell 2016), the impact of freshwater flow on the distribution of *Vibrio* in the estuary and adjacent basins is unknown. Chl *a* concentrations range from 1 to 26 µg/mL and are highest in mesohaline portions of the Bay (Caffrey and Murrell 2016; Murrell and Lores 2004; Murrell et al 2007). Bacterial abundances and production are also influenced by freshwater inputs from the Escambia River (Murrell 2003). Cyanobacterial abundances in these systems are low at the marine ends and undetectable in freshwaters but dominate in mesohaline zones (Murrell and Caffrey 2005).

In the PBS, chl *a* and phytoplankton productivity peak about a month following seasonal maximum freshwater flow from the Escambia River (Murrell et al 2007). Summer benthic hypoxia occurs during periods of stratification (Hagy and Murrell 2007) but is moderated by light that supports sub-pycnocline phytoplankton and benthic primary production (Murrell et al 2009). However, regional strong storm events do result in high particle loads (>6,000 particles/mL), particularly in the summer. In winter (February 2014 and 2015), total particle abundances ranged from 500 to >3500 particles/mL, as determined by FlowCam analysis (Sieracki et al 1998) of Lugols-preserved whole water samples from the Escambia Bay (Michael Murrell, per. com). Interestingly, the detrital contribution to total particulate matter composition is low (Murrell 2003), suggesting the majority of particulate matter in the estuary is comprised of zoo- and phytoplankton. Phytoplankton are diverse, with picocyanobacteria (<5 µm) dominating during the summer, representing 70 to 100% of total chl *a* (Murrell and Lores 2004), a pattern found in other GoM estuaries (Murrell and Caffrey 2005).

Perdido Bay is another shallow estuarine system whose watershed includes southeast Alabama. Waters here are generally more turbid than in the PBS, and major sources of

freshwater input include the Perdido River and Elevenmile Creek (Macauley et al 1995). While Escambia Bay/Pensacola Bay and Perdido Bay are major river-dominated systems with freshwater inflow, Big Lagoon is a mesohaline system connecting the PBS and Perdido Bay, where sediments are more sandy than muddy, light attenuation is generally low, and seagrasses are more abundant than in the Escambia or Perdido Bays (Hester et al 2016; Murrell et al 2018). Creeks provide freshwater inputs into the three urban bayous in this study: Grande, Texar, and Chico. They are the largest bayous in the PBS that are impacted by stormwater runoff (Lewis et al 2016). Other inputs of freshwater to the bayous include adjacent creeks, but runoff contributes greatly to eutrophication and sedimentation, as well as contamination with heavy metals and pesticides (Lewis et al 2002; Nature Conservancy 2014). Septic tank systems within the Bayou Chico and Grande watersheds contribute to eutrophication, and Bayou Chico fails to meet total maximum daily load goals of US and FL standards (Nature Conservancy 2014).

We hypothesized that abundances of *Vibrio* species in the Perdido and Pensacola Bay Systems would be higher in water column samples with high turbidity. We also expected *Vibrio* species to thrive where dissolved or total nutrient concentrations were high, especially when salinity and temperature fell within optimal ranges as described by previously-published studies (Hsieh et al 2007; Kaspar and Tamplin 1993; Motes et al 1998). Temperature was not considered a major factor in this short-term study, as all sampling was done within one winter month (February 2020).

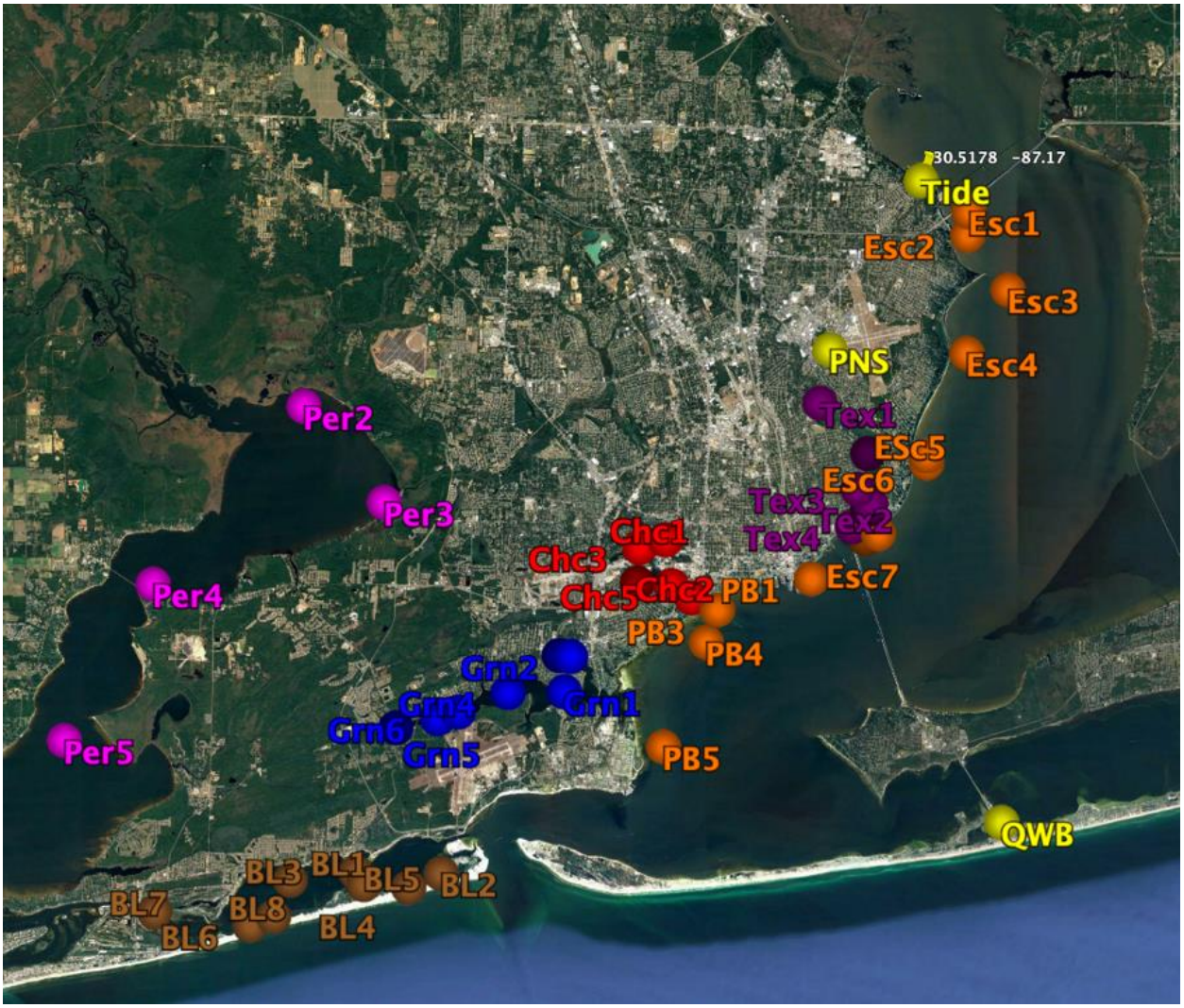

Fig. 1 Locations and dates of sampling. Colors of pins indicate dates on which samples and in situ measurements were obtained. Orange, Pensacola/Escambia Bay (stations V1 to V12), 02/03/20; Dark purple, Bayou Texar (V13-V18), 02/07/20; Red, Bayou Chico (V19-23), 02/12/20; Blue, Bayou Grande (V24-V30), 02/21/20; Brown, Big Lagoon (V31-38), 02/28/20; Light purple, Perdido Bay (V39-43), 03/02/20; Yellow, QWB, QuietWater Beach in Santa Rosa Sound, 02/10/20; Yellow, PNS, Pensacola Regional Airport weather station (precipitation and wind data); Yellow, Tide, Lora Point tidal gauge (tidal data)

Materials and Methods

Field sampling

Forty-three stations were chosen, representing a wide range of salinities, stratification, eutrophication, and freshwater influence. We surveyed surface waters and sediments on seven dates between 02/03/20 and 03/02/20 (Fig. 1). All sampling and *in situ* measurements were performed from small vessels. Hydrographic data (surface water and bottom water) were measured with a YSI multimeter (Xylem, Yellow Springs, OH). Parameters measured *in situ* at all stations included surface and bottom water column readings of salinity (PSU), temperature (°C), and dissolved oxygen (mg/L). Surface and bottom water pH were determined with a ProDSS pH sensor, which became available on 02/21/20; thus, surface and bottom pH was reported only for Bayou Grande (02/21/20), Big Lagoon (02/28/20), and Perdido Bay (03/02/20). Statistical analyses for pH data reflect the correct sample size (n = 20). Light attenuation coefficient (K_d, m^{-1}) was calculated from the slope of attenuation of photosynthetic photon flux fluence rate (PPFFR) at 0.5-meter intervals measured with a LiCor 4II spherical underwater quantum sensor. Total water column depth was measured with the line on a Secchi disk and with the vessel's on-board instrumentation. Total precipitation and cumulative maximum wind speeds were recorded in the three days leading up to sampling, including the mornings of sampling events in which windy conditions delayed the start of sampling. Precipitation and wind speed data were obtained from the NOAA station ID: GHCND:USW00013899, 30.47 °N, 87.2 °W located at Pensacola Regional Airport (WUnderground 2020). Tidal coefficient (m) at Lora Point (Escambia Bay, 30.5178° N, 87.1700° W), also within our sampling area and in one of the seven basins, was also recorded (TidalCoefficient 2020). Precipitation, wind speed, and tidal coefficient were considered reflective of the entire basin. Thus, the sample size was n = 7.

Forty-three surface water samples were collected *via* bucket cast and held in an acid-washed 1-L Nalgene bottle (one for each site) in coolers maintained at *in situ* temperature. Sediment samples were collected using a PONAR grab sampler. Forty-two sediment samples (0.5 to 2.0 mL of superficial sediment) were collected from the top 0 to 30 cm with sterile, single-use plastic spatulas and resuspended in 0.5 mL of phosphate-buffered saline (1X solution contains 0.137M NaCl, 0.0027M KCl, 0.0119M phosphates, pH 7.4) (Fisher BioReagents, Pittsburgh, PA), and held in sterile 50-mL centrifuge tubes in coolers maintained at *in situ* temperature. An additional 50 mL of sediment was collected for analysis of sediment water content, organic matter content (loss on ignition), sediment chl *a* and phaeopigment concentrations. Surface water was filtered on-site through Whatman GF/F filters to collect filtrates which were collected in acid-washed bottles and immediately preserved in coolers on ice and later stored at the laboratory at -20°C for subsequent dissolved nutrient analyses. Filters were also immediately cooled on site and preserved at -20°C for subsequent chl *a* analyses. Whole water was preserved with H_2SO_4 as per EPA method 351.2 and held at 4ºC for total Kjeldahl nitrogen (TKN) analyses. Where invertebrates were present (on marker poles or in sediment grabs), we collected invertebrate surface (presumptive biofilm) samples *via* surface-swab, henceforth referred to as biofilm or biofilm swab samples. A total of 13 samples of these biofilms, approximately 1 cm^2 surface area each, were collected with sterile cotton swabs, resuspended in 0.1 mL of sterile phosphate-buffered saline in centrifuge tubes and held at *in situ* temperature until processed.

All surface water samples were analyzed using the following methods: dissolved inorganic phosphate (DIP) as in (Parsons et al 1984), NH_4^+ as in (Holmes et al 1999), and NO_3^- + NO_2^- as in (Schnetger and Lehners 2014). Dissolved inorganic nitrogen (DIN) is the sum of

NH_4^+, NO_3^-, and NO_2^-. Whole water was preserved with acid and analyzed for TKN with EPA method 351.2 on a Lachat Quikchem FIA Model autoanalyzer. Samples for chl *a* were extracted in 90% acetone for 24 hours and analyzed as in (Welschmeyer 1994). Sediment samples were evaluated for biomass of benthic microalgae using the acidified chl method to determine concentrations (µg/g) of sediment chl *a* and phaeopigment as in (Parsons et al 1984). Sediment aliquots were also processed for water content and organic carbon (ash content) percentages. Ash-free dry weight combustion was at 500°C. Surface water concentrations of TSS were determined using EPA method 160.2.

Putative Viable Vibrio abundances

To determine abundances of presumptive viable *Vv* and *Vp,* all samples (surface water, sediment suspension, and biofilm surface-swab suspension) were plated on CHROMagar™-*Vibrio* (DRG International, Inc., Springfield, NJ), an agar medium with chromogenic substrates (15.0 g/L agar, 8.0 g/L peptone and yeast extract, 51.4 g/L salts, 0.3 g/L chromogenic mix, pH 9.0). In winter (January) and summer (June) of 2019, we had performed preliminary end-point PCR testing to narrow color ranges of presumptive *Vv* (bright blue, with early color development before 24 hours) and *Vp* (bright mauve, also with early color development). To assess accuracy of presumptive *Vv* colored colonies on CHROMagar™, *vvhA* was assayed using primer pair F-vvh785/R-vvh990 as previously described (Panicker et al 2004). Presumptive *Vp*, appearing as bright pink, not purple, were confirmed as *Vp* with either *tdh*- or *trh*-positive end-point PCR, employing primer pairs tdh-F/R and trh-F/R as previously described (Nordstrom et al 2007). All samples of colony biomass were also tested by end-point PCR for prokaryotic 16S rRNA (BACT1369+PROK1541R), to verify there were no false-negatives. None of the 2019 preliminary data (abundances based on colony counts or end-point PCR results) are presented

here, since data collection in 2019 did not include environmental data. In the preliminary work, depending on the body of water sampled, the percent bright blue colonies scoring *vvhA*-positive ranged from ~50% to 85%, with an average of 75% among all summer and winter 2019 samples for *Vv* bright blue colony-*vvh*+ and *Vp*-bright pink colony-*tdh*/*tlh*+. The same person (L. Waidner) who observed *vvhA*-positive and *trh*- or *tdh*-positive colonies was also the one who counted colonies in the winter 2020 data presented in this study.

In this study, to assess presumptive *Vv* and *Vp* abundances, water samples were plated undiluted on CHROMagar™-*Vibrio;* fresh sediment samples were diluted 2-, 3-, and 4-log-fold with phosphate-buffered saline before plating, and presumptive biofilm surface-swab samples were similarly diluted 1- and 2-log-fold. After dilutions and plating, exact volumes of each sediment sample were determined. Each abundance calculation accounted for the variability in volume of sediments collected in the field. Presumptive biofilm, sediment, and undiluted surface water samples were vigorously shaken (water) or mixed *via* vortex (sediment and biofilm) prior to plating. Three aliquots (0.15 mL each) of each dilution of each sample, in triplicate, were plated on Petri plates as previously described (Huq et al 2012; Oliver 2003; Thomas et al 2014; Yeung and Thorsen 2016). Plating was followed by incubation in the dark at room temperature (24°C, chosen since this was most like *in situ* temperature) for 24, 48, and 72 hours. At each 24-hour interval, the number of each of the colored colony types was recorded and reported as CFU of presumptive *Vv* or *Vp*. The abundances of each type of *Vibrio* were calculated in the same manner for all sample types and included all abundances of dilutions that could be accurately assessed (between 3 and 300 CFU/plate). Abundances lower than the limit of detection (15 CFU/mL) were recorded as zero. For presumptive abundance determination across all samples, abundances at t = 48 were used, and average cell abundances were normalized to milliliters

(mL), since abundances per cm^3 are equivalent to abundances per volume (mL). We did not use molecular methods to confirm *Vv* and *Vp* (i.e., bright blue and bright pink colonies, respectively) in this study.

Statistical analyses

Mathematical relationships and each corresponding significance were performed using the "Analyze" function of the Statistical Package for the Social Sciences (SPSS). All surface water and sedimentary *Vibrio* abundances were log-transformed to accommodate normality for Pearson (parametric) correlation analysis. SPSS was used to generate one-way analysis of variance (ANOVA) tests to determine differences between log-transformed *Vibrio* abundances and environmental parameters among all seven basins. Parameters that showed relatively strong evidence ($r \geq 0.30$) for a difference among basins were followed with multiple comparison procedures (Tukey's *Post Hoc*) to determine wherein the seven basins lies the difference. In addition to basin-by-basin comparisons, one-way ANOVAs were also generated to determine differences between open and enclosed basins. Pearson correlation coefficients were calculated in the statistical package Plymouth Routines in Multivariate Ecological Research (PRIMER) version 7. Box- and surface-plots showing the distribution of measured abundances and ecological parameters across all basins were also generated using PRIMER.

Results

Overview of bodies of water sampled

In all stations of all basins surveyed, the minimum depth was approximately 0.4 meters, with a maximum depth at any station of 6.1 meters. The average surface water temperature of all stations was 15.4°C, and temperatures ranged from 12.3 to 22.2°C (Table 1). Surface water salinities ranged from 0.9 to 18.2 PSU. Among all seven basins, Bayou Chico had the greatest

average water chl *a* (8.6 ± 5.4 µg/L), TKN (53.5 ± 16.7 µM), and DIN (39.0 ± 38.7 µM) concentrations. Of all basins examined, the surface waters' temperature and salinity in Bayou Chico were overall the highest and lowest, respectively (Fig. 2). Additionally, salinity stratification was high at two of the 5 locations sampled within Bayou Chico: V-20 and V-23, with surface-bottom values of 9.4 and 21, respectively. Perdido Bay had the lowest average water chl *a* concentration (1.9 ± 1.0 µg/L), and Big Lagoon had the lowest average TKN (24.2 ± 3.0 µM) and DIN (1.7 ± 0.5 µM) concentrations. DIP concentrations were negligible or undetectable in surface water samples (Table 1; Fig. 2). Bottom water temperatures and salinities ranged from 13.0 to 22.0°C and 1.9 to 28 PSU, respectively (Table 2). Bayou Texar had the greatest average sediment chl *a* concentration (3.7 ± 2.4 µg/g). Escambia Bay had the greatest average concentration of sediment phaeopigment (4.7 ± 1.5 µg/g) and average sediment water content (58.0 ± 22.7%). Perdido Bay had the greatest average sediment organic content (8.3 ± 6.0%), with Pensacola Bay as the lower bound (1.8 ± 2.8%).

In seven of the 43 surface water samples, *Vv* was below detection limits of the chromogenic agar assay. In the remaining 36 locations, *Vv* concentrations ranged from 15 to 3,556 CFU/mL, with a median concentration of 44 CFU/mL. In contrast, *Vp* abundance was below the limit of detection at 28 of the 43 stations (Table 3). In the 15 surface water samples where it was detected, *Vp* concentrations ranged from 15 to 8,919 CFU/mL, with a median concentration of 104 CFU/mL. Bayou Texar greatly outnumbered the other basins with regards *Vp* abundances, with Pensacola Bay and Perdido Bay having the lowest surface water *Vp* abundances (Fig. 3). Conversely, Bayou Chico had the greatest abundance of surface water *Vv* of the seven basins, as well as the largest range in *Vv* surface water abundance at the sites within the basin (Table 3).

Table 1 Means ± standard deviations of physical and chemical water parameters

Site [f]	Depth ranges (m)	Surface water						
		K_d [a] (m^{-1})	Temperature (°C)	Salinity (PSU)	Chl *a* (µg/L) [b]	TKN (µM) [c]	DIN (µM) [d]	DIP (µM) [d]
PB	0.9 - 3.5	0.9 ± 0.1	12.9 ± 0.4	14.7 ± 1.6	2.8 ± 1.1	27.1 ± 1.4	3.0 ± 2.4	0.0 ± 0.0
EB	1.5 - 3.4	1.1 ± 0.2	13.9 ± 0.3	9.6 ± 4.0	4.1 ± 0.9	32.7 ± 3.7	2.8 ± 3.1	0.0 ± 0.0
BT	1 - 2.7	1.3 ± 0.4	15.1 ± 0.6	8.5 ± 1.0	2.9 ± 1.1	40.6 ± 3.7	20.7 ± 4.8	0.1 ± 0.1
BC	0.4 - 4.3	1.8 ± 0.8	20.7 ± 0.9	4.1 ± 2.1	8.6 ± 5.4	53.5 ± 16.7	39.0 ± 38.7	0.0 ± 0.0
BG	0.9 - 2.9	1.2 ± 0.3	16.5 ± 0.7	8.8 ± 3.3	3.4 ± 1.5	38.1 ± 6.5	5.7 ± 1.5	0.1 ± 0.1
BL	1.1 - 6.1	0.7 ± 0.1	13.8 ± 0.5	16.7 ± 1.2	2.3 ± 0.8	24.2 ± 3.0	1.7 ± 0.5	0.1 ± 0.1
PD	1.1 - 3	1.0 ± 0.3	16.1 ± 0.4	9.8 ± 3.0	1.9 ± 1.0	41.1 ± 5.6	4.7 ± 2.2	0.1 ± 0.1

[a] K_d, light attenuation coefficient
[b] chl *a*, chlorophyll *a*
[c] TKN, total Kjeldahl nitrogen
[d] Total dissolved inorganic nitrogen DIN
[e] DIP, dissolved inorganic phosphate
[f] Site abbreviations: PB, Pensacola Bay; EB Escambia Bay; BT, Bayou Texar; BC, Bayou Chico; BG, Bayou Grande; BL, Big Lagoon; PD, Perdido Bay

Putative Overview of Vibrio in sediment samples

Basin-wide analyses indicated there was no body of water with low concentrations of *Vibrio* in sediments. At the 43 locations sampled, 42 sediment samples were obtained. Sediment types ranged from sand to sand-mud mix to mud. When *Vv* was detected, concentrations ranged from 169 to 607,222 CFU/mL, with a median concentration of 18,160 CFU/mL. In three of the seven major basins, there were exceptionally high *Vv* concentrations in at least one location each. In Bayous Chico and Texar, *Vv* was found in some locations at concentrations >300,000 CFU/mL, and in one location of Big Lagoon at >600,000 CFU/mL (Table 4). In contrast, *Vp* was generally less in the sediments and was below detection limits in nine of the sediment samples.

In the remaining 33 stations, *Vp* ranged from 28 to 77,333 CFU/mL, with a median concentration of 652 CFU/mL. The highest densities of *Vp* were observed in the sediments of Bayou Chico (77,333 CFU/mL) and in Big Lagoon (19,185 CFU/mL). In four of the five Perdido Bay sites, *Vp* was undetectable. In Bayou Grande, *Vp* was undetectable in two of the seven locations. In the Pensacola Bay basin (Pensacola Bay and Escambia Bay), we collected 11 sediment samples. Of those, three contained undetectable levels of *Vp*, one site had 1,649 CFU/mL, and the remaining eight sites contained fewer than 655 CFU/mL in the sediments (Table 4).

The variation in sediment *Vibrio* abundance, both among and within the seven basins, was high. The upper bound of *Vv* was similar across all basins, with Pensacola and Perdido Bay having the largest range (Fig. 4; Fig. 5). *Vp*, however, was more abundant in Bayou Chico, with Bayou Texar and Big Lagoon following closely behind. Sites within Pensacola Bay and Bayou Grande generally had the lowest sediment *Vp*. Given that the average concentration of total active aerobic bacterial cells are present in a mL of estuarine, riverine, or coastal marine sediments is 1 to 500 x 10^6 (Proctor and Souza 2001; Luna et al 2002; Glavin et al 2004; Kirchman 2018), the data suggest *Vv* make up from 0.2% to 60% of total sediment bacteria; whereas *Vp* could comprise 0.003% to 0.2% of all bacteria in sediments. On average, *Vv* outnumbered *Vp* by approximately 18-fold in all sediments. Very high abundances of sediment *Vv* and *Vp* in were found in stations V24 and V25, two sites in Bayou Grande. In these locations, bottom pH and stratification were closely tied and showed the greatest variation among all sites.

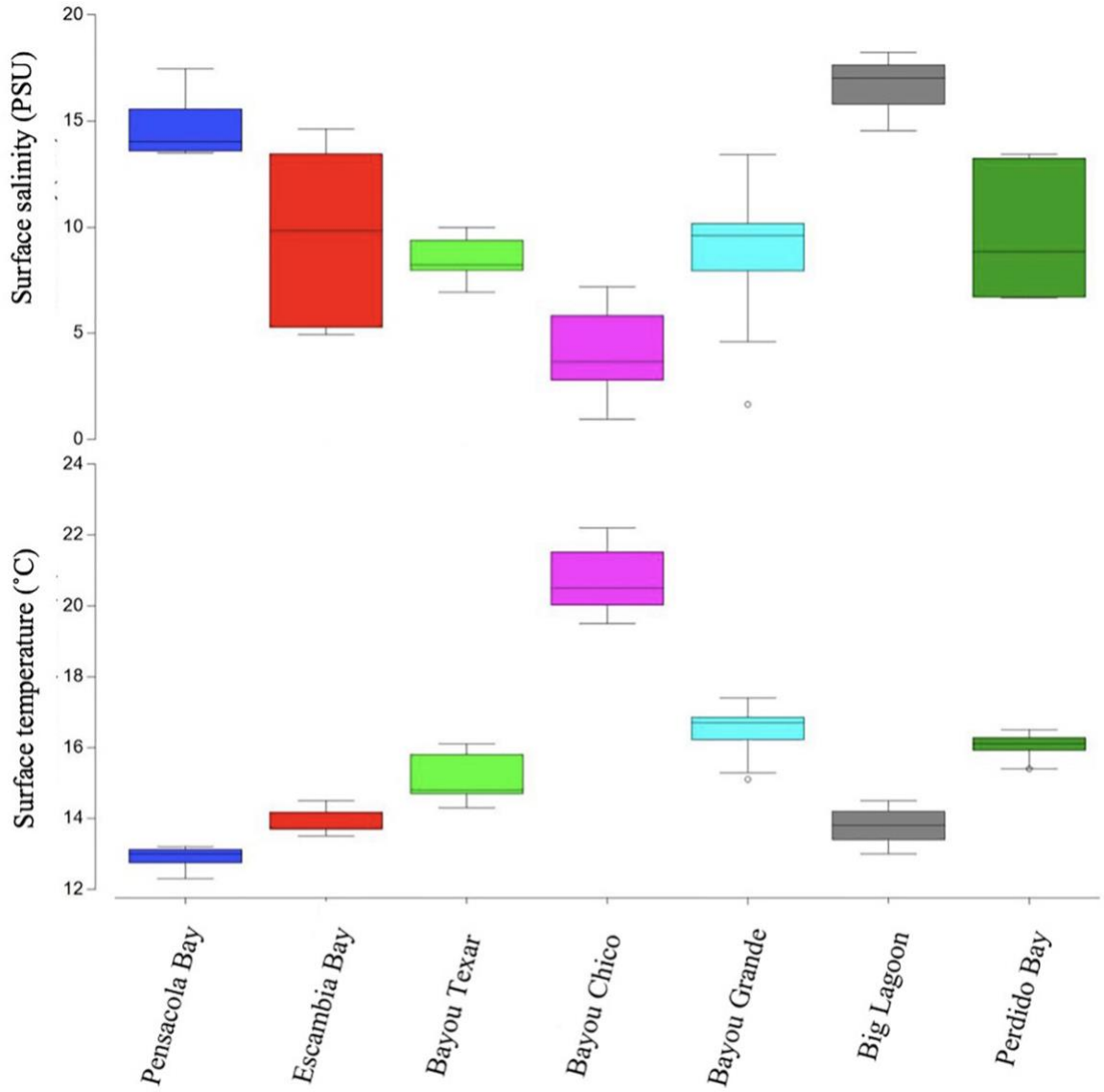

Fig. 2 Boxplots of surface water salinity and temperature. Open circles denote extreme values; box-tops and -bottoms show the 25th and 75th percentiles; lines within boxes mark mean values; and whiskers indicate minimums and maximums

Table 2 Means ± standard deviations of parameters of bottom water and sediment

Site [a]	Depth ranges (m)	Bottom water and sediment parameters					
		Temp. (°C)	Salinity (PSU)	Chl *a*[c] (µg/g)[b]	Phaeopig. (µg/g)[b]	% OC[d] Content[b]	% H_2O Content[b]
PB	0.9 - 3.5	13.4 ± 0.3	18.0 ± 2.8	3.3 ± 1.0	3.4 ± 1.3	1.8 ± 2.8	35.1 ± 20.3
EB	1.5 - 3.4	13.4 ± 0.1	11.3 ± 3.8	2.1 ± 2.1	4.7 ± 1.5	7.0 ± 5.6	58.0 ± 22.7
BT	1 - 2.7	15.8 ± 0.6	12.1 ± 3.4	3.7 ± 2.4	4.1 ± 1.0	6.0 ± 6.1	49.8 ± 29.0
BC	0.4 - 4.3	19.7 ± 1.9	11.6 ± 7.0	2.9 ± 1.7	4.0 ± 1.4	6.8 ± 8.0	41.2 ± 23.7
BG	0.9 - 2.9	17.1 ± 0.5	10.5 ± 3.9	1.9 ± 1.0	3.5 ± 1.2	5.1 ± 5.1	45.8 ± 22.5
BL	1.1 - 6.1	15.3 ± 0.9	22.4 ± 3.3	3.4 ± 1.4	3.9 ± 1.9	3.4 ± 5.0	40.5 ± 25.7
PD	1.1 - 3	16.0 ± 0.3	10.5 ± 3.0	1.5 ± 0.6	4.2 ± 1.7	8.3 ± 6.0	56.8 ± 22.1

[a] Basin abbreviations: PB, Pensacola Bay; EB Escambia Bay; BT, Bayou Texar; BC, Bayou Chico; BG, Bayou Grande; BL, Big Lagoon; PD, Perdido Bay
[b] sediment parameter
[c] chl *a*, chlorophyll *a*
[d] organic content, OC

Putative Vibrio in biofilm samples

The median concentrations of *Vv* and *Vp* in all presumptive biofilms were 2,281 and 163 CFU/mL, respectively (Table 6). Only two invertebrate biofilm samples resulted in undetectable *Vibrio* – one from a polychaete worm in Pensacola Bay, and the other from an oyster located at Bayou Grande. In the remaining 11 samples, mostly from swabbed oyster or barnacle shells, *Vv* abundances ranged from 81 to 28,844 CFU/mL, and *Vp* from 81 to 14,422 CFU/mL. There was not a statistical difference between oysters (n = 5) and barnacles (n = 6) for *Vv* (*t-test*, p = 0.750) nor *Vp* (*t-test*, p = 0.560).

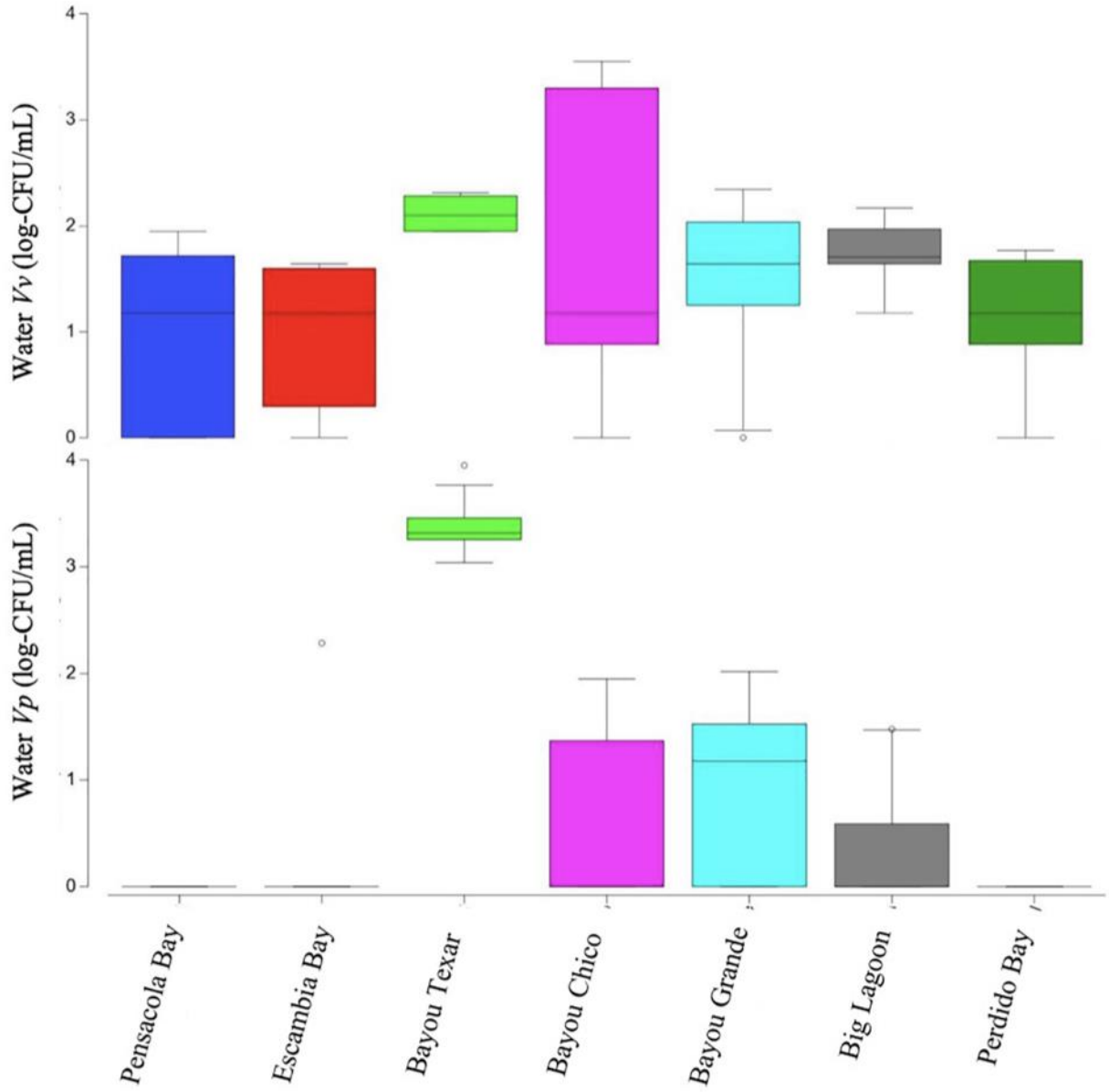

Fig. 3 Boxplots of surface water *Vibrio* abundances. Open circles denote extreme values; box-tops and -bottoms show the 25th and 75th percentiles; lines within boxes mark mean values; and whiskers indicate minimums and maximums

Table 3 Abundances of culturable *Vv* in sediments and surface waters. Medians and ranges in each basin are provided

Basin	Sediment (CFU / mL)					Surface water (CFU / mL)				
	n[a]	# samples undetect.[b]	Min. >0[c]	Max.	Basin Median	n[d]	# samples undetect.[b]	Min. >0[c]	Max.	Basin Median
Pensacola Bay	4	0	762	21,055	7,590	5	2	15	89	15
Escambia Bay	7	0	1,653	42,218	14,926	7	2	15	44	15
Bayou Texar	6	0	169	388,338	10,499	6	0	89	207	126
Bayou Chico	5	0	188	314,667	51,839	5	1	15	3,556	15
Bayou Grande	7	0	475	17,333	8,757	7	1	15	222	44
Big Lagoon	8	0	36,681	607,222	70,274	8	0	15	148	51
Perdido Bay	5	1	4,665	164,273	20,993	5	1	15	59	15

[a] Number of sediment samples obtained in each basin
[b] Number of samples in which *Vibrio* species was below detection limit
[c] Minimum CFU/mL in which *Vibrio* species was above detection limit
[d] Number of surface water samples obtained from each basin

Table 4 Abundances of culturable *Vp* in sediments and surface waters. Medians and ranges in each basin are provided

Basin	Sediment (CFU / mL)					Surface water (CFU / mL)				
	n[a]	# samples undetect.[b]	Min. >0[c]	Max.	Basin Median	n[d]	# samples undetect.[b]	Min >0[c]	Max.	Basin Median
Pensacola Bay	4	2	73	655	36	5	5	0	0	0
Escambia Bay	7	1	92	1,649	187	7	6	193	193	0
Bayou Texar	6	0	132	3,124	1,445	6	0	1,096	8,919	2,066
Bayou Chico	5	0	586	77,333	2,689	5	3	15	89	0
Bayou Grande	7	2	28	392	30	7	3	15	104	15
Big Lagoon	8	0	227	19,185	1,444	8	6	15	30	0
Perdido Bay	5	4	130	130	0	5	5	0	0	0

[a] Number of sediment samples obtained in each basin
[b] Number of samples in which *Vibrio* species was below detection limit
[c] Minimum CFU/mL in which *Vibrio* species was above detection limit
[d] Number of surface water samples obtained from each basin

Correlation of abundances with abiotic environmental parameters

Vibrios were generally most abundant in Bayou Chico (with the exception of *Vp* water abundances, which were greatest in Bayou Texar) (Tables 2-3, Fig. 3). Prior wind speeds showed strong evidence for a positive correlation between surface water abundances of both *Vv* ($r = 0.84$, $p < 0.05$) and *Vp* ($r = 0.83$, $p < 0.05$), but not with sedimentary *Vibrio* abundances (Table 5). Water *Vv* abundances were also positively correlated with bottom water pH ($r = 0.46$, $p < 0.05$) and tidal coefficient ($r = 0.86$, $p < 0.01$); and surface water *Vv* moderately correlated with average sediment chl *a* concentrations ($r = 0.29$, $p = 0.057$) (Table 5). Surface water *Vv* did not covary strongly with salinity. Surface water *Vp* abundances correlated with seven parameters, the greatest number of correlations among the four calculated species abundances. Parameters that showed negative correlations with surface water *Vp* included surface salinity ($r = -0.36$, $p < 0.05$), surface pH ($r = -0.45$, $p < 0.05$), and bottom pH ($r = -0.47$, $p < 0.05$). Positive correlations with surface *Vp* included total DIN ($r = 0.32$, $p < 0.05$) and TKN ($r = 0.36$, $p < 0.05$) concentrations. Maximum cumulative wind speed ($r = 0.83$, $p < 0.05$) also showed evidence for a positive correlation with water *Vp* (Table 5).

In sediments, *Vv* abundances positively correlated with both surface ($r = 0.50$, $p < 0.05$) and bottom ($r = 0.52$, $p < 0.05$) pH (Table 5). Sedimentary *Vp* was correlated with average sediment chl *a* concentrations ($r = 0.31$, $p < 0.05$) and tidal coefficient ($r = 0.77$, $p < 0.05$). Interestingly, both *Vv* and *Vp* sediment abundances shared a correlation with one parameter: salinity stratification. Although winter levels of salinity stratification among all basins were generally low, stratification positively correlated with sedimentary abundances of both *Vv* ($r = 0.31$, $p < 0.05$) and *Vp* ($r = 0.33$, $p < 0.05$). Within the salinity values measured at locations in this study, there was no optimal salinity range where *Vv* or *Vp* was more abundant (Fig. 5).

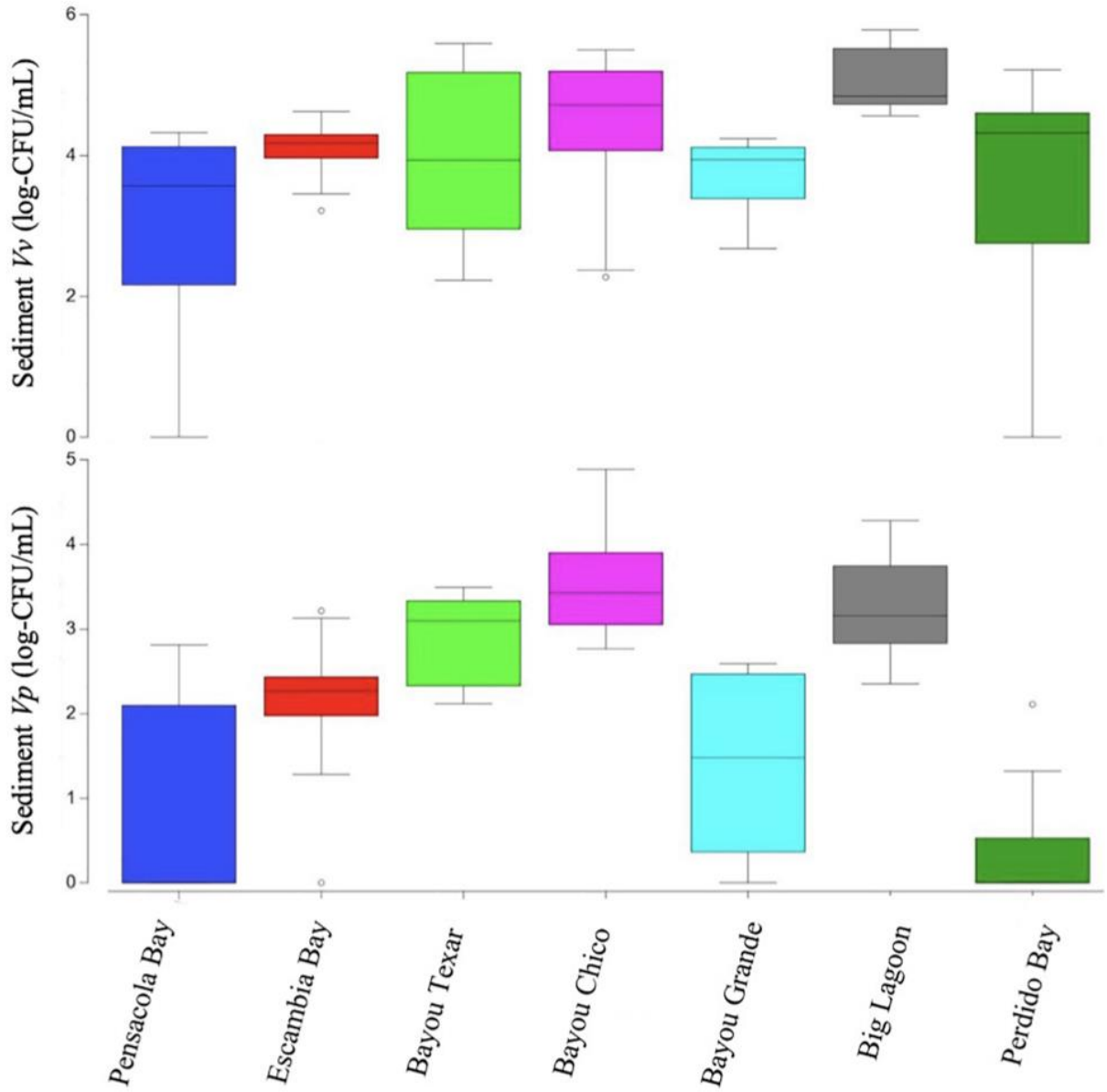

Fig. 4 Boxplots of *Vibrio* abundances in sediments. Open circles denote extreme values; box-tops and -bottoms show the 25th and 75th percentiles; lines within boxes mark mean values; and whiskers indicate minimums and maximums

To further examine the relationship of salinity with these presumed *Vv* and *Vp* abundances, we also examined *Vibrio* abundances within a subset of stations that had salinities only between 5-25 PSU. For these additional correlation tests, five stations (V7, V19, V20, V23, V27) with surface or bottom water salinities outside this range were excluded from this additional correlation analysis. Even when salinity did fall within the optimal range, there still was no significant relationship with abundance, whether in the water column (*Vv*; r = -0.0089, p = 0.958, n = 38) or in the sediments (*Vv*; r = 0.0875, p = 0.596, n = 39 and *Vp*; r = 0.1107, p = 0.542, n = 39). Only surface *Vp* showed a strong relationship with optimal salinity conditions, but it did so negatively (r = -0.435, $p < 0.01$, n = 38).

Table 5 Numbers of *Vv* and *Vp* present in biofilms on invertebrates

Waterbody	Organism type[d]	*Vv* (CFU/mL)	*Vp* (CFU/mL)	Ratio *Vv*:*Vp*	Total DIN[a] (µM)	TKN[b] (µM)	DIP[c] (µM)	Chl *a* (µg/L)
Pensacola Bay	barnacle	7,822	489	16	2.74	27.00	0.00	3.55
	barnacle	2,281	326	7	1.42	28.14	0.00	2.81
	oyster	28,844	0	n/a	2.28	26.93	0.00	1.83
	worm	0	0	n/a	7.11	28.36	0.00	1.57
Escambia Bay	worm	27,215	0	n/a	3.48	29.14	0.00	5.30
Bayou Texar	oyster	1,630	4,726	0.34	22.73	38.64	0.00	2.88
	oyster shell	1,548	163	9.5	25.78	39.00	0.00	3.09
Bayou Chico	barnacle	17,519	14,422	1.2	3.82	42.43	0.00	8.57
	barnacle	244	163	1.5	9.21	46.43	0.00	8.46
	oyster shell	9,289	81	114	9.39	43.29	0.00	5.60
Bayou Grande	barnacle	10,267	163	63	6.45	33.36	0.06	5.41
	oyster	0	0	n/a	7.66	42.57	0.19	5.36
	barnacle	81	326	0.25	4.30	50.64	0.00	0.86

[a] DIN, dissolved inorganic nitrogen
[b] TKN, total Kjeldahl nitrogen
[c] DIP, dissolved inorganic phosphorus
[d] Exact taxonomic identification was not determined for sampled invertebrates. Worm, polychaete worm

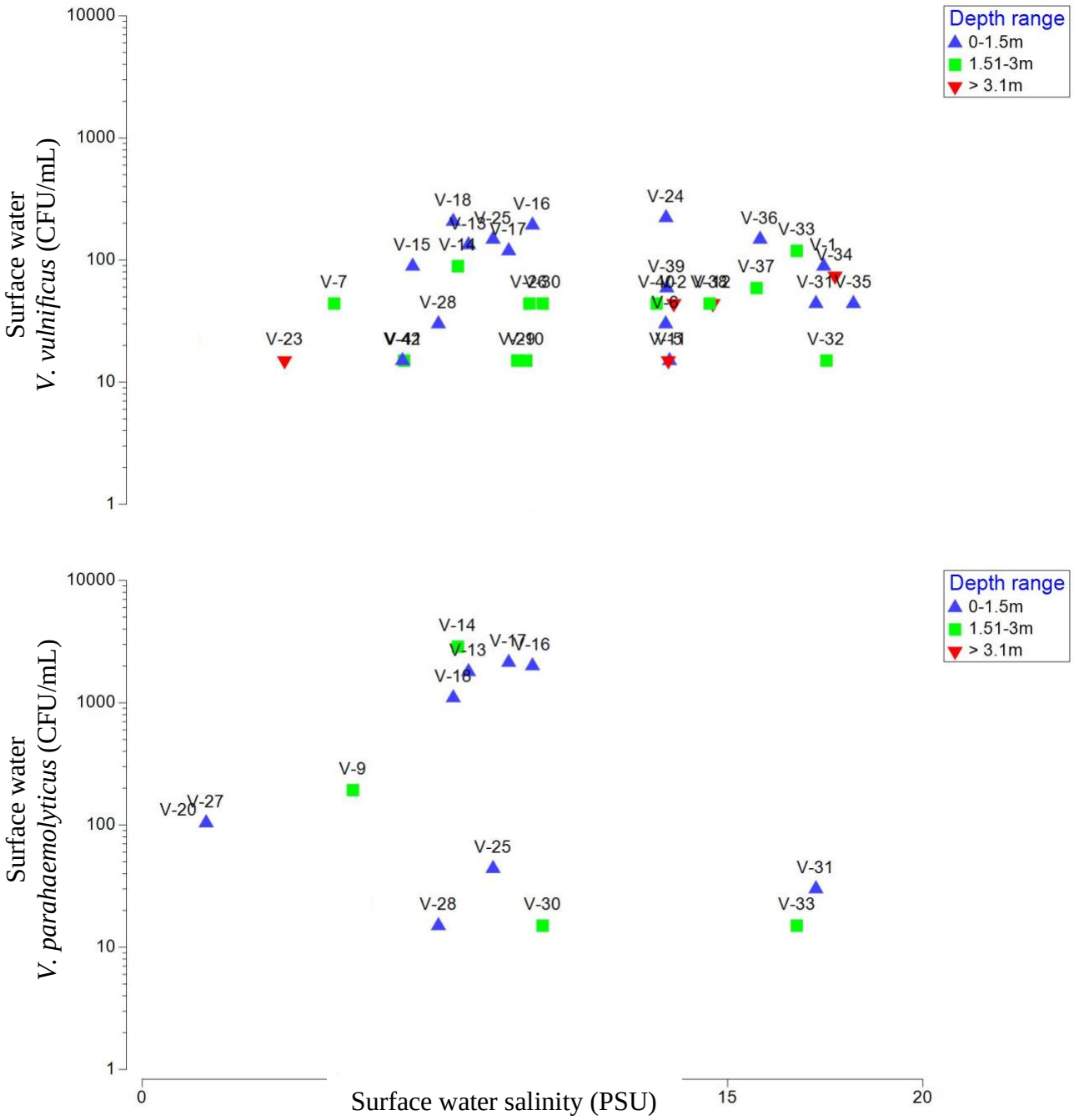

Fig. 5 Surface water *Vv* and *Vp* with respect to salinity, delineated by basin and water column depths. Surface water *Vv* (above) and *Vp* (below) abundances vs. surface water salinity. Data symbols are delineated by total water column depths

Table 6 Correlations between *Vibrio* abundances and environmental parameters

Environmental parameter	Surface water				Bottom water/sediment			
	Vv (log)		*Vp (log)*		*Vv (log)*		*Vp (log)*	
	r[b]	p[a]	r[b]	p[a]	r[b]	p[a]	r[b]	p[a]
Surface salinity (PSU)	N.S.	0.22	**-0.36**	** **0.018**	N.S.	0.57	N.S.	0.48
Surface pH	N.S.	0.080	**-0.45**	** **0.044**	**0.50**	** **0.025**	N.S.	0.065
Bottom pH	**0.46**	** **0.040**	**-0.47**	** **0.035**	**0.52**	** **0.018**	N.S.	0.17
Salinity stratification	N.S.	0.66	N.S.	0.75	**0.31**	** **0.040**	**0.33**	** **0.029**
Total surface DIN (µM)	N.S.	0.52	**0.32**	** **0.037**	N.S.	0.57	N.S.	0.092
Total Kjeldahl Nitrogen (µM)	N.S.	0.57	**0.36**	** **0.017**	N.S.	0.85	N.S.	0.37
Avg. sediment chl *a* (µg/g)	**0.29**	* **0.057**	N.S.	0.21	N.S.	0.29	**0.31**	** **0.043**
Max. cumulative wind (mph)	**0.84**[c]	** **0.018**	**0.83**[c]	** **0.022**	N.S.	0.70	N.S.	0.46
Tidal coefficient[c] (m)	**0.86**	*** **0.008**	N.S.	0.28	N.S.	0.64	**0.77**	** **0.045**

[a] Significance levels indicated: *$p \approx 0.05$; **$p < 0.05$; ***$p < 0.01$; N.S., not significant

[b] Bacterial abundances, Pearson correlation coefficient (r) of log(CFU/mL) with parameter. Degrees of freedom for these analyses was 42 (surface water abundances) and 41 (sediment abundances). Bottom and surface water pH was $n = 20$

[c] D.F. for these analyses was 6, and basin-wide means of *Vv* or *Vp* were used. Values in bold indicate strong evidence ($p \geq 0.05$) for a significant correlation between parameters

Water column *Vibrio* abundances were not correlated with concentrations of TSS, dissolved oxygen, DIP, chl *a*, or K_d. Sedimentary *Vibrio* abundances were not correlated with the following sediment characteristics: percent water, percent organic content, and sediment phaeophyte pigments; additionally, neither presumptive *Vv* nor *Vp* abundances were correlated with water column K_d.

Analysis of variance (ANOVA) among basins

ANOVA tables were generated for each environmental parameter and subsequently used to determine factors that indicated strong evidence for a difference among basins (Table 6). Bottom pH (F = 16.548), bottom salinity (F = 7.771), bottom temperature (F = 33.328), log-DIN concentrations (F = 10.684), log-*Vp* sediment abundances (F = 9.421), log-*Vp* water abundances (F = 19.735), surface pH (F = 21.012), surface salinity (F = 13.750), surface temperature (F = 96.284), and TKN concentrations (F = 9.732) were different at $a < 0.001$. Additionally, TSS (F = 3.225, p = 0.01), water chl *a* concentrations (F = 4.791, p = 0.001), DIP (F = 5.210, p = 0.001), and K_d (F = 4.817, p = 0.001) showed strong evidence for a difference among basins.

ANOVA between open and enclosed waterbodies

Statistical analysis was also performed to determine evidence of a difference between open estuaries (Pensacola Bay, Escambia Bay, and Perdido Bay) and enclosed estuaries (Bayou Texar, Bayou Chico, Bayou Grande, and Big Lagoon). Log-*Vv* water abundance (F = 9.973, p = 0.003), log-*Vp* water abundance (F = 9.662, p = 0.003), log-*Vp* sediment abundance (F = 17.271, $p < 0.001$), surface temperature (F = 7.838, p = 0.008), bottom temperature (F = 24.197, $p <$ 0.0001), salinity stratification (F = 4.257, p = 0.045), log-DIN concentrations (F = 8.305, p = 0.006), and tidal coefficient (F = 25.809, p = 0.004) were different between open and enclosed estuaries (Table 7).

Table 7 ANOVA for factors significant at $p < 0.05$ among the seven basins

Parameter tested		SS[a]	df[b]	MS[c]	F-value	Significance[d]
Bottom pH	*Between*	2.1	2	1.0	16.6	1.02E-04
	Within	1.1	17	0.1		
	Total	3.2	19			
Bottom salinity (PSU)	*Between*	889.6	6	148.3	7.8	2.10E-05
	Within	686.9	36	19.1		
	Total	1576.5	42			
Bottom temperature (˚C)	*Between*	160.0	6	26.7	33.3	2.79E-13
	Within	28.8	36	0.8		
	Total	188.8	42			
DIP (µM)	*Between*	0.1	6	0.01	5.2	0.001
	Within	0.1	36	0.002		
	Total	0.2	42			
K_d (m^{-1})	*Between*	4.4	6	0.7	4.8	0.001
	Within	5.5	36	0.2		
	Total	9.9	42			
log-DIN (µM)	*Between*	8.0	6	1.3	10.7	8.37E-07
	Within	4.5	36	0.1		
	Total	12.6	42			
log-*Vp* sediment (CFU/mL)	*Between*	48.9	6	8.1	9.4	3.00E-06
	Within	31.1	36	0.9		
	Total	80.0	42			
log-*Vp* water (CFU/mL)	*Between*	50.1	6	8.4	19.7	4.78E-10
	Within	15.2	36	0.4		
	Total	65.4	42			
NH_4 (µM)	*Between*	103.5	6	17.3	6.6	8.00E-05
	Within	93.7	36	2.6		
	Total	197.2	42			
Surface pH	*Between*	1.8	2	0.9	21.0	2.50E-05
	Within	0.8	17	0.04		
	Total	2.6	19			
Surface salinity (PSU)	*Between*	655.2	6	109.2	13.8	4.68E-08
	Within	285.9	36	7.9		
	Total	941.1	42			
Surface temp. (˚C)	*Between*	221.9	6	37.0	96.3	1.15E-20
	Within	13.8	36	0.4		
	Total	235.8	42			
TKN (µM)	*Between*	3401.4	6	566.9	9.7	2.00E-06
	Within	2097	36	58.3		
	Total	5498.3	42			
TSS (mg/L)	*Between*	163.5	6	27.3	3.2	0.012
	Within	304.2	36	8.5		
	Total	467.8	42			
Water chl *a* (µg/L)	*Between*	159.2	6	26.5	4.8	0.001
	Within	188.3	34	5.5		
	Total	347.6	40			

[a] Type I sum of squares

[b] Degrees of freedom

[c] Mean square

[d] Significance of <0.05 is strong evidence to reject the null hypothesis that basins were similar with regards to the given parameter

In surface waters, *Vv* median abundance was approximately 2-fold greater in open basins than in the enclosed basins. In only three of the 25 stations, *Vp* abundances were above the minimum detection limit in open basins (12%), whereas it was found in surface waters in 12 of the 18 locations in enclosed waterbodies (67%). In open basins, the median *Vv* sediment abundance exceeded that of enclosed waterbodies by approximately 1.8-fold, while median sediment *Vp* was approximately 2-fold greater in enclosed systems than in open systems.

Table 8 ANOVA for factors significant at $p < 0.05$ between open and enclosed basins

Parameter tested		**SS[a]**	**df[b]**	**MS[c]**	**F-value**	**Significance[d]**
Log-*Vv* water (CFU/mL)	*Between*	5.6	1	5.7	10.0	0.003
	Within	23.2	41	0.6		
	Total	28.9	42			
Log-*Vp* water (CFU/mL)	*Between*	12.5	1	12.5	9.7	0.003
	Within	52.9	41	1.3		
	Total	65.4	42			
Log-*Vp* sediment (CFU/mL)	*Between*	23.7	1	23.7	17.3	1.61E-04
	Within	56.3	41	1.4		
	Total	80.0	42			
Surface temperature (˚C)	*Between*	37.8	1	37.8	7.8	0.008
	Within	197.9	41	4.8		
	Total	235.8	42			
Bottom temperature (˚C)	*Between*	70.1	1	70.1	24.2	1.50E-05
	Within	118.7	41	2.9		
	Total	188.8	42			
Salinity stratification	*Between*	67.9	1	67.9	4.3	0.045
	Within	654.2	41	16.0		
	Total	722.1	42			
Log-DIN (µM)	*Between*	2.1	1	2.1	8.3	0.006
	Within	10.4	41	0.3		
	Total	12.6	42			
Tidal coefficient (m)	*Between*	2708.7	1	2708.7	25.8	0.004
	Within	524.8	5	105.0		
	Total	3233.4	6			

[a] Type I sum of squares
[b] Degrees of freedom
[c] Mean square
[d] Significance of <0.05 is strong evidence to reject the null hypothesis that basins were similar with regards to the given parameter

Table 9 Overview of salinity zone, stratification and oxygen levels in all waterbodies examined. The maximum salinity stratification (absolute value of salinities in surface water – bottom water) at any station sampled in each waterbody is indicated

Waterbody	System Type	No. of stations	Salinity Zone[a]	Mean surface salinity[b]	Surface water[c]		Sediment[d]		Mean bottom water salinity[b]	Salinity stratification at any location in waterbody		DO (mg/L) ranges	
					Vv	*Vp*	*Vv*	*Vp*		Min.	Max.	Surface water	Bottom water
Pensacola Bay	open	5	mesohaline	14.7 ± 1.6	15	0	7,590	36	18.0 ± 2.8	0.75	7.3	10.0 - 10.8	8.9 - 10.5
Escambia Bay	open	7	mesohaline	9.6 ± 4.0	15	0	14,926	187	11.3 ± 4.1	0.02	6.8	9.9 - 10.8	9.4 - 10.5
Bayou Texar	enclosed	6	oligohaline	8.5 ± 1.0	126	2066	10,499	1,445	12.1 ± 3.7	0.01	8.7	8.7 - 9.8	7.2 - 8.8
Bayou Chico	enclosed	5	oligohaline	4.1 ± 2.1	15	0	51,839	2,689	11.6 ± 7.9	0.2	21.1	5.2 - 9.7	5.1 - 9.5
Bayou Grande	enclosed	7	mesohaline	8.8 ± 3.3	44	15	8,757	30	10.5 ± 4.2	0.02	4.4	7.9 - 9.4	5.8 - 9.5
Big Lagoon	open	8	mesohaline	16.7 ± 1.2	51	0	70,274	1,444	22.4 ± 3.5	0.02	9.8	9.8 - 10.2	8.7 - 10.6
Perdido Bay	open	5	mesohaline	9.8 ± 3.0	15	0	20,993	0	10.5 ± 3.4	0	3.3	9.2 - 9.7	8.7 - 9.5
			Median, all open basins		44	0	21,024	207					
			Median, all enclosed basins		89	29	11,950	489					

[a] Salinity zone defined by basin mean salinity: 0-9.99 PSU, oligo-; 10-20 PSU, meso-; and >20 PSU, euryhaline
[b] Mean salinity ± SD
[c, d] Median *Vv* and *Vp* abundances (CFU / mL) in surface water and sediment, respectively

Discussion

Salinity, among others, is often considered a predictive variable for *Vibrio* in the water column, with optimal conditions ranging from 5 to 25 PSU (Hsieh et al 2008; Kaspar and Tamplin 1993; Motes et al 1998). However, this was not the case in this study. In the seven basins examined, locations chosen for the survey represented waterbodies with a wide range of salinities and stratification (Table 2). Within the salinity values measured at these different locations, there was no optimal salinity range where presumptive *Vv* or *Vp* was found to be more abundant (Fig. 5). Moreover, bottom pH and stratification also correlated with one another, though not as dramatically ($r = 0.4541$, $p = 0.044$). This could have been attributed to the lower sample size ($n = 20$), as pH measurements were only taken for approximately half of all basins (Bayou Grande, Big Lagoon, and Perdido Bay). *Vv* abundances can increase with depth, particularly in bottom waters within shallow estuaries (Wetz et al 2014). This trend may be attributed to variation in salinity and/or temperature at different depths, suggesting covariation between temperature and salinity in regard to estimating *Vibrio* abundance.

However, in our study, putative abundances of *Vv* and *Vp* did not significantly vary with total water column depth, and there was no consistent pattern of depth, salinity, and *Vibrio* abundances. In some basins, water *Vibrio* abundances may have been greater than usual due to high wind speeds, which likely promoted mixing in the water column and resuspension of sediments. Therefore, it would have been unlikely to see a relationship between *Vibrio* abundances and depth. However, there was a relationship between *Vibrio* abundances and stratification, which does in fact align with findings in previous studies, especially for shallow estuaries (Wetz et al 2014). Although the method here assesses only abundances based on viable CFU, this broad range of data is useful in determining baseline abundances in the region.

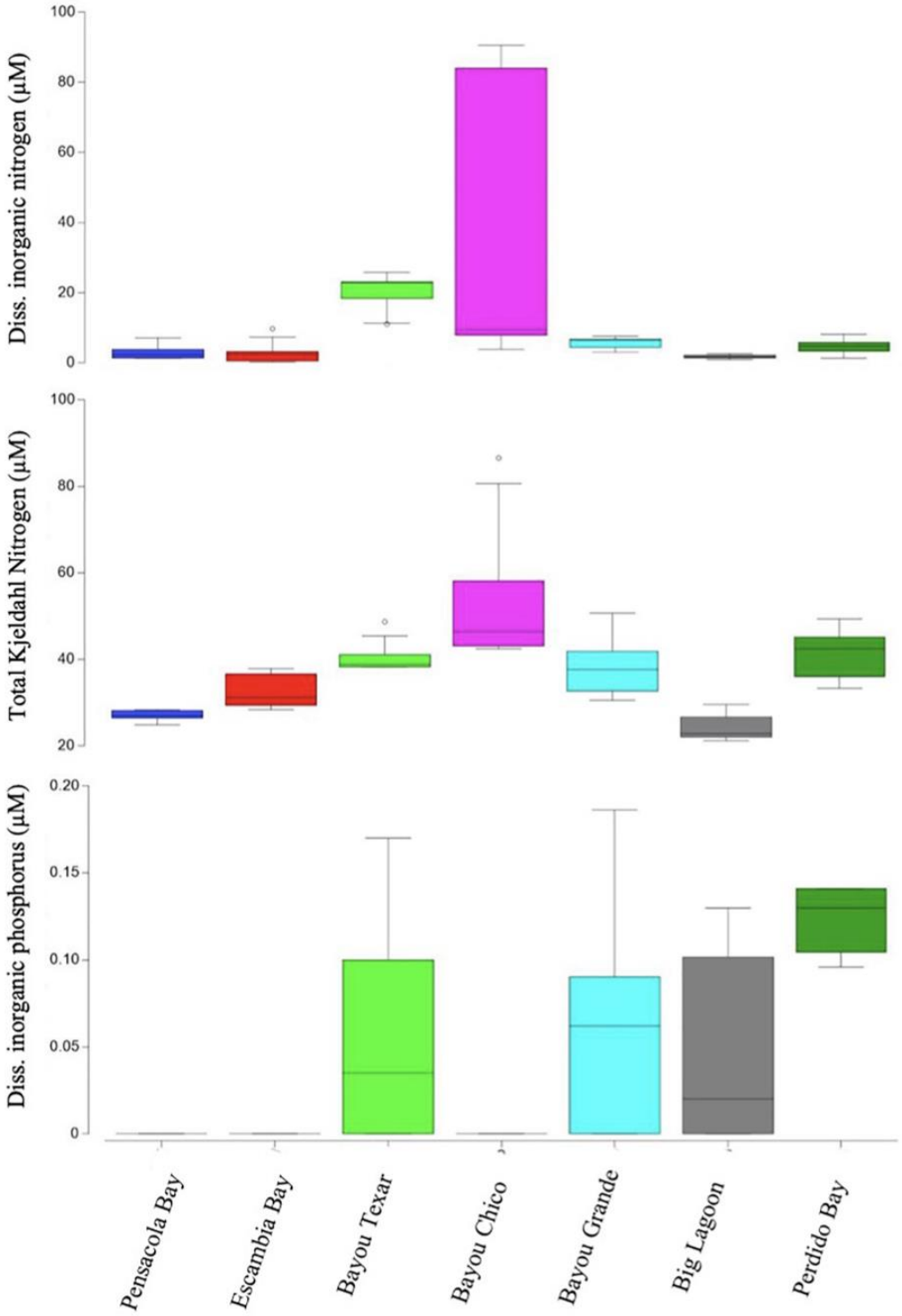

Fig. 6 Boxplots of dissolved inorganic nitrogen (DIN), phosphorus (DIP) and total Kjeldahl nitrogen (TKN). Open circles denote extreme values; box-tops and -bottoms show the 25th and 75th percentiles; lines within boxes mark mean values; and whiskers indicate minimums and maximums

Correlations of *Vibrio* abundance with temperature are often linked to seasons (Hsieh et al 2008; Wetz et al 2014). For example, (Wetz et al 2014) reported seasonal data over a four-year period for environmental parameters that may influence surface and bottom water abundances of *Vv* within the Neuse River Estuary. Certainly, the length of this survey capacitates the reporting of seasonal data. Although the Neuse River Estuary and the PBS are both shallow, river-dominated estuarine systems, and despite the contrast in duration of the study, actual relationships between water or sedimentary *Vibrio* abundances and environmental parameters differ depending on the influence of physicochemical factors (i.e., runoff, mixing, resuspension). Evidently, seasonal data reported for temperature, salinity, turbidity, and chl *a* all showed strong correlations to *Vv* abundances, whereas none of the four covaried with *Vibrio* abundances in our study (Wetz et al 2014). In fact, surface water temperatures in this winter survey were less than optimal for maximum concentrations of *Vv* or *Vp*, presumed to be in the range of 20 to 37°C (Johnson et al 2012; Johnson 2013; Tantillo et al 2004). Maximum abundances of surface water putative *Vv* were in Bayou Chico, the one basin with the highest overall *Vv* surface water abundances (Fig. 3). In this basin, surface water salinities were lowest of all, but temperatures and salinity stratification were the highest (Fig. 2; Table 8). It was surprising to see very high winter abundances in surface waters, sediments, or both, in particular basins of this study.

Surface water presumptive *Vp* were maximal in Bayou Texar where total DIN concentrations were high, and sedimentary presumptive *Vp* was greatest in Bayou Chico where chl *a* concentrations were high – factors that are both associated with eutrophication suspected to promote *Vibrio* success (Froelich et al 2019; Han et al 2020; Turner et al 2009; Wetz et al 2008). It is feared that eutrophication will promote higher concentrations of pathogens such as *Vibrio* species (Malham et al 2014). Estuarine eutrophication alone, often measured by chl *a*

concentrations, does not necessarily assess the number of higher trophic levels (Van Meerssche and Pinckney 2019). Genomic evaluation of *Vv* and *Vp* suggests most are chitinolytic (Grimes et al 2009), and *Vibrio* may be attached to zooplankton- or eukaryotic phytoplankton (Takemura et al 2014). Abundances of particle-associated estuarine *Vibrio* may be strongly correlated with chl *a*, but this relationship may vary seasonally or from year to year (Main et al 2015). These data suggest much of the particulate material in these estuaries, terrestrial-derived and autochthonous, drives and is associated with primary production. If *Vibrios* in subtropical estuaries are largely associated with diatoms or zooplankton (Martinez-Urtaza et al 2012), one might expect a positive relationship of *Vibrio* abundances with increased turbidity and phytoplankton biomass (chl *a*). However, surface water *Vibrio* abundances were not significantly correlated with TSS or chl *a* in this study. A lack of, or negative, correlation of abundance with chl *a* and/or TSS is consistent with findings of previous temperate estuarine studies (Deeb et al 2018; Wetz et al 2014). Culture-dependent methods of total *Vibrio* counts do suggest their abundances are strongly and positively correlated with turbidity and DIN (Froelich et al 2019).

Here, we observed culturable presumptive *Vp* positively correlating with DIN and TKN, similar to the findings of (Froelich et al 2019) in a temperate estuary. However, neither surface water putative *Vv* nor sedimentary putative *Vp* or *Vv* significantly covaried with nitrogen. Additionally, an earlier study (Wetz et al 2008) of culture-dependent enumeration of total *Vibrio* found abundances strongly correlated with temperature during two significant storms, but abundances were correlated with salinity and TSS in only one of the two events. These findings were explained by the different wind directions and levels of sediment resuspension. Therefore, in addition to nutrients, turbidity, and phytoplankton biomass, estuarine dynamics such as tidal influence, salinity stratification, and wind-driven mixing may also be important considerations.

Salinity and stratification, both affected by wind and/or rain events, can affect *Vibrio* concentrations (Fries et al 2008). Therefore, we evaluated the effect of maximum cumulative wind speeds recorded in the Pensacola metropolitan area in the three days leading up to and on the mornings of our sampling events. Wind mixing introduces sediment-dwelling bacteria into surface waters and may partly explain increased *Vibrio* concentrations in surface waters, particularly in Bayou Texar (02/07/20), the basin with the highest cumulative wind speeds (84 MPH). While wind-driven resuspension could explain the very high numbers of presumptive *Vp* in all stations sampled there, corresponding water abundances of *Vv* do not support wind as the sole cause for high *Vp* numbers on that sampling date. For example, in Bayou Texar, *Vv* water levels were between 89 and 207 CFU/mL, while *Vp* concentrations ranged from ~1,000 to 9,000 CFU/mL. In contrast, concentrations of both species in sediments showed the opposite trend. In two of the six locations sampled, putative *Vv* in sediments roughly equaled those of putative *Vp*. At the remaining four stations, *Vv* exceeded *Vp* by at least eight-fold. It is clear that other factors, in addition to wind, are likely responsible for high *Vibrio* concentrations in the water column and within the sediments.

In sediments of subtropical coasts or temperate estuaries, *Vp* are generally more prevalent than *Vv* (Pfeffer et al 2003; Vezzulli et al 2009), but this overall pattern was not seen in this study. The relative abundances of these two species in sediments varied widely, with an approximate 1500:1 ratio of presumptive *Vv:Vp* in Perdido Bay, but approximately 50:1 in all other basins, except Bayou Chico, where *Vv:Vp* was only 6:1 (Table 4). Multiple comparison procedures (Tukey's *Post Hoc*) determined *Vp* sedimentary abundances in Pensacola and Perdido Bays were significantly lower than in the other basins. Interestingly, *Vibrio* abundances covaried with tidal coefficient and maximum wind speeds, indicating the influence of sediment

resuspension. In this study, bottom water oxygen concentrations and putative *Vibrio* abundances in the sediments were not correlated. Generally, there is a lack of hypoxia in bottom waters of these basins in winter (Caffrey and Murrell 2016), which was also found in winter 2020. Since all types of putative *Vibrio* we enumerated (with the exception of sediment *Vv*) were significantly correlated with prior cumulative wind speeds, resuspension may be a contributing factor in explaining *Vibrio* in the surface waters of the Pensacola and Perdido Bay water basins.

To determine the effects of rain events prior to our sampling dates, we evaluated precipitation with respect to *Vibrio* abundances and environmental parameters. In all basins, total precipitation did not positively covary with turbidity as expected. K_d, not unexpectedly, was positively correlated with TSS ($r = 0.30$, $p = 0.05$) and chl *a* ($r = 0.73$, $p < 0.0001$). Pensacola Bay cyanobacterial abundances in these waters are lowest in winter (Murrell and Caffrey 2005; Murrell and Lores 2004), and while we did observe different chl *a* concentrations among the basins examined, there was no significant relationship with *Vibrio* abundances (Table 5 and 6). We anticipated increased *Vibrio* densities in waters with higher turbidity, as observed previously with *Vp* in subtropical waters of coastal northern GoM (Zimmerman et al 2007), but abundances may not consistently covary with turbidity, where patterns are either site- or season-specific (Blackwell and Oliver 2008; Johnson et al 2012; Zimmerman et al 2007). Our findings suggest terrestrial inputs of nutrients concomitant with mixing and increased turbidity are alone not sufficient to explain *Vibrio* success, as previously suggested for temperate estuaries (Davis et al 2017; Froelich et al 2019).

For the purposes of initial surveys to determine baseline levels, culture-dependent methods can provide notable ecological insights, yet be limited in scope. For example, the false-positive rate of *Vv* on CHROMagar™ as a bright blue colony was previously tested from a low-

salinity body of water (Lake Ponchartrain) in the same approximate latitude as the waterbodies surveyed here (Nigro and Steward 2015). In this typically oligohaline environment, with a salinity in the range of our study sites Bayous Texar and Chico (Table 2; Table 3), winter abundances of *Vv* and *Vp* may be overestimated by 50% (Nigro and Steward 2015). Additionally, enumeration of *Vv* and *Vp* using the colony method likely underestimates the count, as a single particle may contain numerous *Vibrio* cells but still appear as a single colony on media (Joux et al 2015).

False-positives may also be due to cross-reactivity of the substrate, such as blue colonies presenting as putative *Vv* confirmed by other methods to be *V. cholerae* or *V. mimicus* (Hara-Kudo et al 2001). In our preliminary testing (winter and summer of 2019) of similar bodies of water, molecular method verification indicated that *Vv* presented not only as bright blue on this solid medium, but also *vvhA*-positive in end-point colony PCR, using established primers for the *vvhA* gene, a species-marker for *Vv*. Similarly, bright pink (not purple, which may be *Aeromonas* species) were determined to be either *tdh*- or *trh*-positive (data not shown). Molecular analyses (either end-point PCR of colonies or qPCR on DNA extracted directly from the sample) may also provide over- or underestimates of *Vv* abundance data, due to possible cross-reactivity of *vvhA* PCR primers with related *Vibrio* species (Canizalez-Roman et al 2011; Klein et al 2014). However, this is not the case for *Vp*-specific PCR primers, such that they do not cross-react with other species of *Vibrio* (e.g., *V. mimivus*, *V. fluvialis*, *V. cholerae*).

Another limitation of the plating method may be a potential underestimate of the *Vibrio* abundance due to incubation temperatures or other factors affecting bacterial growth on solid agar. Conversely, not all putative *Vibrio* detected on plates will contain the established marker genes (e.g., *tdh*, *trh* for *Vp* or *vvhA*, *vcgC* for *Vv*). Therefore, a combination of plating and

molecular methods is ideal for enumerating putative *Vibrio* species in water column or sediments. For example, in a study of *Vibrio* abundances responding to hurricanes, low percentages of the colonies detected on plates of water or sediment samples contained genes associated with virulence (*vcgC* and *tdh*), and none of the sediment or water colonies were positive for *trh.* Notably, in that study, abundances of sedimentary and water column *Vv* and *Vp,* detected with culture methods, were not significantly impacted by wind nor freshening due to the storm (Shaw et al 2014). In contrast, in our study, putative *Vibrio,* based on only the culture method employed here, did significantly covary with prior wind speeds. Cultivable *Vv* and *Vp* abundance determination is dependent on culture substrate, time and temperature of incubation, among other factors. In a GoM estuary near our study site, for instance, *Vibrio* abundances associated with finfish or shellfish were previously determined using simultaneous culture-dependent and -independent methods (Givens et al 2014). The abundances determined by both approaches were similar, but it should be noted that molecular methods may be more sensitive when attempting to enumerate all *Vibrio,* culturable and non-culturable, or when enumerating only pathogenic species (Gutierrez West et al 2013).

Additionally, both *Vv* and *Vp* can be underestimated by culture-dependent techniques as compared to molecular methods (Froelich et al 2012; Kirchman et al 1982; Williams et al 2017). There was variability of putative *Vibrio* abundances among the few surface swab samples collected (Table 5), but this could be explained by the diversity of strains enumerated, some of which may have missed being counted due to slow recovery after plating. Recovery of *Vv*, *Vp,* or other *Vibrio* on various types of culture media is variable and possibly dependent on the nutrient state of the environment from which the sample was derived (Warner and Oliver 2008). In this study, low abundances from swab samples may have been rectified by a longer period of

incubation on agar plates or use of different media (DePaola et al 2003; Warner and Oliver 2008). We enumerated colonies after 24, 48, and 72 hours, but there were no significant increases in numbers of *Vv* nor *Vp* colonies after 48 hours. Therefore, the variability of *Vibrio* in the biofilms opportunistically sampled in this study may be more dependent on the abundances of *Vv* and *Vp* in the surrounding water column, but this was not seen in oysters and water samples in Tampa Bay, FL (Chase et al 2015).

Consistent with similar studies, *Vv* and *Vp* in sediments outnumbered those in waters by at least 10-fold. In surface waters of temperate or subtropical estuaries, *Vv* distributions are highly variable (Franco et al 2012; Givens et al 2014; Heidelberg et al 2002), but this may be explained by underestimates in the culture method, due to overwintering, in which *Vv* enter a "viable but not culturable" (VBNC) state when conditions are not optimal (Foster 2004; Franco et al 2012; Oliver and Bockian 1995). In temperate systems, culture-dependent abundances in winter sediments are low compared to those in surface waters, also suggesting overwintering (Pfeffer et al 2003), but bottom water temperatures in systems such as those examined here are generally warmer. Subtropical lagoon sediments did not yield cultivable *Vv*, even when incubations were performed at higher temperatures (41°C) (Cantet et al 2013) than in this study.

The design of this study was not to enumerate pathogenic *Vv* and *Vp*, but rather to determine baseline *Vibrio* loads in winter for a set of waterbodies yet to be examined. Although the method employed here assesses only "presumptive" *Vv* and *Vp* abundances based on viable CFU, this wide range of data is useful in determining baseline abundances in the region. Cultivable abundance estimates, representative of consistent sample-to-sample comparison (Zimmerman et al 2007), are valuable in and of themselves for determining relative risk factors in each waterbody of interest. Pathogenic strains' abundances vary extensively – within samples,

between sampling dates in the same location, among samples with different source salinities, among seasons, or after significant storm events (Kaufman et al 2003; Liu et al 2016; Nigro et al 2011; Zimmerman et al 2007). Therefore, to confirm estimated culturable loads of either species, future efforts will be directed towards species-specific enumeration, upon additional culture-dependent methods. The results of the bioinformatics and initial PCR testing I performed, for the purpose of this thesis work, are described in the following chapter (**Chapter III**).

Chapter III

EVALUATING VIBRIO PATHOGENICITY-RELATED GENES EVALUATING VIBRIO PATHOGENICITY-RELATED GENES WITH IN SILICO AND PCR APPROACHES

Virulence, or pathogenicity, factor genes in genomes of *Vibrio* are often important markers for the pathogenic potential of various *Vibrio* species and strains (Gutierrez West et al 2013). In *Vp,* the gene encoding the thermostable direct hemolysin (*tdh*) and its homolog, the thermostable direct hemolysin-related hemolysin (*trh*), are markers for virulence. The functions of *tdh* and *trh* are similar, in that these proteins embed in and disrupt human cell membranes, acting as toxic porins and altering cell membrane ion flux (Table 10). While the clinical symptoms of *tdh* and *trh* pathogenicity mechanisms present as diarrhea in mammals, infection may also begin with low-grade fever, advance to skin lesions, and/or lead to uncontrolled septicemia and death if left untreated (Jia et al 2010).

Though contested for its inconsistency, a positive result of the Kanagawa phenomenon is characterized by the presence of *beta*-hemolysin on Wagatsuma agar in a modified Elek test method (Honda et al 1980). Briefly, this method relies on an immuno-halo appearing around bacterial colonies on the plate, in which the immunogenic reagent applied to the plate is antihemolysin serum. When colonies contain actively expressed hemolysin genes, a "precipitation halo" around the hemolysin-positive colonies typically forms during an overnight incubation at 37˚C. The Kanagawa phenomenon test is usually validated by more precise and culture-independent (molecular) methods, a now common practice complementing culture-dependent assays.

Sequencing of conserved taxonomic marker genes, such as 16S, 23S, and *rpoA*, can help taxonomic identification of various *Vibrio* isolates, regardless of species, strain or pathogenicity status (Dalmasso et al 2009; Main et al 2015). However, these markers cannot be used in

screening for virulence, and thus cannot be used to reliably differentiate between pathogenic and non-pathogenic strains. Current primers that target virulence genes in *Vv* and *Vp* have not been reexamined in nearly a decade. In this study, published primers were reassessed and redesigned in hopes of addressing these limitations, aiming to ultimately produce more accurate methods for enumerating pathogenic *Vv* and *Vp,* including the first *Vv*-specific primer set for detection of *tdh*.

Table 10 Descriptions of *Vibrio* spp. hemolysin gene families of interest and each corresponding mechanism of pathogenesis

Gene	Species	Gene product (protein) name	Major mechanism(s) of pathogenesis
tdh	*Vp*	thermostable direct hemolysin	Increases permeability of host cell membranes, acts as toxic porins (cell lysis) (Narayanan et al 2020)
trh	*Vp*	thermostable direct hemolysin-related hemolysin	
vvhA	*Vv*	*Vv*-specific hemolysin	Kanagawa phenomenon positive: exhibits *beta*-hemolysis on Wagatsuma agar (Honda et al 1980)

Genes of interest for this study focused on those in pathogenic *Vv* and *Vp,* including *tdh, trh,* and *vvhA.* A 1999 study successfully defined and developed a 5’ nuclease probe-based qPCR method for quantifying *Vp* in oyster tissue homogenate (Bej et al 1999). When comparing to positive detection in pure culture strains, *trh,* but not *tdh,* was detected in one strain, suggesting assaying for both genes may be necessary to detect all hemolysin-producing strains of pathogenic (Bej et al 1999). Some published primer pairs also exist for detection and enumeration of *Vv* with qPCR forgoing the use of probes (Panicker et al 2004) relying solely on SYBR Green I fluorescence for detection of amplicon production during the course of the PCR (Malinen et al 2003; Rasmussen 2001). This method is more cost-effective than probe-dependent assays, and is a reliable method for the general use of pathogen detection (Aarts et al 2001; Malinen et al 2003; O’Mahony and Hill 2002; Rantakokko-Jalava and Jalava 2001).

Enumeration of *Vp* pathogenicity marker genes *tdh* and *trh* can be done with multiplex qPCR for detection and enumeration of total and pathogenic *Vp* (Nordstrom et al 2007). Multiplex methods use an internal amplification control (IAC), a nontarget DNA fragment that is simultaneously amplified with the target sequence, acting as a "standard" by accounting for potential PCR inhibitors that produce false negatives. However, multiplex methods require inclusion of multiple fluorogenic probes, such as "TaqMan" probes (Heid et al 1996). While TaqMan probes add a layer of specificity or sensitivity (Malinen et al 2003), developing or using probe-based methods is more costly (due to the need for a fluorogenic probe for each target amplicon) and more difficult in designing a third (probe) sequence that matches well to the gene sequence between the forward and reverse primers.

Pathogenicity target genes may appear to be present in species other than *Vp*. For example, *trh,* a target gene that was only reported to be present in *Vp* (Iida et al 1998) was found in what was later identified as *V. alginolyticus*, a near-neighbor species, suggesting a positive PCR result could be associated with presence of pathogenic *Vp* (González-Escalona et al 2006). More recently, the lineage of a newly evolved pathogenic *Vp* strain expanded its distribution along the North American Atlantic coast. It was dubbed as a new "sequence type," number 631 (ST631) that exhibited a similar virulence gene profile to members of a related ST36 clade, a group of *Vp* known to contain both *tdh* and *trh* (Xu et al 2020). Ergo, methods of detecting such highly adaptable pathogens need to be attuned often to accommodate the effects of a rapidly changing environment.

Pandemic *Vibrio* spp. have been detected in various aquatic environments as well. *Vp* strains positive for *tdh* and *trh* were identified in four cultured mollusk species on the Spanish Mediterranean coast (Roque et al 2009) and in natural mussel populations in coastal waters of

Chile (Bacian et al 2021). Similarly, in the lagoons of the French Mediterranean coast, temperature and salinity showed significant influence on the occurrence and distribution of pathogenic *Vibrio* spp. during short, but intense, autumnal freshwater flash floods (Esteves et al 2015). The 2015 study applied *tdh* oligonucleotide primers or qPCR detection of enteropathogenic *Vp* (Cantet et al 2013; Tall et al 2012;). Lower salinity favored growth and proliferation of pathogenic *Vibrio* detected with this particular qPCR method, especially in DNA samples from brackish waters. Temperature positively correlated with pathogenic *Vibrio*, specifically between 15 and 24˚C. This was the first report of *in situ* rapid proliferation following coastal flooding and a sudden decrease in salinity (Esteves et al 2015). Increasing global temperatures due to climate change portends an increase in frequency and/or intensity of heavy rainstorms, which could promote *Vibrio* abundance.

Using *in silico* techniques, I designed primers to be more specific to match well to known pathogenic groups of *Vv* and *Vp*. To refine previously published primers, for each gene, I created two separate multiple sequence alignments (MSAs) – one containing gene sequences known to be from DNA of clinical sources, and another from environmental sources (i.e., sequences of yet-uncharacterized pathogenicity). I retrieved various published primer sets and located their position within each alignment, at times altering nucleotide positions to better match to the pathogenic sequences, while maintaining distinctiveness from environmental sequences. Previously published primer pairs and cycling conditions can provide a starting point to screen DNA samples for positive signals and indicate whether or not *Vibrio* are present in the collected samples. However, some primer sets are limited and result in amplicons that are either too large [e.g., the 410 bp amplicon of *trh* (Gutierrez West et al 2013)] or match poorly to sequences of

currently known pathogens (Bej et al 1999). Aligning newer sequences from the NCBI database aids in creating new forward and reverse primers that abide by the following criteria:

a. accurately and specifically hybridize (i.e., anneal) to the target gene of interest at a temperature of least 55˚C (Waidner and Kirchman 2007; Waidner and Kirchman 2008);
b. are within 5˚C of one another (Breslauer et al 1986; Kibbe 2007; Sugimoto et al 1996);
c. do not require the addition of a third (e.g., "Taqman") probe, which can be costly (Heid et al 1996);
d. result in an amplicon no less than 175 bp and no greater than 275 bp for maximum amplification efficiency (Bustin and Huggett 2017).

Methods

Design of qPCR primers and cycling parameters

To make internal databases of nucleotide sequences containing the functional gene of interest from known pathogenic species [*tdh*, (*Vv* and *Vp*) *trh*, and *vvhA*], I subjected nucleotide sequences to the BLASTn algorithm (Morgulis et al 2008; Zhang et al 2018) and retrieved hits with the greatest percent nucleotide identity to the gene of interest. The following accession numbers were used as reference sequences: CP011885 for *tdh*, KU244684 for *trh*, and CP037932 for *vvhA*. Entries that denoted they had been isolated from a human or clinical source were termed "pathogenic" isolates. The rest of the sequences (typically indicating an ambiguous or environmental source) were dubbed "environmental" isolates. For each gene of interest, pathogenic and environmental sequences were aligned by codons in an MSA using the MUSCLE algorithm in the MEGA-X software (Kumar et al 2018), and their locations noted of each of the primers in the MSA. When warranted, nucleotides in the primer sequences were altered to better match to the pathogenic strains in the MSA, resulting in newly refined primer pairs (Table 11).

Table 11 Number key used to refer to primer pairs used in PCR

Primer Pair #	Primer Pair Name	*Reference*
1	TVP-vvhA-F1 / R2	*This study*
6	vvh L / R	*Panicker et al. 2004*
4	TVP-tdh-Vv-F2 / R2	*This study*
5	TVP-tdh-Vv-F1 / R1	*This study*
2	TVP-tdh-Vp-F2 / R2	*This study*
8	tdhF / R	*Nordstrom et al. 2007*
3	TVP-trh-Vp-F2 / R2	*This study*
7	trh F / R	*Nordstrom et al. 2007*
9	UtoxF / vptoxR	*Bauer & Rørvik, 2007*

DNA templates

Primers were tested in PCR on DNA samples obtained from pure cultures of *E. coli, Vv* and *Vp* type strains and from environmental sediment samples. Previously, an enumeration of *Vv* and *Vp* using culture-dependent methods was performed (Potdukhe et al 2021); a selection of DNA samples from these sediment samples were used for the PCR tests described here. DNA from a bacterium with presumably none of the virulence markers of *Vibrio* species was isolated from a recombinant *E. coli* containing a fosmid clone of a segment of environmental DNA (Waidner and Kirchman 2005). Representative pathogenic strains of *Vibrio,* ATCC® type strains of each *Vv* (#27562) and *Vp* (#17802), were each grown in pure culture on plates and in liquid media. Type strains were initially plated on Marine Agar (for 1 L: 1.0 g yeast extract, 5.0 g peptone, 35.0 g Instant Ocean® Sea Salt, 15.0 g agar) and incubated at 27˚C for 24 to 48 hours. Single colonies were inoculated into test tubes containing 5 mL of Difco™ Marine Broth (#2216). Liquid cultures of *Vibrio* and *E. coli* were incubated at 27˚C and 37˚C, respectively, with shaking at 100 RPM for approximately 16 hours. From each of the liquid growth cultures,

E. coli, Vv, and *Vp* cells were pelleted from 1.8 mL of culture by centrifugation at 12,000 x g for 5 minutes. After removal of the supernatant, the resulting pellets were stored at -20˚C until subsequent DNA isolation.

DNA extractions

Total genomic DNA was extracted from the three pure cultures and 42 sediment samples. For isolation of DNA from pelleted cells of each of the three pure cultures, the standard procedure of the GeneJet isolation kit for isolation of DNA from Gram-negative bacteria was performed. The DNA from each type strain of *Vv* and *Vp* DNA was eluted twice for maximum recovery of DNA from the purification column. The first elution (A) was with the standard 200 µL of elution buffer, and the second elution (B) was with 50 µL. Only one elution was performed during the DNA isolation from the recombinant *E. coli.* For isolation of DNA from the estuary sediment samples, I used a method specific for isolating DNA from microbes associated with soils and sediments (ZymoBIOMICS™ DNA Miniprep Kit, #D4300T, #D4300, & #D4304). In all extractions, DNA was eluted from the purification column by room-temperature incubation in a low-salt, but buffered, solution (either 10 mM Tris or $T_{10}E_1$), assayed by spectrophotometry, and aliquots were stored at -20˚C until use in PCR. A ThermoFisher Scientific NanoDrop™ 2000C UV/VIS Spectrophotometer was used to assess quality and quantity of DNA for use in PCR. Aliquots of all sediment DNA samples were diluted to 0.5 ng uL^{-1}, *E. coli* DNA was diluted to 0.5 ng/µL, and DNA of the *Vibrio* type strains was diluted to 1.0 ng μL^{-1} prior to use in PCR. For all 42 sediment samples, end-point PCR with the universal 16S rRNA primers BACT1369F & PROK1541R (Suzuki et al 2000) was performed with a 60˚C annealing temperature to qualitatively assess for PCR inhibitors (Fig 7).

Endpoint PCR

To assess presence or absence of *Vibrio*-specific genes in a subset of sediment DNA samples and DNA from pure cultures of *Vibrio* and *E. coli*, the oligonucleotide primer pairs listed in Table 11 were used in end-point PCR. The DNA of three of the February 2020 sediment samples were chosen because they were previously determined (Potdukhe et al 2021) to contain *Vv* at 3,702; 2,275; and 8,757 cells mL^{-1} of sediment, and *Vp* at 73, 325, and 0 cells mL^{-1} of sediment. Every end-point PCR was also performed with a no-template control (NTC), with molecular grade water added in place of a DNA template. Initial tests of the 16S primer pair BACT1369F & PROK1541R on the DNA of the type strains resulted in no amplicons (not shown), since the match of the 16S genes in these *Vv* and *Vp* strains with the reverse primer in the above-mentioned primer pair was poor. An alternate primer pair [BACT1369F & PROK1492R, (DeLong 1992)] was examined *in silico*, determined to match better to the 16S rDNA of the type strains, and used on all eight templates listed in Table 12.

Eight DNA samples were used as templates for all end-point PCR tests, including primer pairs for 16S rDNA (Fig. 8) and published and newly developed primer pairs for functional genes. All reactions were set up the same way, with each template used in 20-µL PCR reactions, each containing 1 µL of template DNA and 19 µL of Master Mix (molecular grade H_2O, 1X *Taq* Buffer with KCl (75 mM Tris-HCl, pH 8.8 at 25°C; 375 mM KCl; 0.01%, v/v; Nonidet P40), 2.5 mM $MgCl_2$, 0.16 mM dNTPs, 0.08 µM 16S rDNA primer mix (F&R), and 0.05U μL^{-1} *Taq* DNA Polymerase) (ThermoFisher Scientific). End-point PCR was run for 35 cycles of the following conditions: denaturation for 15 seconds at 94˚C, annealing for 30 seconds at the below-indicated annealing temperatures, and extension for 45 seconds at 72˚C. Reactions were then held at 72˚C for an additional 5 minutes, then cooled to 4˚C. One half volume of each of the reactions (10 µL)

were subjected to electrophoresis in 2.0% agarose gels containing 0.4 μg mL^{-1} EtBr and 1X Tris-acetate-EDTA (TAE) buffer. One lane in each gel panel contained GeneRuler 1 kb Plus DNA ladder (catalog # SM1331, ThermoFisher Scientific) to help estimate approximate sizes of PCR products and non-specific amplicons. The same templates, reagents, and conditions above were used for all primer pairs in this study (Table 12), with the exception of the annealing temperatures, which were chosen based on the calculated nearest-neighbor melting temperature estimated by the OligoCalc online tool (Kibbe 2007).

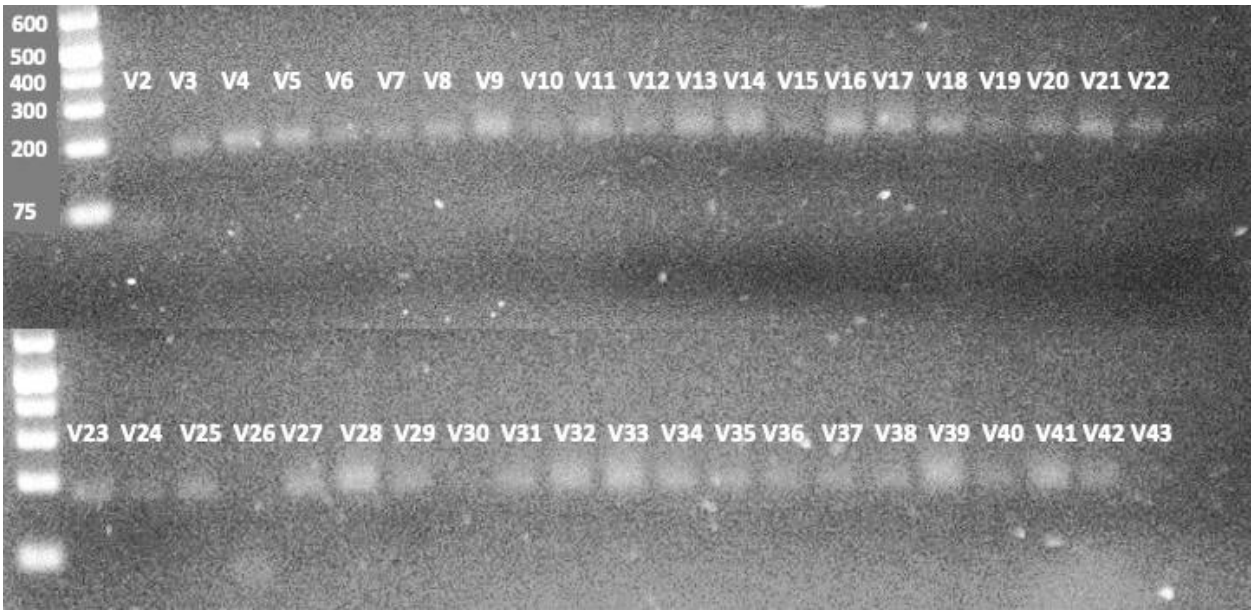

Fig. 7 Sediment DNA quality assessed by PCR amplification of a 192-bp portion of the SSU 16S rRNA gene. The universal primer pair, BACT1369F & PROK1541R (Suzuki et al 2000) was used in end-point PCR for 35 cycles. The first lane is GeneRuler 1 kb Plus DNA ladder (catalog # SM1331, ThermoFisher Scientific). Top panel: sediment samples V2-V22; bottom panel: sediment samples V23-43 (Potdukhe et al 2021)

Table 12 Gel electrophoresis results from all primers pairs used in end-point PCR reactions. Asterisk (*) indicates a band at the target amplicon size band was observed in a template expected to show a negative result

	Primer pair	*#1*	*#6*	*#2*	*#8*	*#3*	*#7*	*#4*	*#5*	*#5*	*#9*
	Annealing temperature	**60˚C**	**52˚C**	**60˚C**	**52˚C**	**57˚C**	**52˚C**	**57˚C**	**57˚C**	**60˚C**	**60˚C**
	Target amplicon size (bp)	**203**	**205**	**234**	**342**	**214**	**273**	**179**	**240**	**240**	**297**
	Target gene and species	***vvhA* (*Vv*)**	***vvhA* (*Vv*)**	***tdh* (*Vp*)**	***tdh* (*Vp*)**	***trh* (*Vp*)**	***trh* (*Vp*)**	***tdh* (*Vv*)**	***tdh* (*Vv*)**	***tdh* (*Vv*)**	***ToxR* (*Vp*)**
Template #											
1. Vv type A[a]		+	+	-	-	-	-	+	+	+	-
2. Vv type B[a]		+	+	-	-	-	-	+	+	+	-
3. Vp type A[b]		-	-	+	+	+	-	-	+*	-	+
4. Vp type B[b]		-	-	+	+	+	-	-	-	-	+
5. Sed 3A[c]		-	-	-	-	-	-	-	-	-	-
6. Sed 27A[c]		-	-	-	-	-	-	-	-	-	-
7. Sed 28A[c]		-	-	-	-	-	-	-	-	-	-
8. E. coli		-	-	-	-	-	-	-	+*	+*	-
9. NTC[d]		-	-	-	-	-	-	-	-	-	-

[a] duplicate DNA elutions of *Vp* type strain ATCC® #17802
[b] duplicate DNA elutions of *Vv* type strain ATCC® #27562
[c] sediment DNA extracted from samples obtained in **Chapter II** (Escambia County *Vibrio* Project)
[d] no-template control (NTC), in which the DNA template was molecular grade water

Results

Primer accuracy and specificity

For all four functional genes examined (*tdh, Vv*; *tdh, Vp*; *trh, Vp*; *vvhA, Vv*), the refined primer pairs presented in this study matched better to pathogenic sequences from the NCBI database than did previously published primers. The accuracy of this primer design was also informed by how well the primer matched to the corresponding gene sequence in the *Vv* and *Vp* type strains used here. Out of the total 16 primers designed, only one did not match exactly to the corresponding sequence of its respective type strain, whereas 18 of the 24 previously published sequences did not match to its type strain (Appendices A-D).

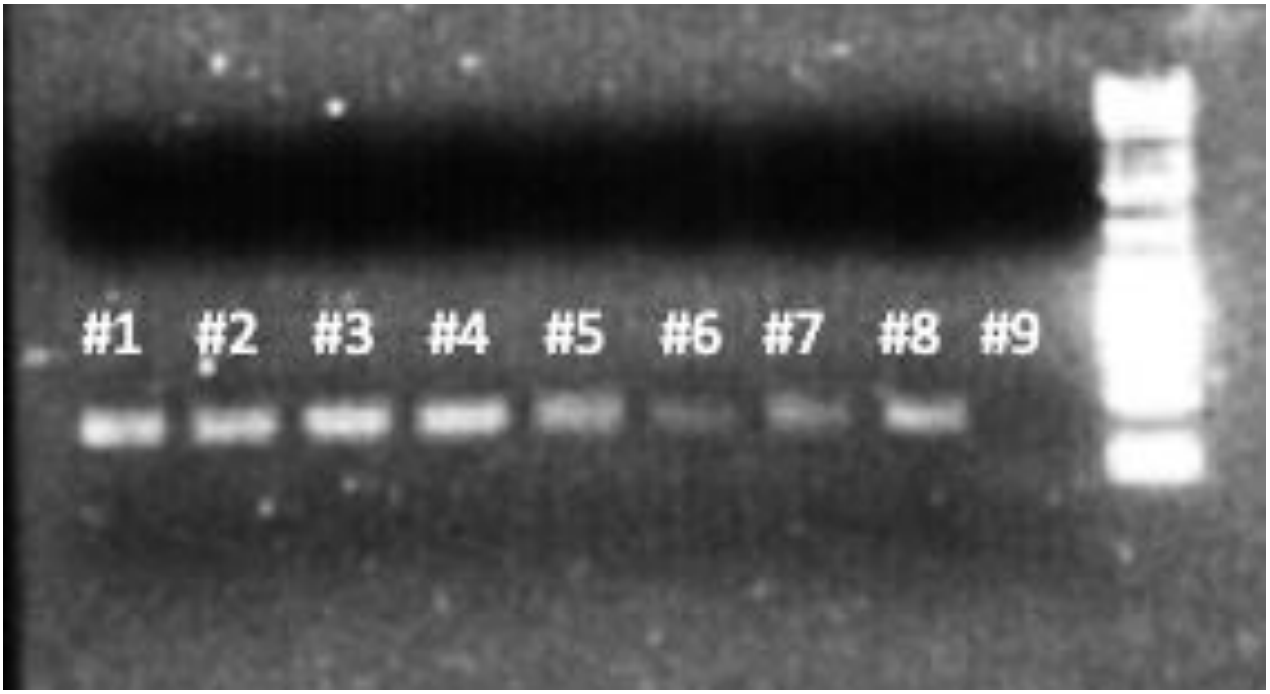

Fig. 8 Partial SSU 16S rDNA gene product amplified in end-point PCR. The universal primer pair (target amplicon size ~180 bp) BACT1369F & PROK1492R was used as previously described (DeLong 1992)

Primer efficacy

To verify the quality of DNA samples to be used in functional gene tests, eight DNA samples were subjected to PCR amplification with a universal SSU 16S rRNA primer pair (Fig. 8). PCR amplification with these primers resulted in a product of the expected size (~180 bp) from all samples, and these same templates were used in all end-point PCR tests described below. In all figures shown here, the images of the agarose gels are marked with template DNA numbers as indicated in Table 11, where amplicons of the expected sizes are observed.

Expected results were obtained from the reactions containing new pathogenic *Vv*-specific primers for a portion (203 bp) of the *vvhA* gene (Fig. 9, left panel). PCR with the newly designed primer pair yielded faint ~250 bp bands in reactions with *Vv* DNA elutions A and B. Additionally, PCR with this pair resulted in non-specific amplicons (~70 bp) for most of the eight total DNA samples used. PCR with a published primer pair for *vvhA* (Panicker et al 2004), primer pair #6, resulted in more intense, correctly-sized amplicons with both elutions of the *Vv* type strain. However, as with amplification in tubes containing non-*Vv* DNA samples, PCR resulted in substantial non-specific amplification of a ~70-bp fragment.

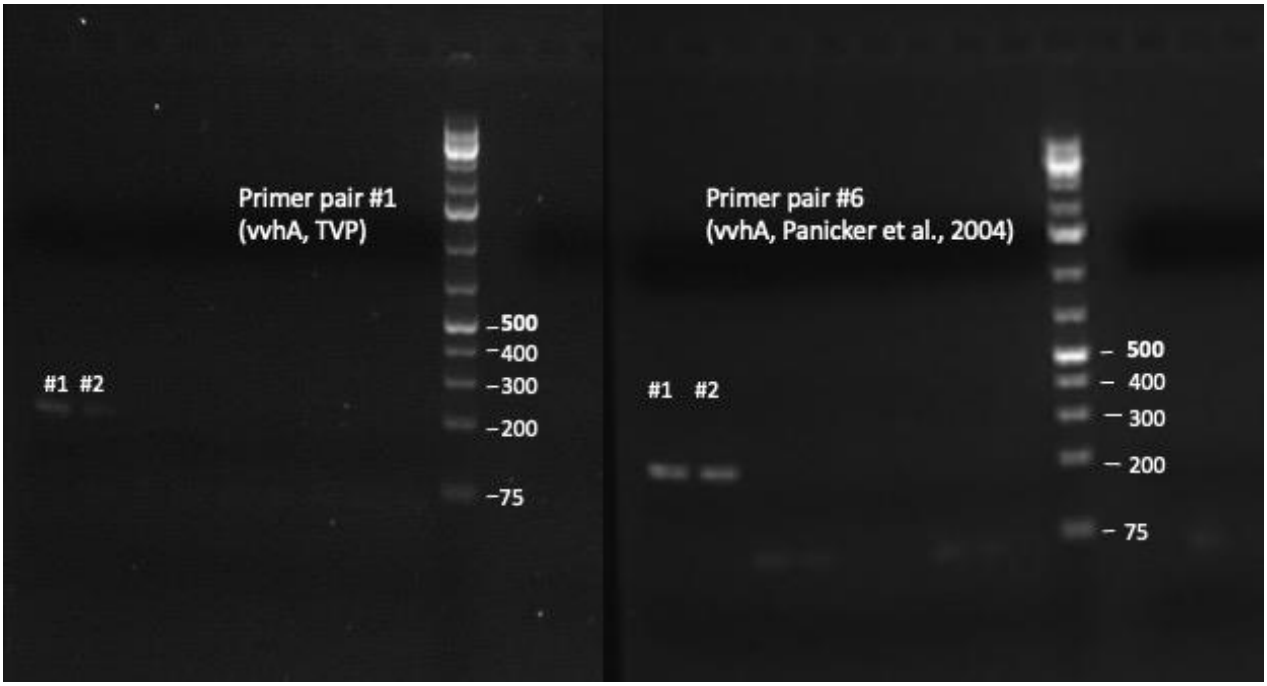

Fig. 9 PCR products of primer pairs targeting *vvhA* in *Vv.* Left panel: *vvhA*-specific primer pair #1 designed in this study, target amplicon size 203 bp. Right: published primer pair (Panicker et al 2004), target amplicon size 205 bp

Primer pairs #2 and #8 (Fig. 10) targeted *tdh* in *Vp*. Both the previously published (Nordstrom et al 2007) and newly designed primer pairs yielded PCR products at the target amplicon size for both elutions of the target species (*Vp*). Amplification with both *tdh* primer pairs resulted in only expected-sized fragments, with no detectable non-specific amplification. A larger-than-expected amplicon size may be due to discrepancies related to forward and reverse primer pairs overlapping –expected amplicon size determined from *in silico* methods may have been different from actual amplicon size.

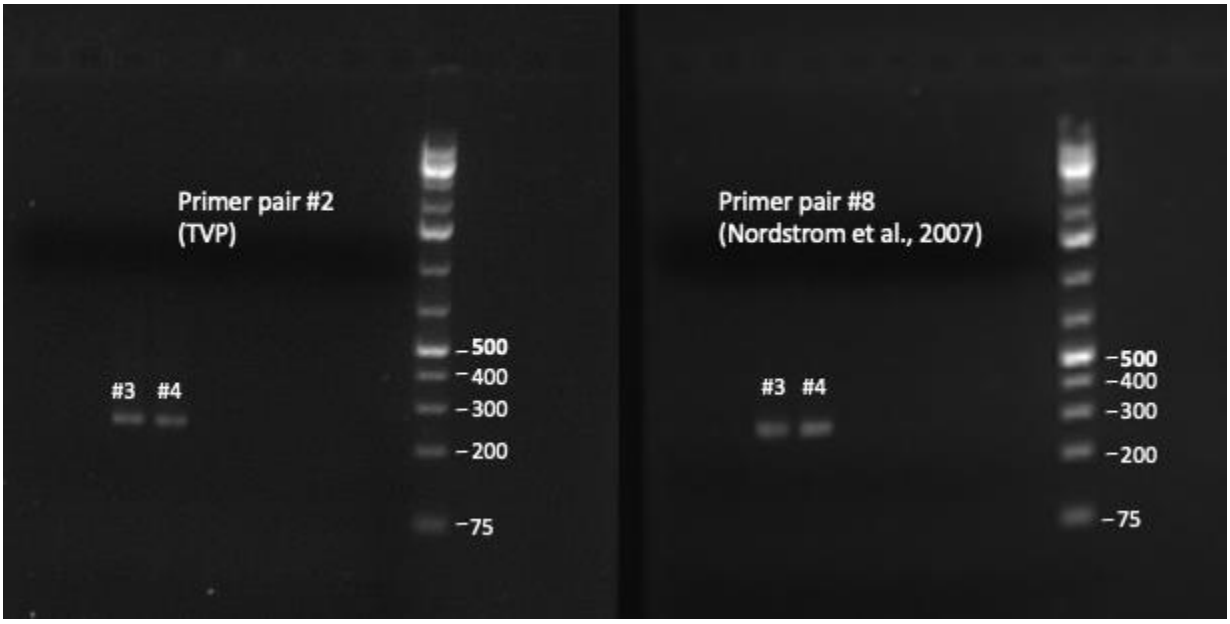

Fig. 10 PCR products of primer pairs targeting *tdh* in *Vp*. Left panel: primer designed in this study, target amplicon size 234 bp. Right: published primer (Nordstrom et al 2007), target amplicon size 342 bp

PCR products from newly designed primer pair #3 and previously published primer pair #7 (Nordstrom et al 2007), both of which targeted *trh* in *Vp*, are shown in Fig. 11. PCR with the new primer pair #3 yielded fragments at the target amplicon length for elutions A and B of the target species (*Vp*) with no non-specific amplification, whereas PCR using the published primer pair did not result in any PCR products other than non-target amplification ~75 bp. A larger-than-expected amplicon size may be due to discrepancies related to forward and reverse primer pairs overlapping –expected amplicon size determined from *in silico* methods may have been different from actual amplicon size.

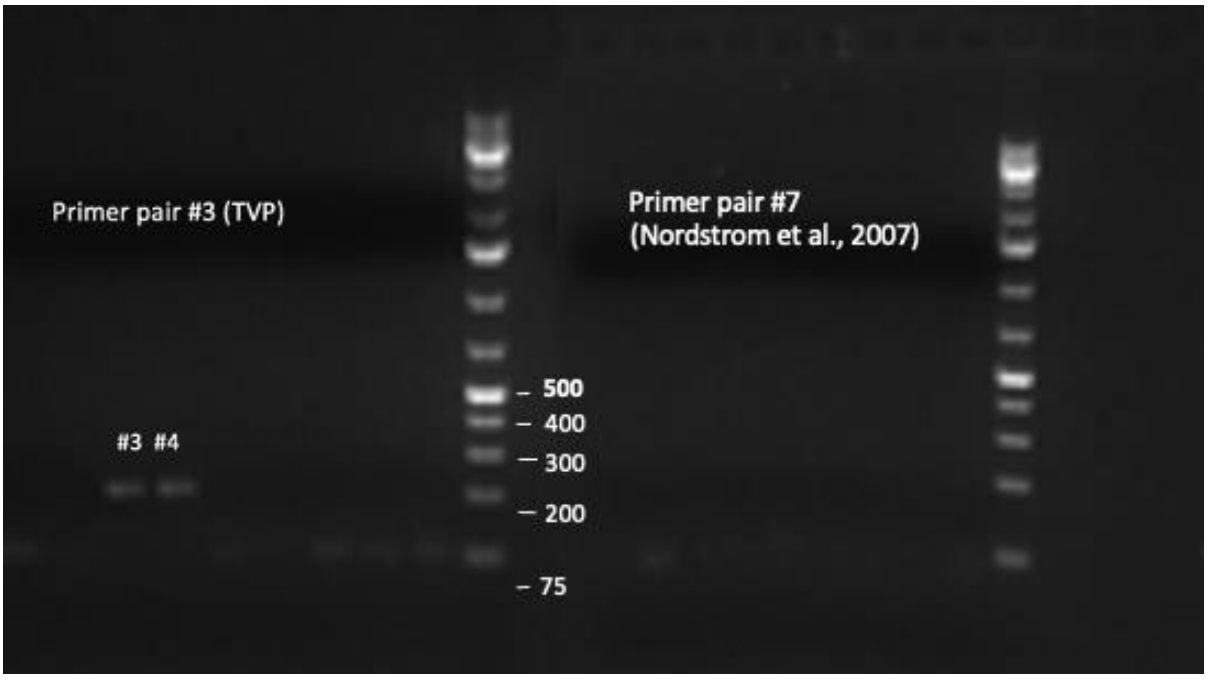

Fig. 11 PCR products of primer pairs targeting *trh* in *Vp*. Left panel: primer designed in this study, target amplicon size 214 bp. Right: published primer (Nordstrom et al 2007), target amplicon size 273 bp

Newly designed primer pair #4 was used to target a novel *Vv*-specific *tdh*, an otherwise *Vp*-specific gene. PCR amplification resulted in gene products for elutions A and B of the *Vv* type strain DNA. Primer pair #5, also a *Vv*-specific *tdh* primer pair, did not follow suit (Fig. 13). Primer pair #5 was initially subjected to PCR reactions at a 57˚C annealing temperature. An amplicon was observed for a *Vp* type strain and the *E. coli* template, neither being target species. Additionally, there was substantial non-target amplification at the ~75 bp length. Primer pair #5 was rerun at 60˚C annealing temperature. The product for *Vp* did not show this time, however *E. coli* still showed a band at the target amplicon size.

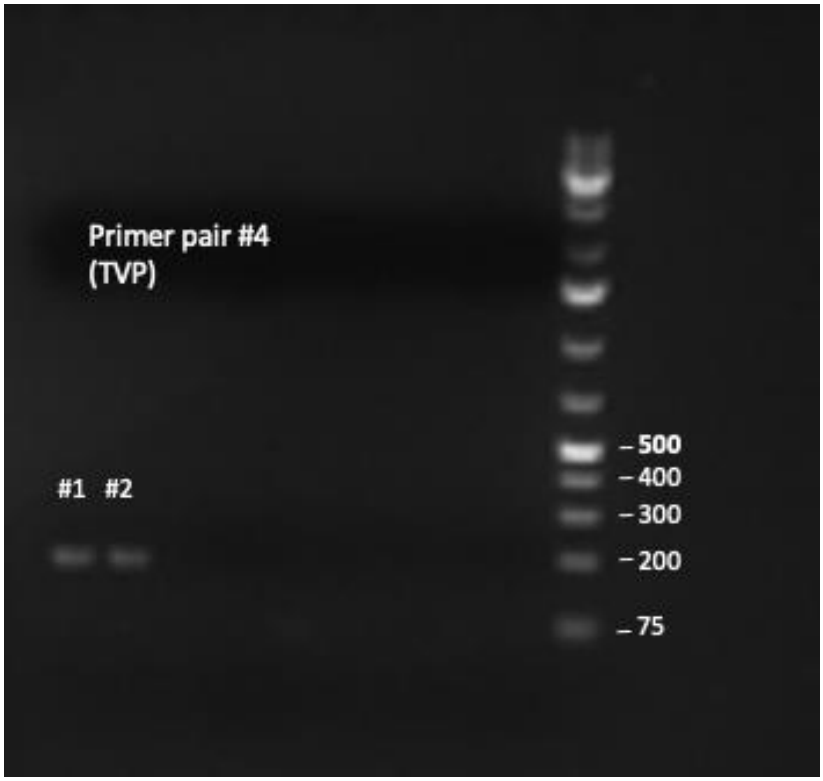

Fig. 12 PCR products of newly designed primer pair #4 targeting *tdh* in *Vv*, target amplicon size 179 bp

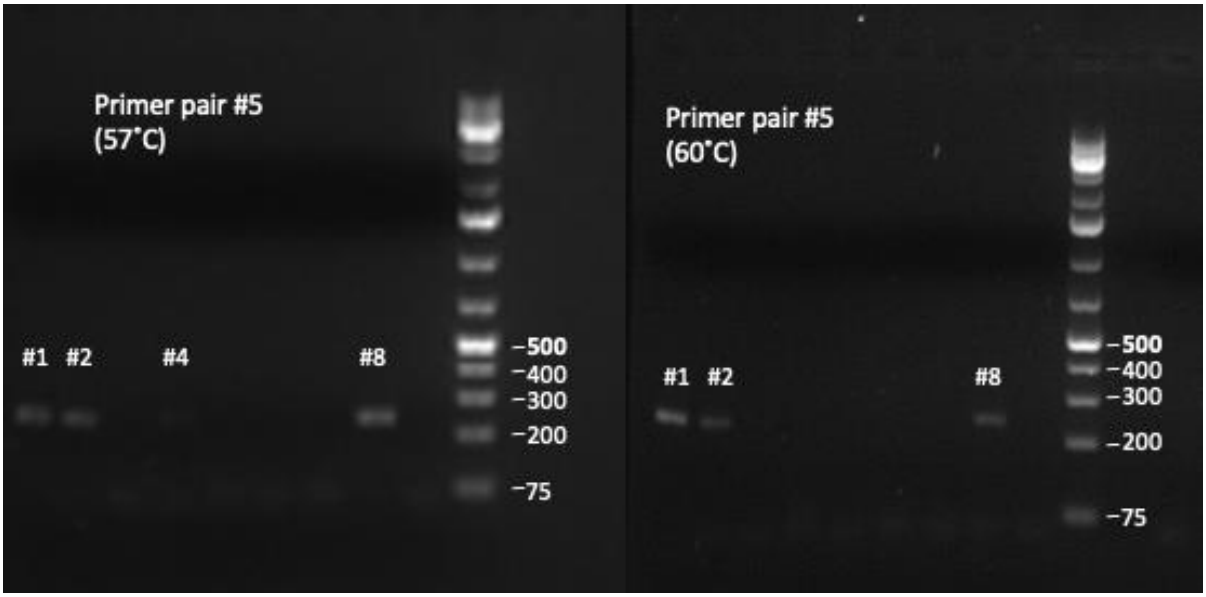

Fig. 13 PCR products of newly designed primer pairs targeting *tdh* in *Vv* subjected to PCR at 57˚C (left) and 60˚C (right) annealing temperatures

Previously published primer pair #9 was designed to target *ToxR* in *Vp* (Bauer and Rørvik 2007). Although there was non-target amplification at the ~75 bp band, there were also PCR products observed for both elutions of the *Vp* type strains (Fig. 14). A larger-than-expected amplicon size may be due to discrepancies related to forward and reverse primer pairs overlapping –expected amplicon size determined from *in silico* methods may have been different from actual amplicon size.

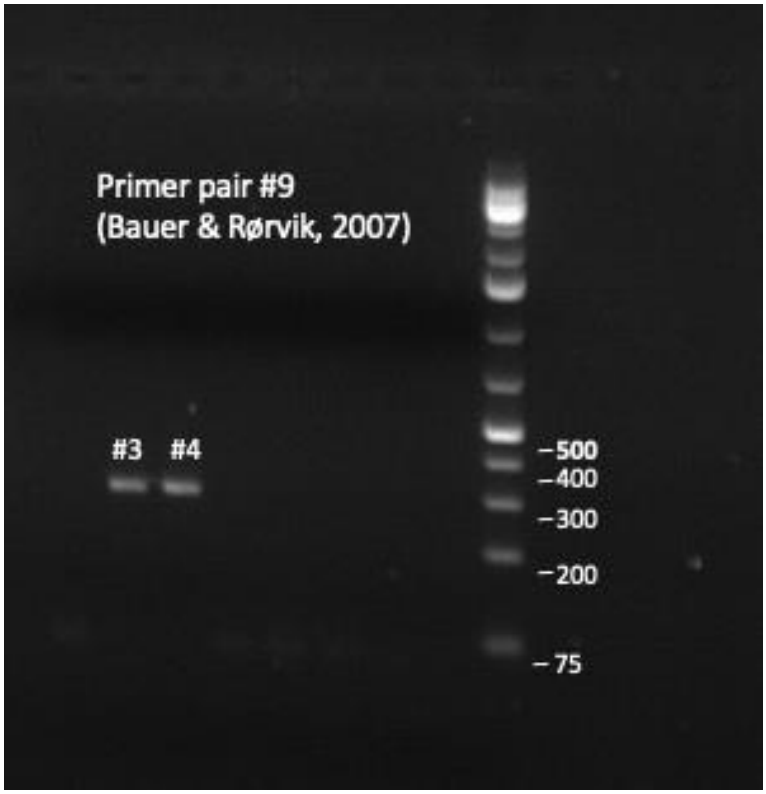

Fig. 14 PCR products of previously published (Bauer and Rørvik 2007) primer pair targeting *ToxR* in *Vp* with an expected amplicon size of 297 bp.

Discussion

Previously published vs. newly designed primers

Hemolysin genes *trh* and *tdh* are the most commonly-employed virulence (and at times, taxonomic) markers of *Vp*. In our hands, PCR with *trh* primer pair #7, a published method (Nordstrom et al 2007), did not result in amplification from any of the eight DNA templates tested, except for non-target amplification at ~75 bp in all lanes. The new *trh* primer set here (#3) did result in non-specific PCR amplification at ~70 bp, but also showed the intended amplicon size for the target species (*Vp*). This new primer set was acceptable, in that gene products at the target amplicon length were observed, but the percent match to pathogenic sequences in the NCBI database was relatively low (forward primer, 63%; reverse primer, 46%) compared to general percent match to the various other gene-markers primers presented here, which were upwards from ~90%. It may be worth reexamining this primer design, or perhaps exploring additional published primer sets. For example, another study (Gutierrez West et al 2013) designed a primer set for *trh* based on the *Vp* type strain used in this study (ATCC® #17802), and both primers exactly matched this strain's *trh* sequence. Furthermore, this primer pair showed a 100% match to all 24 pathogenic strains in the *trh* MSA made for this study. Based on these data, this third proposed primer set shows promise to be used in qPCR for specific detection of pathogenic *Vp*.

Most notably, separate *Vv*- and *Vp*-specific *tdh* primers were effectively delineated and targeted in each type strain. New primer pair #2 (*tdh*) was specific to *Vp* and resulted in low non-specific amplicons from PCR amplification. These results were similar to those of published primer set #8 (Nordstrom et al 2007). Admittedly, there are two minor but notable advantages the new primers may have over the published ones: i) match to the *Vp* type strain, and ii) percent

match to other known pathogenic sequences in the MSA's produced for this study. The published primers did not seem to match any of the pathogenic sequences extracted from the NCBI database, whereas the new primer pairs were designed to match them very well (forward primer, 100%, reverse primer: 97%). Considering the absence of non-target amplification for both primer sets, one is not objectively better than the other, and would therefore be considered equally sound choices to use in PCR. However, when considering *tdh* in *Vv*, new primer pair #4 was highly accurate in detecting both replicates of the *Vv* type strain and neither of the *Vp* replicates, with little to no non-specific amplification in any of the lanes, including the NTC. The primer set proposed here is an excellent tool that can be used for detection of *tdh* as a virulence gene marker specifically in *Vv*.

Most of the small amplicons (~50-100 bp) due to non-specific amplification observed in primer pairs #3 (*trh*), #5 (*tdh*), #6 (*vvhA*), #7, and #9 (*ToxR*) are likely due to off-target binding of the forward primer, the reverse primer, or both, wherein the binding could have occurred anywhere within the thousands of genes or non-coding DNA regions present in these samples, even in the no-template control sample, that can contain trace amounts of contaminating *E. coli* DNA from the Taq DNA polymerase enzyme (see below). In all these cases, it is impossible to predict where the primer(s) bound in an off-target manner, but we do know that, in the NTC reactions, non-specific binding was within *E. coli* DNA, because in these samples, the only DNA present was trace amounts of *E. coli* DNA could have originated from the *Taq* DNA polymerase. This brings more validity to the presentation of these novel *Vv*-specific *tdh* gene primers.

Additional considerations

Often, non-specific amplification is observed in end-point and qPCR and can confound qPCR conclusions (Ruiz-Villalba et al 2017). Therefore, we must carefully evaluate each primer pair in end-point PCR for possible non-specific amplification, before using these primer sets in qPCR. Poor annealing of primers to template DNA is another common primer design issue that may involve non-target artifacts, one which can be caused by a variety of factors. Increasing annealing temperatures can decrease sensitivity but increase specificity for only intended target DNA sequences (Jansson and Hedman 2019; Roque et al 2009). However, caution must be used in decreasing the annealing temperature to increase sensitivity, since annealing at lower temperatures will possibly give way to false positives of the correctly-sized amplicons or of lower sized products from off-target amplification (Ruiz-Villalba et al 2017). Examples of this were seen in PCRs with primer pair #5, a *Vv*-specific primer, which when run at 57˚C annealing temperature, showed a false positive PCR product for one replicate of the *Vp* type strains and no non-specific amplification in the lane with *E. coli*. Increasing the annealing temperature to 60˚C resulted in the disappearance of the untargeted *Vp* band but with more non-specific amplification, including in the *E. coli* lane, where the target gene product was observed. This was likely due to the high G-C% content of primer pair #5 (F, 57%; R, 61%). Another cause for poor annealing properties is designing primers with more than three guanines (G) or cytosines (C) at the 3’ end. This configuration of repeating characters significantly decreases the binding capacity, potentially causing “slippage” and preventing proper annealing at the 3’ end (Ruiz-Villalba et al 2017; Shinde et al 2003). On a similar note, high G-C% content of the primer can affect primer binding ability to DNA at a given temperature. Since there are three bonds between G and C, and only two bonds between adenine and thymine, G-C% content is a primary

determinant of primer melting/annealing temperatures (Kibbe 2007). This phenomenon was observed in *vvhA* and analyzed here.

Hemolysin gene *vvhA* is unique, in that it can act both as a virulence-marker and is species-specific for *Vv*. The newly designed *vvhA* primer set (#1) correctly amplified the *Vv* type strain used in this study (ATCC® #27562). Since there was some non-target amplification at ~75 bp, in all lanes, including the NTC, this suggests either that there was contamination of extraneous DNA or the remnant *E. coli* originally present in *Taq* polymerase (Koponen et al 2002; Spangler et al 2009) was picked up and amplified by the primer, thus producing an amplicon at that an arbitrary region that happened to match the primer sequence. For primer pairs #1 and #2, the target template DNA did result in PCR products at the target amplicon length, though all bands were very faint and difficult to decipher. This could have been due to the design of the primer sequence, which was designed with "CCC" at the 3' end (Appendix A) and may have caused "slippage," resulting in fewer DNA templates being amplified. Similarly, the G-C% content was much higher in the designed primers than in the published primers, which likely compromised the primer specificity. Despite the presence of faint bands, the template DNA was successfully amplified, thus these primers proved more effective than the published primer pair that yielded intense bands with ample non-specific amplification.

While primer dimerization may explain the presence of non-target artifacts, these artifact bands all had molecular weights just below or around the 75-bp mark. Thus, the non-target fragments of this length could not have been due to primer dimerization. Only very long primers (greater than 38 bp long), annealing to each other at the extreme 3' ends of both forward and reverse primers, would yield an amplicon at 75 bp. Rather, these non-target products result from primers binding non-specifically to trace amounts of *E. coli* DNA that was present in the *Taq*

Polymerase prior to PCR (Koponen et al 2002). *Taq* polymerase, acquired from the bacterium ***T****hermas* ***aq****uaticus,* is often gene-transformed and subcloned into laboratory strains that are easy to manipulate, grow, and induce for protein production, most often in a genetically-engineered strain of *E. coli*. Most commercial Taq DNA polymerase enzyme preparations contain trace amounts of *E. coli* DNA, due to the recombinant nature of these enzyme manufacturing practices. Though the polymerase production process is designed for enzyme purification that captures the over-expressed protein on a protein-specific purification column, residual *E. coli* DNA remains with the protein, leaving the *Taq* inevitably "contaminated" with unwanted DNA (Koponen et al 2002; Spangler et al 2009).

Future directions

Though present in most all pathogenic strains, *Vp*-specific *tdh* and *trh* are relatively rare in "environmental" isolates (Theethakaew et al 2013). These "environmental" strains may very well be human pathogens and may have potential to cause vibriosis, but since they were not directly collected from an infected individual, the status of each is uncertain. The nature of environmental isolates validates the need for additional molecular analyses, so to specify virulence gene expression of non-clinical isolates, and not just determine its presence or absence.

The primer pairs from this study were tested and proven to be robust and sensitive tools for detecting pathogenic *Vv* and *Vp* at the species level. The *Vv*-specific *tdh* primer pair presented here is the first of its kind, with excellent nucleotide similarities of both primers to i) sequences from known pathogens submitted to the NCBI database and ii) the sequence from a known culturable pathogenic *Vv* strain. These *in silico* and preliminary end-point PCR data serve as a foundation on which to take future efforts examining environmental samples for enumerating potentially pathogenic *Vv* and *Vp* strains.

Chapter IV

DETERMINING THE IN VITRO ECOLOGY BETWEEN VIBRIO SPP. AND KARENIA BREVIS IN SOUTHWEST FLORIDA BAYS AND WATERWAYS

Phytoplankton comprise the largest group of oceanic primary producers (Buchan et al 2014), forming the very foundation of the aquatic trophic food chain. Harmful phytoplankton, however, can impose on ecosystem function if "bloom" status is reached. *Karenia brevis* (*Kb*), in particular, is the dinoflagellate species responsible for one of the most common harmful algal blooms (HABs) in the Gulf of Mexico: Florida red tide. In southwest Florida, *Kb* blooms can reach densities between 10^4 to $>10^6$ cells L^{-1} (Brand and Compton 2007). *Kb* is often of major concern because of its production of potent neurotoxins and hemolytic toxins, or more generally termed brevetoxins. Typically considered a stress response, the release of these types of toxins causes large fish kills, and negatively affects larger nekton and marine mammals with acute negative effects (Bercel and Kranz 2019). Brevetoxins can become airborne and aerosolized, potentially causing respiratory distress and sinus infection in humans recreating or living near the affected body of water; those predisposed to breathing difficulties are most at risk for developing these symptoms. When *Kb* cells die, brevetoxin is released when the cell membrane ruptures. Depending on the initial size of the bloom, the brevetoxin can cause fatalities in marine life up to a 16-kilometer away (Fire et al 2021).

Kb cytolysis may remove attached bacterial host cells (Mayali et al 2007; Roth et al 2008), particularly algicidal bacteria, or bacteria that cause death in algal cells like *Kb*. Algicidal bacteria have a wide geographic and spatiotemporal range, versatile metabolisms, and in some cases, can resist protistan grazing (Kirchman et al 1984; Zou et al 2020). Additionally, heterotrophic bacteria are principal agents in aquatic nutrient regeneration, a process which promotes conditions for a bloom event, another potential explanation of this coincidence (Vargo

2009). As metabolically versatile, opportunistically-pathogenic facultative anaerobes, ecological dynamics of *Vibrio* bacteria often mirror those of HAB species. Both are often seasonally driven, and optimal environmental conditions are similar (i.e., nutrient-rich, warm waters, in meso- to halophilic salinities, etc.) (Diner et al 2021). This commonality suggests that bacterial and algal species may thrive in co-existence, which may even extend to the potential for algicidal properties in *Vibrio* species. Since both *Kb* and algicidal bacteria are often present in naturally-occurring microbial communities, bacterial algicides may have potential as safe and effective HAB mitigation tools (Buchan et al 2014; Doucette et al 1999; Hare et al 2005; Heil and Muni-Morgan 2021; Roth et al 2008). Conversely, in the Great Bay Estuary, both chl *a* concentrations (proxy for phytoplankton biomass) and nutrient concentrations were poorly associated with *Vp*-plankton dynamics (Urquhart et al 2016). Another study noticed that there was no apparent interaction between toxic dinoflagellates and *Vibrio* spp. in bivalve larvae upon release of their respective toxins (De Rijcke et al 2016). Considering these disparities in *Vibrio-Kb* dynamics, few studies directly address interactions between *Vibrio* and *Kb* in aquatic ecosystems, much less potential algicidal capabilities.

In this study, I address *Vibrio-Kb* relationships in lab culture experiments by examining the interactions between *Kb* cultivated from southwest Florida blooms and type strains of *Vv* and *Vp*. The presence, if any, of algicidal activity in pathogenic *Vv* and/or *Vp* was tested by comparing observations of *Kb* growth in the absence and presence of *Vibrio* type strains. The null hypotheses for this study were that i) *Kb* had no effect on culturable viability of *Vv* or *Vp* type strains, and that ii) neither of the two *Vibrio* type strains influenced *Kb* viability.

Methods

Algal culture experimental setup

In the summer of 2021, a large, 10-L carboy of whole seawater from the New Pass Dock at Longboat Key (Sarasota Bay, FL, USA) was collected and transported by interns from the Main Campus of Mote Marine Laboratory; these samples contained concentrations of *Kb* that were representative of a *Kb* bloom, in which algal abundances were up to 3 x 10^7 cells L^{-1} (FWC 2021). These *Kb* cultures were divided into 2-L glass bottles or flasks and diluted with *f*/2 sterile algal liquid medium for 1 L: 70.0 g Instant Ocean® Sea Salt, 1.0 g Tris, pH adjusted to 8.00 ± 0.05 using 6M HCl, 2.0 mL *f*/2 vitamins, 2.0 mL trace metals, 2.0 mL $NaNO_3$, 2.0 mL NaH_2PO_4) (Guillard and Hargraves 1993). The diluted algal cultures were grown at 21˚C in a diurnal incubator under a 12:12 light regime. Cells were harvested at early-exponential phase, or when concentrations were ≥10^4 cells L^{-1} (as determined by microscopy), typical of *in situ* abundances during high bloom conditions (Brand and Compton 2007).

Bacterial inoculation setup

Stock solutions of type strains *Vv* (ATCC® 27562™) (Reichelt et al 1976) and *Vp* (ATCC® 17802™) (Fujino et al 1965) were each streaked onto modified Marine Agar (for 1 L: 1.0 g yeast extract, 5.0 g peptone, 35.0 g Instant Ocean® Sea Salt, 15.0 g agar), and plates were incubated at 26˚C for 24 – 36 hours. A single colony was used to aseptically inoculate a 100-mL flask containing a nutrient-enriched dinoflagellate-bacterial liquid growth medium (250 mL of *f*/2, 0.16 g peptone, 0.16 g yeast extract, 0.16 g casamino acids) (Provasoli et al 1957). The inoculated broth was incubated at 26˚C on a rolling drum at 120 RPM for 24 – 36 hours, until turbid. Cultures were then harvested to be pelleted; each *Vv* and *Vp* cultures were centrifuged in at 5,550 x g for 5 minutes, and the supernatant was poured off. Centrifugation and wash steps

were repeated, and the resulting pellet was resuspended once more in 5 mL of *f*/2 media. Using an OD600 DiluPhotometer™ (Implen©), absorbance readings of ~0.669 equate to approximately 10^6 cells mL^{-1}. Using *f*/2, bacterial cultures were serially diluted to 10^6 cells m^{-1}, then subsequently diluted 1:99 twice, to a final concentration of 10^4 cells mL^{-1}. These bacterial concentrations are possibly higher than the concentrations expected in nature, where total bacterial communities are at abundances of approximately 10^6 cells mL^{-1} (Fig. 20) (Kirchman 2018). In subtropical estuarine or coastal waters of Florida, anywhere from <0.01% to >1% the total bacteria community can be comprised of *Vibrio*, with culturable *Vv* or *Vp* abundances as high as 4,000 – 9,000 CFU mL^{-1}, respectively. However, for the purposes of this controlled experiment, the same loads of each algal and bacterial species were mixed in a controlled co-culture, with abundances chosen to reflect naturally-occurring abundances of the algal species during which blooms occur.

Assay preparation

To assemble the co-cultures for the assay, I assembled five different flasks: two co-cultures containing a 1:1 (v/v) ratio of the bacteria (*Vv-Kb* and *Vp-Kb*, respectively) with the *Kb* to arrive at equal concentrations. I prepared three controls by combining each *Vv*, *Vp*, and *Kb* with *f*/2 in a similar manner (1:1, v/v), resulting in three cultures, with each species at a final concentration of 10^2 cells L^{-1} *Vv-Kb* and *Vp-Kb* in each flask (*Vv-f*/2, *Vp-f*/2, and *Kb-f*/2). The five total cultures (two bacterial controls *Vv- f*/2 and *Vp- f*/2, two co-cultures *Vv-Kb* and *Vp-Kb*, and one algal control *Kb- f*/2) were subsequently distributed into the 48-well plates. In a sterile 48-well non-tissue culture plate, 1 mL of phosphate-buffered saline was distributed into the 12 lateral wells (six on each side), acting as a barrier, and preventing the interior samples from evaporating. The remaining 36 wells were divided into four quadrants, each representing one

timepoint. Nine wells in total were allocated per timepoint, with each of the three treatments in triplicate: three wells of bacterial culture, three wells of the algal culture, and three wells of the algal-bacterial co-culture. Well allocation was randomized using a random number generator (Fig. 15). Plates were incubated at 21˚C under a 12:12 light regime for 14 days (Fig. 16).

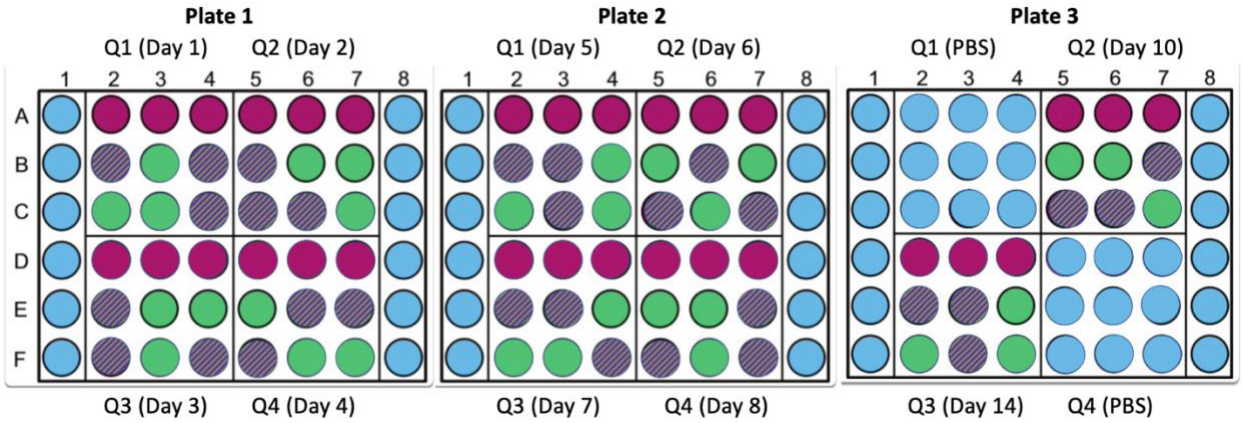

Fig. 15 The 48-well microassay design as previously described (Bramucci et al 2015). Blue, phosphate-buffered saline; purple, *Vibrio* (either *Vp* or *Vv*); green, *Kb*; dashed, *Vibrio-Kb* co-culture, (v/v, 1:1)

Sample collection

Every 24 hours, bacterial cells were quantified as colony forming units (CFUs) L^{-1} on thiosulfate-citrate-bile salts-sucrose agar (TCBS) (CRITERION™, Hardy Diagnostics, Santa Maria, CA). Dilutions of 1-, 2-, 3-, and 4-log fold were plated for each timepoint. After ~24-36 hours of incubation, average CFUs L^{-1} were enumerated from a plate that most closely resembled 30-300 CFUs. Average CFUs L^{-1} were calculated for bacterial controls (*Vv- f*/2 and *Vp- f*/2) and algal-bacterial co-cultures (*Vv-Kb* and *Vp-Kb*). *Kb* cell viability was determined for relative fluorescence units (RFU) using an *Aqua*Fluor® Handheld Fluorometer/Turbidimeter (Turner Designs, Inc., San Jose, CA) using EPA method 445.0. *Kb* concentration (cells L^{-1}) was determined *via* microscopy using a Nanogeotte Counting Chamber, (catalog #4000, Hausser

Scientific, Horsham, PA), using Utermöhl's solution to stain for viable cells where algae was present – the algal control (*Kb- f*/2) and the two algal-bacterial co-cultures (*Vv-Kb* and *Vp-Kb*).

Statistical analyses

To determine evidence for a significant difference among algal and bacterial concentrations between the control and co-culture treatments, I used a one-way analysis of variance (ANOVA) test with repeated measures to calculate *F* statistics. For *Kb* growth, I performed two ANOVAs per trial: i) *Kb-Vv* vs. *Kb-f*/2 and ii) *Kb-Vp* vs. *Kb-f*/2, totaling 4 ANOVAs. For *Vibrio* growth, I performed an ANOVA comparing i) *Vv-Kb* vs. *Vv-f*/2 and ii) *Vp-Kb* vs. *Vp-f*/2 per trial, totaling two Vv ANOVAs and two Vp ANOVAs. A total of eight ANOVAs for all four trials and four different treatments were used to report *F* values that showed strong evidence ($p < 0.05$) for a significant difference between treatments.

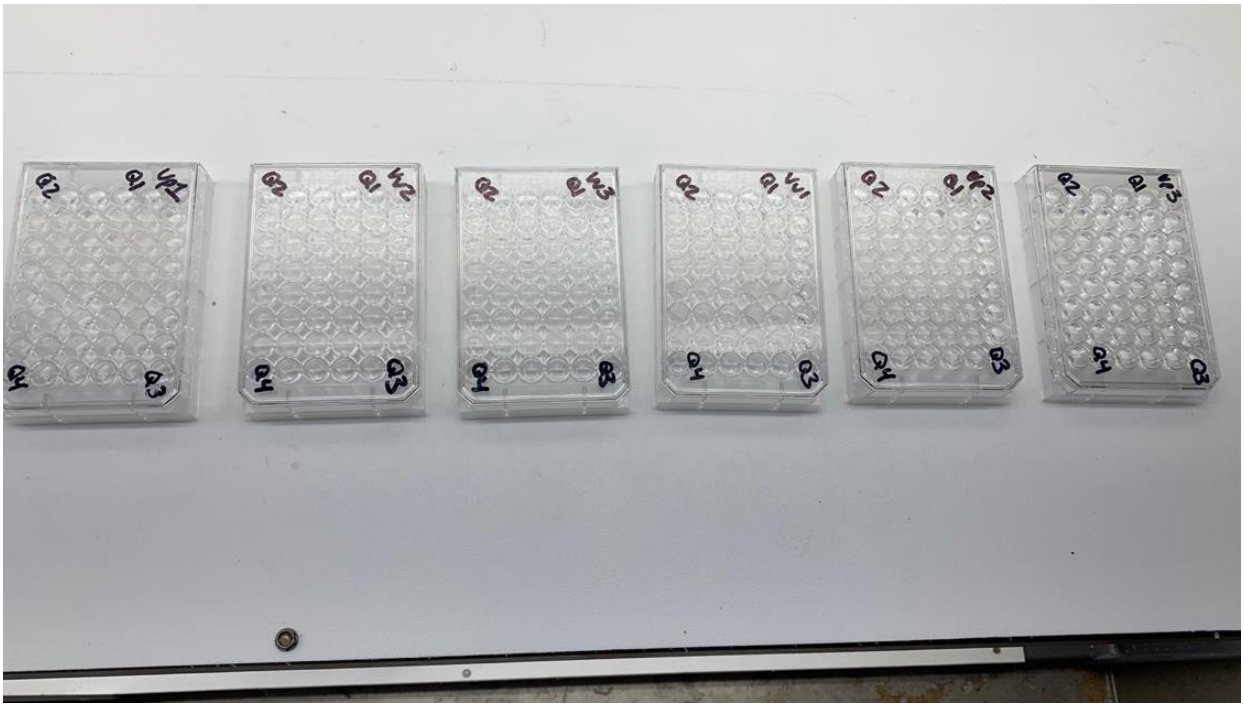

Fig. 16 Set-up of 48-well co-culture assay apparatus. Three plates per species for the 14-day experiment (10 total timepoints)

Results

Preliminary growth trial for harvest

To determine times to harvest exponentially growing *Vp* (*Vv* data not shown), a 12-hour growth curve was performed. Because of the variation among spectrophotometers, this extra step was used as a "standard curve" to confirm that an OD_{600} reading of ~0.669, or 0.03 on the DiluPhotometer, which requires a dilution factor of 20 corresponded to approximately 10^6 CFU L^{-1}. The culture was grown in modified Marine Broth and incubated at 27˚C on a rolling drum at 120 RPM. Abundance was monitored hourly by absorbance readings. Stationary phase was attained approximately ten hours post incubation (Fig. 17).

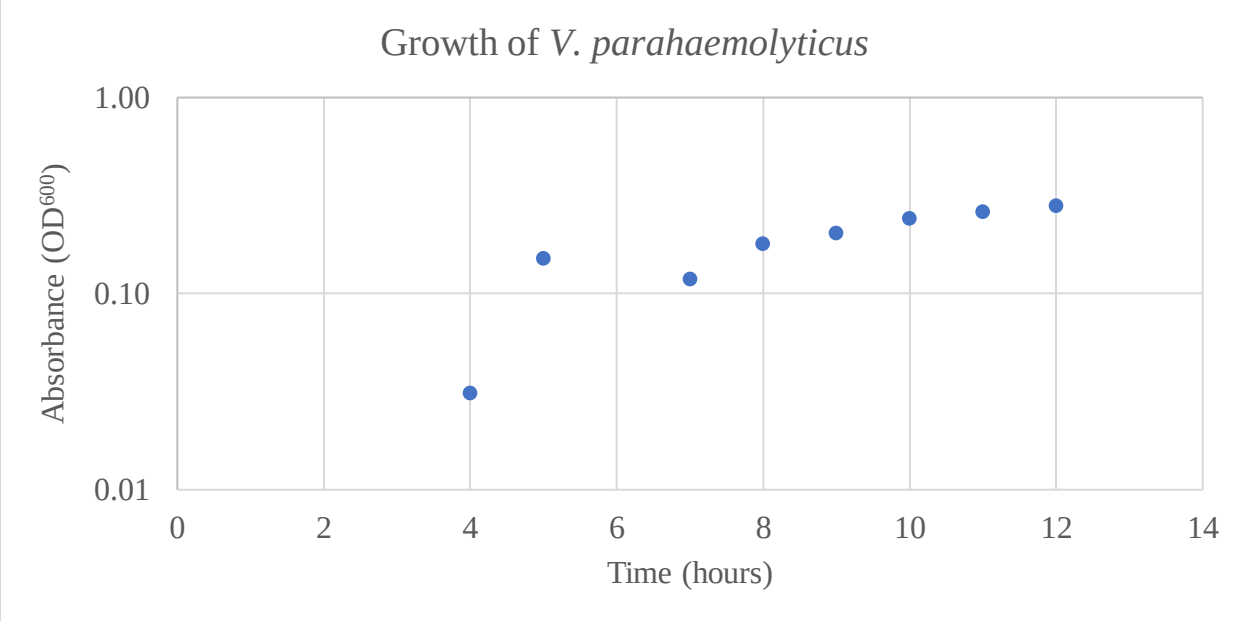

Fig. 17 Concentration (OD_{600}) of *Vp* over 12 hours. These data were used to confirm the timepoint at which cell growth reached late-exponential phase, the optimal time to collect for the co-culture assay (~10^6 CFU L^{-1})

Vv-Kb co-culture

In the first *Vv* trial, initial cell counts of *Kb* were determined as 5.40 x 10^6 cells L^{-1} in both the algal control and the co-culture, and these concentrations were similar to predicted concentrations, based on the inoculation schemes. These concentrations were chosen to reflect concentrations roughly equivalent to large, dense blooms found in nature (Brand and Compton 2007). *Kb* abundance gradually increased over the course of the trial, regardless of culture method (Fig. 18). By day 14, *Kb* had quintupled since day 0 (2.50 x 10^7 cells L^{-1}). This trend occurred for *Kb* in both the control and in the *Vv-Kb* co-culture; *Vv*, on the other hand, was suppressed when co-cultured with *Kb.* These *Vv* cultures were incorrectly diluted, thus the initial *Vv* control concentration was almost 150-fold greater (8.77 x 10^6 CFU L^{-1}) than *Vv* concentration in the co-culture (5.33 x 10^4 CFU L^{-1}). Despite *Vv* starting concentrations starting at higher levels in the control culture than in the *Vv-Kb* co-culture, both treatments still showed complete inhibition of *Vv*, regardless of *Kb* presence.

Kb and *Vv* initial concentrations in trial 2 more closely resembled each other, a key requirement for this assay design (*Vv* control, 1.93 x 10^7 CFU L^{-1}; *Vv-Kb* co-culture, 7.1 x 10^7 CFU L^{-1}). Although *Vv* co-culture abundances decreased to <6 x 10^4 CFU L^{-1}, there was substantial *Vv* growth in the control, reaching 3.24 x 10^9 CFU mL^{-1} on day 3, resulting in an increase of more than 150-fold from initial abundances at this timepoint (Fig. 19). At day 14, Vv in the control ended at 1.16 x 10^6 CFU L^{-1}. At the beginning of the assay, *Kb* were also concentrations were similar (4.83 x 10^6 CFU L^{-1}, control; 4.22 10^6 CFU L^{-1}, co-culture). *Kb* control concentrations peaked on day 3 (7.52 x 10^6 CFU L^{-1}), the same day as *Vv* in the bacterial control. *Kb* concentrations declined in both treatments, but *Kb* control concentrations (1.16 x 10^6 CFU L^{-1}) ended up almost 40-fold greater than of the *Kb* control in trial 2 (3.0 x 10^4 CFU L^{-1}).

Vp-Kb co-culture

The first *Vp-Kb* trial contained similar starting concentrations *Vp* in both treatments (*Vp*-control, 3.89 x 10^6 CFU L^{-1}; co-culture, 4.07 x 10^6 CFU L^{-1}). *Vp* control concentrations stayed relatively low until day 7, when abundance peaked to 1.47 x 10^8 CFU L^{-1}, almost 40-fold greater than day 0. At day 12, *Vp* control was at 5.54 x 10^{10} CFU L^{-1} and *Vp* in the co-culture was at 1.09 x 10^{10} CFU L^{-1}; and by day 14, *Vp* had completely declined to 0 CFU L^{-1} in both treatments. *Vp* growth in the control and co-culture were and days 4 and 7. *Kb* gradually increased, both alone and when cultured with *Vp*, over the course of the assay, with the co-culture just slightly overtaking the control. However, *Kb* growth in the control (2.98 x 10^7 cells L^{-1}) ended up outnumbering the co-culture (2.13 x 10^7 cells L^{-1}). The second trial of *Vp* was consistent with the results from the first – *Vp* growth in the control gradually increased over the course of the assay, with short – although this time with alternating 1–2-day bursts of increases and decreases (Fig. 19). In the co-culture, *Vp* levels quickly declined, ending at a concentration about 20-fold lower than the initial (from 3.47 x 10^6 CFU L^{-1} to 1.80 x 10^5 CFU L^{-1}). Conversely, *Vp* control growth showed a steep incline, from 3.22 x 10^6 CFU L^{-1} to 5.87 x 10^7 CFU L^{-1}, almost a 20-fold increase from the initial.

Statistical tests

In the second trial of the *Vv-Kb* assay, there was strong evidence for a difference between *Kb* growth between the control and co-culture ($F = 7.611$, $p < 0.05$). There was no significant difference in *Vv* growth ($F = 0.167$, $p = 0.693$) nor *Kb* ($F = 1.042$, $p = 0.334$) growth in the first assay. Similarly, *Vp* growth ($F = 4.189$, $p = 0.081$) nor *Kb* growth ($F = 1.677$, $p = 0.693$) differed per treatment in the first assay. However, in the second trial of the *Vp-Kb* assay, there was a significant difference between *Vp* growth in the control and co-culture ($F = 10.371$, $p < 0.05$).

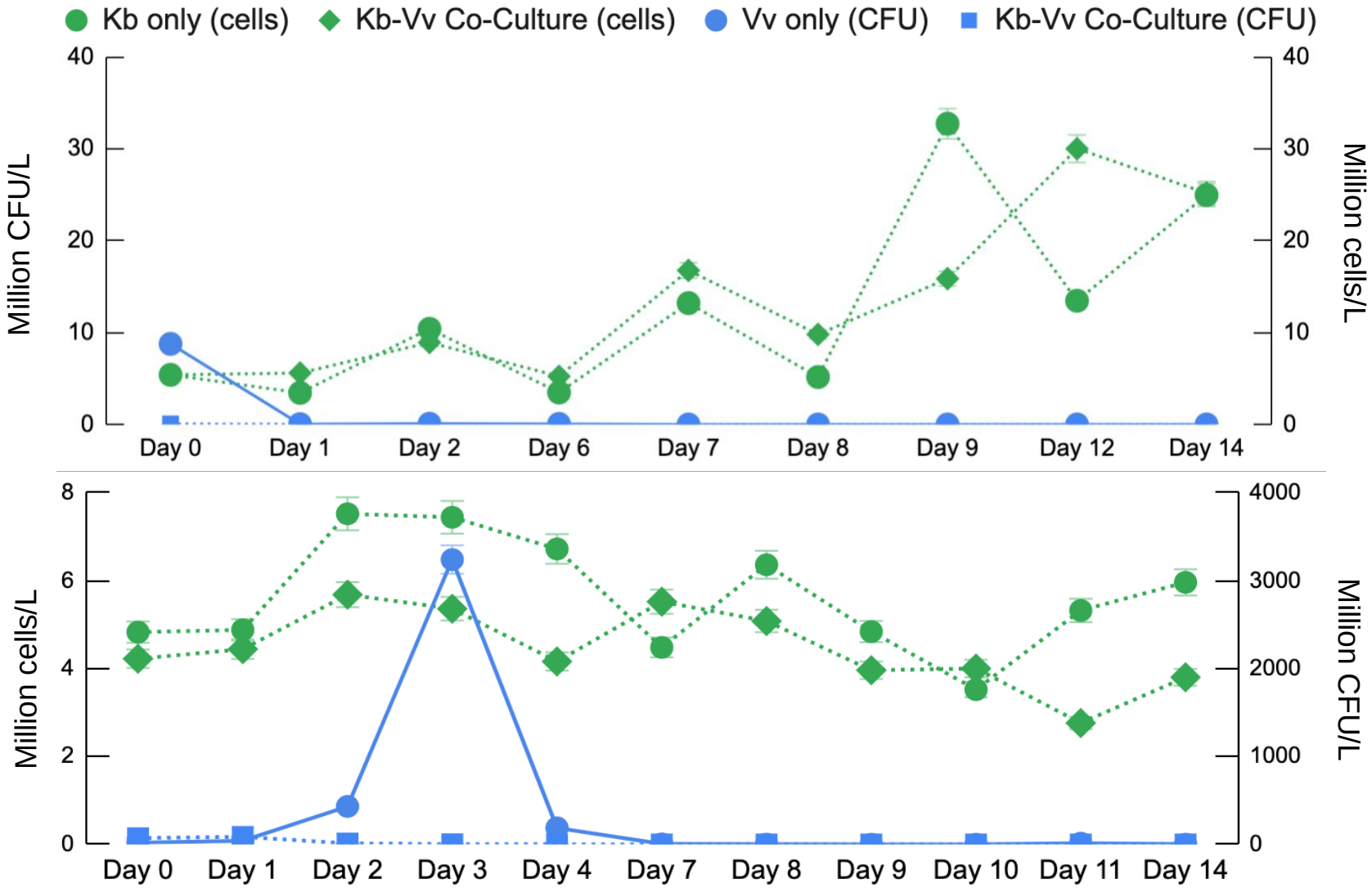

Fig. 18 Growth of *Kb* (circle, control; diamond, co-culture) and *Vv* (circle and solid line, control; square, co-culture) from trial 1 (top panel) and trial 2 (bottom panel)

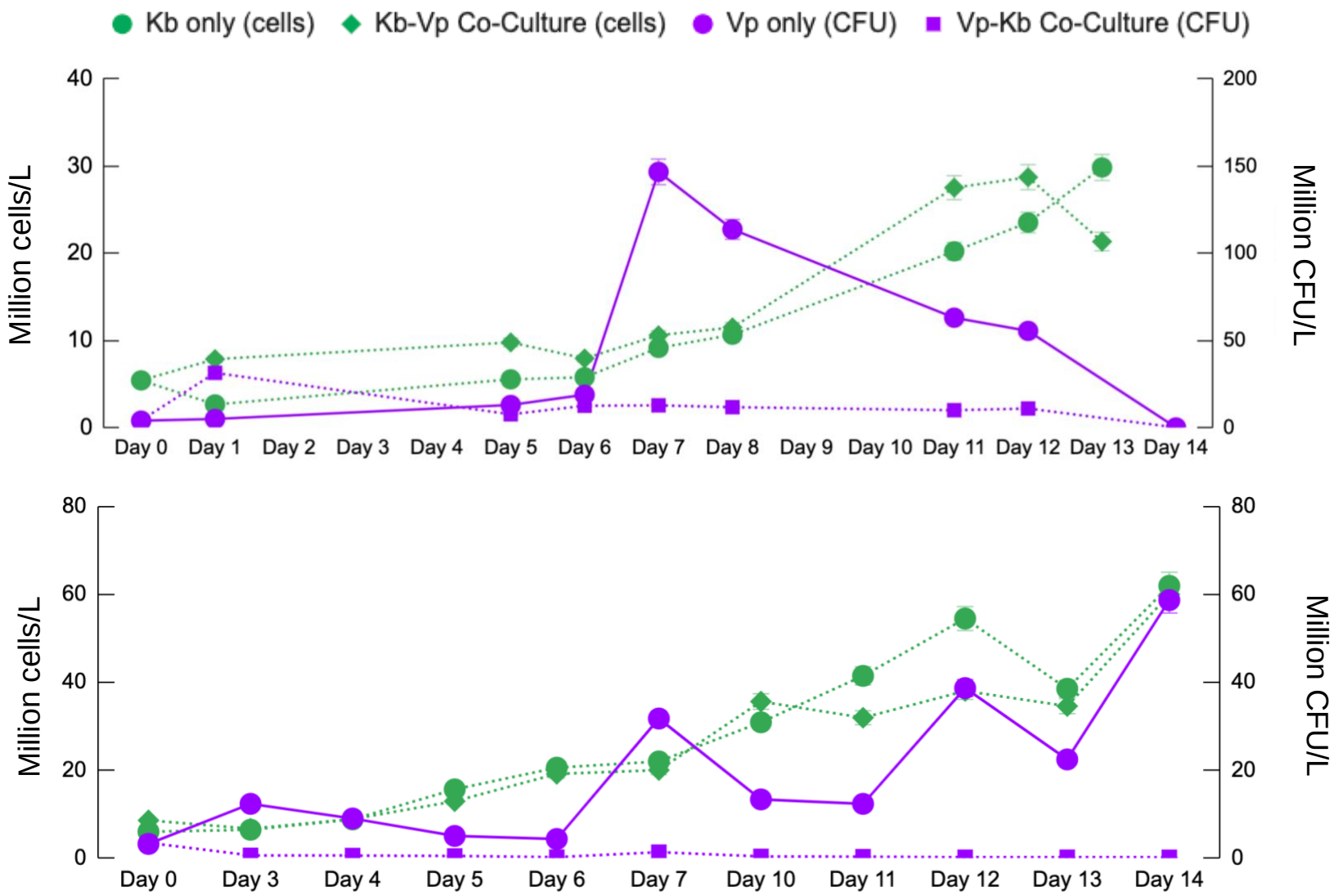

Fig. 19 Growth of *Kb* (circle, control; diamond, co-culture) and *Vp* (circle and solid line, control; square, co-culture) from trial 1 (top panel) and trial 2 (bottom panel)

Discussion

Fluctuations in Kb growth

The goal of this study was to determine, if any, potential algicidal activity of known pathogenic *Vv* and *Vp*, tested by measuring impacts on *Kb* growth under controlled conditions. In the Vv-Kb assay, alternating rises and falls in *Kb* concentrations could be attributed to dissimilarities in the times that samples were collected; certain sampling times took place early in the morning, whereas others during the latter part of the evening. As day shifts to night, *Kb* begins to upregulate respiration in response to shifts in CO_2 (Bercel and Kranz 2019). The relationships between *Vibrio* spp. and *Kb* can be dynamic. Hence, the methodological error committed herein highlights the importance of consistent, and perhaps *bis in die*, sampling to uncover more detailed data of these fluctuations. In addition, suboptimal conditions cause stress and may increase *Kb* susceptibility to predation, as reflected in *Kb* growth rate. For example, in the second trial of the *Vv*-*Kb* assay, *Kb* reached its peak at day 3 (~7 x 10^6 cells L^{-1}), whereas *Vv* concentrations surpassed ~3 x 10^9 CFU L^{-1} on day 3, and eventually decreased to 0 CFU L^{-1} by day 7 (Fig. 18). We predict *Vv* may have initially taken advantage of exudates from *Kb* as an abundant food source, *Vv* was later outcompeted by *Kb* grazing.

Although the general set up of the assay proved sound, some questionable results arose in the *Vv* assay. Culturable *Vv* concentrations consistently decreased to 0 CFU mL^{-1} only six days post incubations (Fig. 18). Thus, neither trial of the *Vv*-*Kb* co-culture assays are particularly helpful in examining *Vv*-*Kb* ecology. These results may be the result of poor aseptic technique when sampling and/or initially preparing the *Vv*-*Kb* co-culture sample Admittedly, a similar pattern occurred ensued in both trials, suggesting other factors may be responsible for algal-bacterial interactions in mixed-culture experiments (e.g., insufficient nutrients).

Future directions

Though experimentally convenient, there were some drawbacks of *in vitro* examinations of these naturally-occurring species. Like most marine organisms, *Vibrio* and *Karenia* abundance and distribution are driven by a variety of environmental fluctuations, many of which are seasonal. HABs are known to bloom following severe storm events and warmer summer months, and *Vibrio* tend to follow suit. Some conditions may also be optimal for *Vibrio* proliferation (Greenfield et al 2017; Hsieh et al 2007; Thickman and Gobler 2017), suggesting some species in bacterial-algal associations would proliferate following severe storms, unusually high temperatures, and myriad other conditions (Zou et al 2020). It is even hypothesized that these algal-bacterial associations may be species-specific, especially between taxa whose ideal environmental conditions (e.g., high water temperatures, meso-halophilic salinities, high nutrient abundance, freshwater influence) are similar (De Rijcke et al 2016; Diner et al 2021). Similarly, salinity may be an important consideration in mixed-culture experiments such as this one; this experiment was performed in culture conditions with a salinity optimal for *Kb* (marine), but *Vibrio* are mesohalophiles (estuarine). Thus, lowering the salinity may yield different results of the *Kb*-*Vibrio* dynamics, depending on the *Vibrio* species or strains tested.

Finally, the controlled *Vibrio*-*Kb* co-culture removes another important ecological consideration: other naturally-occurring bacterial and algal species normally present in brackish or marine waters where *Vibrio* and *Karenia* may co-exist. Mean heterotrophic bacterial abundances in a "typical" drop of seawater are ~1 x 10^6 cells mL^{-1} (Fig. 20) (Kirchman 2018). Competition for resources among heterotrophic bacteria species can dramatically shift the relative abundances of *Vibrio* species (Thorstenson and Ullrich 2021). Additionally, ecological considerations such as particle loads (Liang et al 2019), particle-attachment (Laverty et al 2020),

ocean acidification (Zha et al 2017), freshening (Froelich et al 2019), and temperature (Liang et al 2019) also may lead to rapid shifts in the relative abundances of these bacteria.

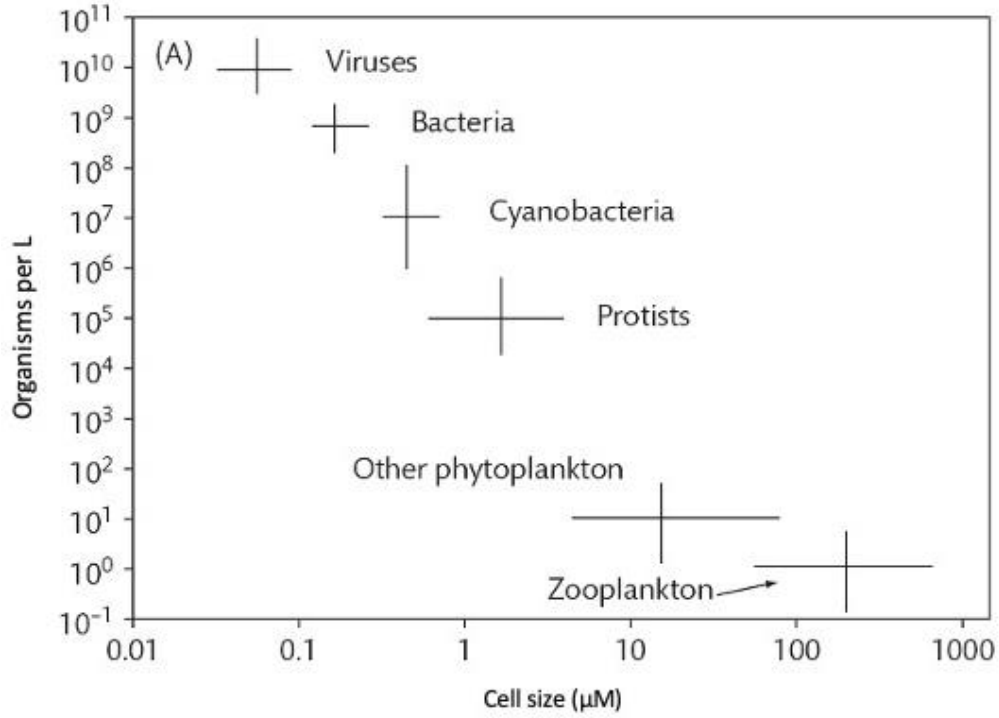

Fig. 20 Cell sizes of various microorganisms and their corresponding average abundances in typical aquatic ecosystems. "Bacteria" refers to the general heterotrophic bacterial community (Kirchman 2018)

Future studies should focus on molecular confirmation of presence and/or relative abundances and activity of bacteria to better reflect the dynamics of these coexisting pathogens. Although TCBS is a commonly employed culturable media for *Vibrio*, further experiments like this study should include a differential chromogenic media, such as CHROMagar™, to more accurately describe *Vv* and *Vp* numbers in environmental samples. Addressing these considerations will uncover deeper aspects of bacterial-algal dynamics in aquatic ecosystems, and perhaps even distinguish driving factors among and within waterbodies.

Conclusions

Predicted rises in eutrophication, surface temperatures, and alterations in salinities may present ideal conditions for pathogenic *Vibrio* proliferation. Using classical microbiological and molecular quantification, we found winter *Vibrio* abundances were high, suggesting that, contrary to popular belief, temperature may not be the most influential driving factor. Rather, a combination or interaction of several attributes, such as physicochemical hydrological factors, storm events (sediment resuspension), freshwater influence (salinity stratification), and nutrient runoff (e.g., chl *a* concentrations), among others should be taken into consideration when studying *Vibrio* dynamics, especially in shallow subtropical estuaries of northwest Gulf of Mexico.

Molecular-based methods for detection and enumeration, therefore, are necessary to complement culture-dependent methods. Primer pairs developed in this study were designed to be used in amplification of genes from known pathogenic strains from the NCBI database and ATCC® type strains of *Vv* and *Vp*. According to gel electrophoresis visualization of end-point PCR products, our newly designed primers were better than previously published primers for detection of *vvhA* (Panicker et al 2004) and *trh* (Nordstrom et al 2007). Our newly designed primer sets and routinely used primers were similarly effective for detection of *tdh* in *Vp* (Nordstrom et al 2007). A previously published primer set for detection of *ToxR* in *Vp* (Bauer and Rørvik 2007) was tested and validated for effectiveness of amplification from DNA of one Vp type strain. Next steps should include improving current *Vv*-specific detection methods of *ToxR* (Lee et al 2007). Most notably, this study discovered a novel *tdh* primer set for *Vv*, the first of its kind, matching with high accuracy and specificity to a known pathogenic *Vv* type strain. Although the literature overwhelmingly points to *tdh* being a *Vp*-specific gene, we were able to

define a new primer set that targeted a novel *tdh* gene in *Vv*. Thus, the results from our new primer design reflects the importance of continually evaluating the match of primer sequences with new *Vibrio* sequences added to the NCBI database.

Investigations of algal-bacterial interactions often seek evidence of bacterial-derived algicidal activity. In this study, I examined *Vibrio-Karenia* interactions in a co-culture microassay, in which *Vv* inhibited *Kb* growth, but *Kb* inhibited *Vp* growth. In this study, *Kb* overall had effects on *Vibrio* viability, with a slight inhibitory effect of *Vv* on *Kb* growth. Altering salinity conditions to be more suitable for *Vibrio* may provide more representative insight into these interactions. Truly, more in-depth studies must confirm these propositions, and this baseline study can be useful for future inquiries.

References

Aagesen AM, Phuvasate S, Su Y-C, Häse CC (2013) Persistence of Vibrio parahaemolyticus in the Pacific Oyster, Crassostrea gigas, Is a Multifactorial Process Involving Pili and Flagella but Not Type III Secretion Systems or Phase Variation. Applied and Environmental Microbiology 79:3303–3305. doi: 10.1128/AEM.00314-13

Aarts HJ, Joosten RG, Henkens MH, et al (2001) Rapid duplex PCR assay for the detection of pathogenic Yersinia enterocolitica strains. Journal of Microbiological Methods 47:209–217. doi: 10.1016/s0167-7012(01)00305-0

Babcock KK, Cesbron F, Patterson WF, et al (2020) Changing Biogeochemistry and Invertebrate Community Composition at Newly Deployed Artificial Reefs in the Northeast Gulf of Mexico. Estuaries and Coasts 43:680–692. doi: 10.1007/s12237-020-00713-4

Bacian C, Verdugo C, García K, et al (2021) Longitudinal Study of Total and Pathogenic Vibrio parahaemolyticus (tdh+ and/or trh+) in Two Natural Extraction Areas of Mytilus chilensis in Southern Chile. Frontiers in Microbiology 12:515. doi: 10.3389/fmicb.2021.621737

Baker-Austin C, Oliver JD (2020) Vibrio vulnificus. Trends in Microbiology 28:81–82. doi: 10.1016/j.tim.2019.08.006

Baker-Austin C, Oliver JD (2018) Vibrio vulnificus: new insights into a deadly opportunistic pathogen. Environmental Microbiology 20:423–430. doi: 10.1111/1462-2920.13955

Bauer A, Rørvik LM (2007) A novel multiplex PCR for the identification of Vibrio parahaemolyticus, Vibrio cholerae and Vibrio vulnificus. Letters in Applied Microbiology 45:371–375. doi: 10.1111/j.1472-765X.2007.02195.x

Bej AK, Patterson DP, Brasher CW, et al (1999) Detection of total and hemolysin-producing Vibrio parahaemolyticus in shellfish using multiplex PCR amplification of tl, tdh and trh. Journal of Microbiological Methods 36:215–225. doi: 10.1016/s0167-7012(99)00037-8

Bercel TL, Kranz SA (2019) Insights into carbon acquisition and photosynthesis in Karenia brevis under a range of CO2 concentrations. Progress in Oceanography 172:65–76. doi: 10.1016/j.pocean.2019.01.011

Blackwell KD, Oliver JD (2008) The ecology of Vibrio vulnificus, Vibrio cholerae, and Vibrio parahaemolyticus in North Carolina Estuaries. The Journal of Microbiology 46:146–153. doi: 10.1007/s12275-007-0216-2

Bramucci AR, Labeeuw L, Mayers TJ, et al (2015) A Small Volume Bioassay to Assess Bacterial/Phytoplankton Co-culture Using WATER-Pulse-Amplitude-Modulated (WATER-PAM) Fluorometry. JoVE (Journal of Visualized Experiments) e52455. doi: 10.3791/52455

Brand LE, Compton A (2007) Long-term increase in Karenia brevis abundance along the Southwest Florida Coast. Harmful algae 6:232–252. doi: 10.1016/j.hal.2006.08.005

Breslauer KJ, Frank R, Blöcker H, Marky LA (1986) Predicting DNA duplex stability from the base sequence. Proceedings of the National Academy of Sciences of the United States of America 83:3746–3750.

Buchan A, LeCleir GR, Gulvik CA, González JM (2014) Master recyclers: features and functions of bacteria associated with phytoplankton blooms. Nature Reviews Microbiology 12:686–698. doi: 10.1038/nrmicro3326

Bustin S, Huggett J (2017) qPCR primer design revisited. Biomolecular Detection and Quantification 14:19–28. doi: 10.1016/j.bdq.2017.11.001

Caffrey JM, Murrell MC (2016) A Historical Perspective on Eutrophication in the Pensacola Bay Estuary, FL, USA. In: Glibert PM, Kana TM (eds) Aquatic Microbial Ecology and Biogeochemistry: A Dual Perspective. Springer International Publishing, Cham, pp 199–213

Campbell MS, Wright AC (2003) Real-time PCR analysis of Vibrio vulnificus from oysters. Applied and Environmental Microbiology 69:7137–7144. doi: 10.1128/AEM.69.12.7137-7144.2003

Canizalez-Roman AC-R, Flores-Villaseñor HF-V, Zazueta-Beltran JZ-B, et al (2011) Comparative evaluation of a chromogenic agar medium – PCR protocol with a conventional method for isolation of Vibrio parahaemolyticus strains from environmental and clinical samples. Canadian Journal of Microbiology. doi: 10.1139/W10-108

Cantet F, Hervio-Heath D, Caro A, et al (2013) Quantification of Vibrio parahaemolyticus, Vibrio vulnificus and Vibrio cholerae in French Mediterranean coastal lagoons. Research in Microbiology 164:867–874. doi: 10.1016/j.resmic.2013.06.005

CDC (2019) Vibriosis Prevention Questions and Answers. In: Centers for Disease Control and Prevention. https://www.cdc.gov/vibrio/faq.html. Accessed 13 Jul 2020

Chase E, Young S, Harwood VJ (2015) Sediment and Vegetation as Reservoirs of Vibrio vulnificus in the Tampa Bay Estuary and Gulf of Mexico. Applied and Environmental Microbiology 81:2489–2494. doi: 10.1128/AEM.03243-14

Coia J, Cubie H (1995) Vibrio species. In: Coia J, Cubie H (eds) The Immunoassay Kit Directory: Volume 1: Part 3 December 1995. Springer Netherlands, Dordrecht, pp 975–976

Dalmasso A, La Neve F, Suffredini E, et al (2009) Development of a PCR Assay Targeting the rpoA Gene for the Screening of Vibrio Genus. Food Analytical Methods 2:317. doi: 10.1007/s12161-009-9089-9

Davis BJK, Jacobs JM, Davis MF, et al (2017) Environmental Determinants of Vibrio parahaemolyticus in the Chesapeake Bay. Applied and Environmental Microbiology 83:e01147-17. doi: 10.1128/AEM.01147-17

Davis CR, Heller LC, Peak KK, et al (2004) Real-time PCR detection of the thermostable direct hemolysin and thermolabile hemolysin genes in a Vibrio parahaemolyticus cultured from mussels and mussel homogenate associated with a foodborne outbreak. Journal of Food Protection 67:1005–1008. doi: 10.4315/0362-028x-67.5.1005

De Rijcke M, Van Acker E, Nevejan N, et al (2016) Toxic dinoflagellates and Vibrio spp. act independently in bivalve larvae. Fish & Shellfish Immunology 57:236–242. doi: 10.1016/j.fsi.2016.08.027

Deeb R, Tufford D, Scott GI, et al (2018) Impact of Climate Change on Vibrio vulnificus Abundance and Exposure Risk. Estuaries and Coasts 41:2289–2303. doi: 10.1007/s12237-018-0424-5

DeLong EF (1992) Archaea in coastal marine environments. Proceedings of the National Academy of Sciences of the United States of America 89:5685–5689.

DePaola A, Nordstrom JL, Bowers JC, et al (2003) Seasonal abundance of total and pathogenic Vibrio parahaemolyticus in Alabama oysters. Applied and Environmental Microbiology 69:1521–1526. doi: 10.1128/AEM.69.3.1521-1526.2003

Diner RE, Kaul D, Rabines A, et al (2021) Pathogenic Vibrio Species Are Associated with Distinct Environmental Niches and Planktonic Taxa in Southern California (USA) Aquatic Microbiomes. mSystems 6:e00571-21. doi: 10.1128/mSystems.00571-21

Doucette GJ, McGovern ER, Babinchak JA (1999) Algicidal Bacteria Active Against Gymnodinium Breve (dinophyceae). I. Bacterial Isolation and Characterization of Killing Activity1,3. Journal of Phycology 35:1447–1454. doi: 10.1046/j.1529-8817.1999.3561447.x

Drake SL, DePaola A, Jaykus L-A (2007) An Overview of Vibrio vulnificus and Vibrio parahaemolyticus. Comprehensive Reviews in Food Science and Food Safety 6:120–144. doi: 10.1111/j.1541-4337.2007.00022.x

Esteves K, Hervio-Heath D, Mosser T, et al (2015) Rapid proliferation of Vibrio parahaemolyticus, Vibrio vulnificus, and Vibrio cholerae during freshwater flash floods in French Mediterranean coastal lagoons. Applied and Environmental Microbiology 81:7600–7609. doi: 10.1128/AEM.01848-15

Fire SE, Miller GA, Sabater ER, Wells RS (2021) Utility of Red Tide (Karenia brevis) Monitoring Data as a Predictive Tool to Estimate Brevetoxin Accumulation in Live, Free-Ranging Marine Mammals. Frontiers in Marine Science 8:284. doi: 10.3389/fmars.2021.611310

Florida Department of Health (2021) Florida Department of Health. http://www.floridahealth.gov/diseases-and-conditions/vibrio-infections/vibrio-vulnificus/index.html. Accessed 6 Sep 2021

Foster JW (2004) Cold-Induced Hibernation of Marine Vibrios in the Gulf of Mexico: A Study of Cell-Cell Communication and Dormancy in Vibrio vulnificus | Research Project Database | Grantee Research Project | ORD | US EPA. In: epa.gov. https://cfpub.epa.gov/ncer_abstracts/index.cfm/fuseaction/display.abstractDetail/abstract/6930/report/0#content. Accessed 23 Nov 2020

Franco S l. m., Swenson G j., Long R a. (2012) Year round patchiness of Vibrio vulnificus within a temperate Texas bay. Journal of Applied Microbiology 112:593–604. doi: 10.1111/j.1365-2672.2011.05229.x

Frank AM, Cains MG, Henshel DS (2021) A Predictive Human Health Risk Assessment of Non-Choleraic Vibrio spp. during Hurricane-Driven Flooding Events in Coastal South Carolina, USA. Atmosphere 12:269. doi: 10.3390/atmos12020269

Fries JS, Characklis GW, Noble RT (2008) Sediment–water exchange of Vibrio sp. and fecal indicator bacteria: Implications for persistence and transport in the Neuse River Estuary, North Carolina, USA. Water Research 42:941–950. doi: 10.1016/j.watres.2007.09.006

Froelich B, Gonzalez R, Blackwood D, et al (2019) Decadal monitoring reveals an increase in Vibrio spp. concentrations in the Neuse River Estuary, North Carolina, USA. PloS One 14:e0215254. doi: 10.1371/journal.pone.0215254

Froelich BA, Daines DA (2020) In hot water: effects of climate change on Vibrio–human interactions. Environmental Microbiology 22:4101–4111. doi: 10.1111/1462-2920.14967

Froelich BA, Noble RT (2014) Factors Affecting the Uptake and Retention of Vibrio vulnificus in Oysters. Applied and Environmental Microbiology 80:7454–7459. doi: 10.1128/AEM.02042-14

Froelich BA, Williams TC, Noble RT, Oliver JD (2012) Apparent loss of Vibrio vulnificus from North Carolina oysters coincides with a drought-induced increase in salinity. Applied and Environmental Microbiology 78:3885–3889. doi: 10.1128/AEM.07855-11

Fujino T, Miwatani T, Yasuda J, et al (1965) Taxonomic studies on the bacterial strains isolated from cases of "shirasu" food-poisoning (Pasteurella parahaemolytica) and related microorganisms. Biken Journal 8:63–71.

FWC (2021) Red Tide Current Status. https://myfwc.maps.arcgis.com/apps/View/index.html?appid=87162eec3eb846218cec711d16462a72. Accessed 12 Sep 2021

Givens CE, Bowers JC, DePaola A, et al (2014) Occurrence and distribution of Vibrio vulnificus and Vibrio parahaemolyticus--potential roles for fish, oyster, sediment and water. Letters in Applied Microbiology 58:503–510. doi: 10.1111/lam.12226

Glavin DP, Cleaves HJ, Schubert M, et al (2004) New Method for Estimating Bacterial Cell Abundances in Natural Samples by Use of Sublimation. Applied and Environmental Microbiology 70:5923–5928. doi: 10.1128/AEM.70.10.5923-5928.2004

González-Escalona N, Blackstone GM, DePaola A (2006) Characterization of a Vibrio alginolyticus strain, isolated from Alaskan oysters, carrying a hemolysin gene similar to the thermostable direct hemolysin-related hemolysin gene (trh) of Vibrio parahaemolyticus. Applied and Environmental Microbiology 72:7925–7929. doi: 10.1128/AEM.01548-06

Greenfield DI, Moore JG, Stewart JR, et al (2017) Temporal and Environmental Factors Driving Vibrio Vulnificus and V. Parahaemolyticus Populations and Their Associations With Harmful Algal Blooms in South Carolina Detention Ponds and Receiving Tidal Creeks. GeoHealth 1:306–317. doi: 10.1002/2017GH000094

Grimes DJ, Johnson CN, Dillon KS, et al (2009) What Genomic Sequence Information Has Revealed About Vibrio Ecology in the Ocean—A Review. Microbial Ecology 58:447–460. doi: 10.1007/s00248-009-9578-9

Grodeska SM, Jones JL, Walton WC, Arias CR (2019) Effects of desiccation practices and ploidy in cultured oysters, Crassostrea virginica, on Vibrio spp. abundances in Portersville Bay (Alabama, USA). Aquaculture 507:164–171. doi: 10.1016/j.aquaculture.2019.03.060

Guillard RRL, Hargraves PE (1993) Stichochrysis immobilis is a diatom, not a chrysophyte. Phycologia 32:234–236. doi: 10.2216/i0031-8884-32-3-234.1

Gutierrez West CK, Klein SL, Lovell CR (2013) High frequency of virulence factor genes tdh, trh, and tlh in Vibrio parahaemolyticus strains isolated from a pristine estuary. Applied and Environmental Microbiology 79:2247–2252. doi: 10.1128/AEM.03792-12

Hagy JD, Murrell MC (2007) Susceptibility of a northern Gulf of Mexico estuary to hypoxia: An analysis using box models. Estuarine, Coastal and Shelf Science 74:239–253. doi: 10.1016/j.ecss.2007.04.013

Han X, Schubert CJ, Fiskal A, et al (2020) Eutrophication as a driver of microbial community structure in lake sediments. Environmental Microbiology. doi: 10.1111/1462-2920.15115

Hara-Kudo Y, Nishina T, Nakagawa H, et al (2001) Improved method for detection of Vibrio parahaemolyticus in seafood. Applied and Environmental Microbiology 67:5819–5823. doi: 10.1128/AEM.67.12.5819-5823.2001

Hare CE, Demir E, Coyne KJ, et al (2005) A bacterium that inhibits the growth of Pfiesteria piscicida and other dinoflagellates. Harmful Algae 2:221–234. doi: 10.1016/j.hal.2004.03.001

Heid CA, Stevens J, Livak KJ, Williams PM (1996) Real time quantitative PCR. Genome Research 6:986–994. doi: 10.1101/gr.6.10.986

Heidelberg JF, Heidelberg KB, Colwell RR (2002) Seasonality of Chesapeake Bay Bacterioplankton Species. Applied and Environmental Microbiology 68:5488–5497. doi: 10.1128/AEM.68.11.5488-5497.2002

Heil CA, Muni-Morgan AL (2021) Florida's Harmful Algal Bloom (HAB) Problem: Escalating Risks to Human, Environmental and Economic Health With Climate Change. Frontiers in Ecology and Evolution 9:299. doi: 10.3389/fevo.2021.646080

Hernández-Cabanyero C, Sanjuán E, Fouz B, et al (2020) The Effect of the Environmental Temperature on the Adaptation to Host in the Zoonotic Pathogen Vibrio vulnificus. Frontiers in Microbiology 11:489. doi: 10.3389/fmicb.2020.00489

Hester C, Smith H, Head M, et al (2016) Comparing Productivity and Biogeochemistry of Native and Transplanted Thalassia testudinum and Halodule beaudettei in Big Lagoon, Florida, USA. Gulf of Mexico Science. doi: 10.18785/goms.3301.02

Holmes RM, Aminot A, Kérouel R, et al (1999) A simple and precise method for measuring ammonium in marine and freshwater ecosystems. Canadian Journal of Fisheries and Aquatic Sciences 56:1801–1808. doi: 10.1139/f99-128

Honda T, Chearskul S, Takeda Y, Miwatani T (1980) Immunological methods for detection of Kanagawa phenomenon of Vibrio parahaemolyticus. Journal of Clinical Microbiology 11:600–603.

Hsieh JL, Fries JS, Noble RT (2007) Vibrio and Phytoplankton Dynamics During the Summer of 2004 in a Eutrophying Estuary. Ecological Applications 17:S102–S109. doi: 10.1890/05-1274.1

Hsieh JL, Fries JS, Noble RT (2008) Dynamics and predictive modelling of Vibrio spp. in the Neuse River Estuary, North Carolina, USA. Environmental Microbiology 10:57–64. doi: 10.1111/j.1462-2920.2007.01429.x

Hughes SN, Greig DJ, Miller WA, et al (2013) Dynamics of Vibrio with Virulence Genes Detected in Pacific Harbor Seals (Phoca vitulina richardii) Off California: Implications for Marine Mammal Health. Microbial Ecology 65:982–994. doi: 10.1007/s00248-013-0188-1

Huq A, Haley BJ, Taviani E, et al (2012) Detection, Isolation, and Identification of Vibrio cholerae from the Environment. Current protocols in microbiology CHAPTER:Unit6A.5. doi: 10.1002/9780471729259.mc06a05s26

Iida T, Park KS, Suthienkul O, et al (1998) Close proximity of the tdh, trh and ure genes on the chromosome of Vibrio parahaemolyticus. Microbiology (Reading, England) 144 (Pt 9):2517–2523. doi: 10.1099/00221287-144-9-2517

Jansson L, Hedman J (2019) Challenging the proposed causes of the PCR plateau phase. Biomolecular Detection and Quantification 17:100082. doi: 10.1016/j.bdq.2019.100082

Jia A, Woo NYS, Zhang X-H (2010) Expression, purification, and characterization of thermolabile hemolysin (TLH) from Vibrio alginolyticus. Diseases of Aquatic Organisms 90:121–127. doi: 10.3354/dao02225

Johnson CN (2015) Influence of Environmental Factors on Vibrio spp. in Coastal Ecosystems. Microbiology Spectrum. doi: 10.1128/microbiolspec.VE-0008-2014

Johnson CN (2013) Fitness Factors in Vibrios: a Mini-review. Microbial Ecology 65:826–851. doi: 10.1007/s00248-012-0168-x

Johnson CN, Bowers JC, Griffitt KJ, et al (2012) Ecology of Vibrio parahaemolyticus and Vibrio vulnificus in the Coastal and Estuarine Waters of Louisiana, Maryland, Mississippi, and Washington (United States). Applied and Environmental Microbiology 78:7249–7257. doi: 10.1128/AEM.01296-12

Johnson CN, Flowers AR, Noriea NF, et al (2010) Relationships between Environmental Factors and Pathogenic Vibrios in the Northern Gulf of Mexico. Applied and Environmental Microbiology 76:7076–7084. doi: 10.1128/AEM.00697-10

Joux F, Bertrand J-C, Wit RD, et al (2015) Methods for Studying Microorganisms in the Environment. Environmental Microbiology: Fundamentals and Applications 757–829.

Kaspar CW, Tamplin ML (1993) Effects of temperature and salinity on the survival of Vibrio vulnificus in seawater and shellfish. Applied and Environmental Microbiology 59:2425–2429. doi: 10.1128/AEM.59.8.2425-2429.1993

Kaufman GE, Bej AK, Bowers J, DePaola A (2003) Oyster-to-Oyster Variability in Levels of Vibrio parahaemolyticus. Journal of Food Protection 66:125–129. doi: 10.4315/0362-028X-66.1.125

Kelly MT (1982) Effect of temperature and salinity on Vibrio (Beneckea) vulnificus occurrence in a Gulf Coast environment. Applied and Environmental Microbiology 44:820–824.

Kibbe WA (2007) OligoCalc: an online oligonucleotide properties calculator. Nucleic Acids Research 35:W43-46. doi: 10.1093/nar/gkm234

Kirchman D, Peterson B, Juers D (1984) Bacterial growth and tidal variation in bacterial abundance in the Great Sippewissett Salt Marsh. Marine Ecology Progress Series 19:247–259.

Kirchman D, Sigda J, Kapuscinski R, Mitchell R (1982) Statistical analysis of the direct count method for enumerating bacteria. Applied and Environmental Microbiology 44:376–382.

Kirchman DL (2018) Processes in Microbial Ecology, 2nd edn. Oxford University Press

Kirchman DL, Dittel AI, Malmstrom RR, Cottrell MT (2005) Biogeography of major bacterial groups in the Delaware Estuary. Limnology and Oceanography 50:1697–1706. doi: 10.4319/lo.2005.50.5.1697

Klein SL, Gutierrez West CK, Mejia DM, Lovell CR (2014) Genes Similar to the Vibrio parahaemolyticus Virulence-Related Genes tdh, tlh, and vscC2 Occur in Other Vibrionaceae Species Isolated from a Pristine Estuary. Applied and Environmental Microbiology 80:595–602. doi: 10.1128/AEM.02895-13

Koponen JK, Turunen A-M, Ylä-Herttuala S (2002) Escherichia coli DNA contamination in AmpliTaq Gold polymerase interferes with TaqMan analysis of lacZ. Molecular Therapy: The Journal of the American Society of Gene Therapy 5:220–222. doi: 10.1006/mthe.2002.0548

Krishna K, Veettil VP, Anas A, Nair S (2021) Hydrological regulation of Vibrio dynamics in a tropical monsoonal estuary: a classification and regression tree approach. Environmental Science and Pollution Research 28:724–737. doi: 10.1007/s11356-020-10486-9

Kumar S, Stecher G, Li M, et al (2018) MEGA X: Molecular Evolutionary Genetics Analysis across Computing Platforms. Molecular Biology and Evolution 35:1547–1549. doi: 10.1093/molbev/msy096

Laverty AL, Primpke S, Lorenz C, et al (2020) Bacterial biofilms colonizing plastics in estuarine waters, with an emphasis on Vibrio spp. and their antibacterial resistance. PLOS ONE 15:e0237704. doi: 10.1371/journal.pone.0237704

Lee JH, Kim MW, Kim BS, et al (2007) Identification and characterization of the Vibrio vulnificus rtxA essential for cytotoxicity in vitro and virulence in mice. Journal of Microbiology (Seoul, Korea) 45:146–152.

Letchumanan V, Chan K-G, Lee L-H (2014) Vibrio parahaemolyticus: a review on the pathogenesis, prevalence, and advance molecular identification techniques. Frontiers in Microbiology. doi: 10.3389/fmicb.2014.00705

Lewis M, Kirschenfeld J, Goodheart T (2016) Environmental Quality of the Pensacola Bay System: Retrospective Review for Future Resource Management and Rehabilitation.

Lewis MA, Weber DL, Moore JC (2002) An evaluation of the use of colonized periphyton as an indicator of wastewater impact in near-coastal areas of the Gulf of Mexico. Archives of Environmental Contamination and Toxicology 43:11–18. doi: 10.1007/s00244-001-0054-x

Li N, Dong K, Jiang G, et al (2020) Stochastic processes dominate marine free-living Vibrio community assembly in a subtropical gulf. FEMS Microbiology Ecology. doi: 10.1093/femsec/fiaa198

Liang J, Liu J, Wang X, et al (2019) Spatiotemporal Dynamics of Free-Living and Particle-Associated Vibrio Communities in the Northern Chinese Marginal Seas. Applied and Environmental Microbiology 85:e00217-19. doi: 10.1128/AEM.00217-19

Lipp EK, Kurz R, Vincent R, et al (2001a) The effects of seasonal variability and weather on microbial fecal pollution and enteric pathogens in a subtropical estuary. Estuaries 24:266–276. doi: 10.2307/1352950

Lipp EK, Rodriguez-Palacios C, Rose JB (2001b) Occurrence and distribution of the human pathogen Vibrio vulnificus in a subtropical Gulf of Mexico estuary. Hydrobiologia 460:165–173. doi: 10.1023/A:1013127517860

Liu B, Liu H, Pan Y, et al (2016) Comparison of the Effects of Environmental Parameters on the Growth Variability of Vibrio parahaemolyticus Coupled with Strain Sources and Genotypes Analyses. Frontiers in Microbiology 7:994. doi: 10.3389/fmicb.2016.00994

Lønborg C, Baltar F, Carreira C, Morán XAG (2019) Dissolved Organic Carbon Source Influences Tropical Coastal Heterotrophic Bacterioplankton Response to Experimental Warming. Frontiers in Microbiology 10:2807. doi: 10.3389/fmicb.2019.02807

Lovell CR (2017) Ecological fitness and virulence features of Vibrio parahaemolyticus in estuarine environments. Applied Microbiology and Biotechnology 101:1781–1794. doi: 10.1007/s00253-017-8096-9

Luna GM, Manini E, Danovaro R (2002) Large Fraction of Dead and Inactive Bacteria in Coastal Marine Sediments: Comparison of Protocols for Determination and Ecological Significance. Applied and Environmental Microbiology 68:3509–3513. doi: 10.1128/AEM.68.7.3509-3513.2002

Macauley JM, Engle VD, Summers JK, et al (1995) An assessment of water quality and primary productivity in Perdido Bay, a Northern Gulf of Mexico Estuary. Environmental Monitoring and Assessment 36:191–205. doi: 10.1007/BF00547901

Main CR, Salvitti LR, Whereat EB, Coyne KJ (2015) Community-Level and Species-Specific Associations between Phytoplankton and Particle-Associated Vibrio Species in Delaware's Inland Bays. Applied and Environmental Microbiology 81:5703–5713. doi: 10.1128/AEM.00580-15

Malham SK, Rajko-Nenow P, Howlett E, et al (2014) The interaction of human microbial pathogens, particulate material and nutrients in estuarine environments and their impacts on recreational and shellfish waters. Environmental Science: Processes & Impacts 16:2145–2155. doi: 10.1039/C4EM00031E

Malinen E, Kassinen A, Rinttilä T, Palva A (2003) Comparison of real-time PCR with SYBR Green I or 5'-nuclease assays and dot-blot hybridization with rDNA-targeted oligonucleotide probes in quantification of selected faecal bacteria. Microbiology (Reading, England) 149:269–277. doi: 10.1099/mic.0.25975-0

Martinez-Urtaza J, Blanco-Abad V, Rodriguez-Castro A, et al (2012) Ecological determinants of the occurrence and dynamics of Vibrio parahaemolyticus in offshore areas. The ISME Journal 6:994–1006. doi: 10.1038/ismej.2011.156

Mayali X, Franks PJS, Azam F (2007) Bacterial induction of temporary cyst formation by the dinoflagellate Lingulodinium polyedrum. Aquatic Microbial Ecology 50:51–62. doi: 10.3354/ame01143

Montánchez I, Ogayar E, Plágaro AH, et al (2019) Analysis of Vibrio harveyi adaptation in sea water microcosms at elevated temperature provides insights into the putative mechanisms of its persistence and spread in the time of global warming. Scientific Reports 9:289. doi: 10.1038/s41598-018-36483-0

Morgulis A, Coulouris G, Raytselis Y, et al (2008) Database indexing for production MegaBLAST searches. Bioinformatics (Oxford, England) 24:1757–1764. doi: 10.1093/bioinformatics/btn322

Motes ML, DePaola A, Cook DW, et al (1998) Influence of water temperature and salinity on Vibrio vulnificus in Northern Gulf and Atlantic Coast oysters (Crassostrea virginica). Applied and Environmental Microbiology 64:1459–1465. doi: 10.1128/AEM.64.4.1459-1465.1998

Murrell M, Caffrey J (2005) High Cyanobacterial Abundance in Three Northeastern Gulf of Mexico Estuaries. Gulf and Caribbean Research 17:95–106. doi: 10.18785/gcr.1701.08

Murrell MC (2003) Bacterioplankton dynamics in a subtropical estuary: evidence for substrate limitation. Aquatic Microbial Ecology 32:239–250. doi: 10.3354/ame032239

Murrell MC, Caffrey JM, Marcovich DT, et al (2018) Seasonal oxygen dynamics in a warm temperate estuary: effects of hydrologic variability on measurements of primary production, respiration, and net metabolism. Estuaries and Coasts: Journal of the Estuarine Research Federation 41:690–707. doi: 10.1007/s12237-017-0328-9

Murrell MC, Campbell JG, Hagy JD, Caffrey JM (2009) Effects of irradiance on benthic and water column processes in a Gulf of Mexico estuary: Pensacola Bay, Florida, USA. Estuarine, Coastal and Shelf Science 81:501–512. doi: 10.1016/j.ecss.2008.12.002

Murrell MC, Hagy JD, Lores EM, Greene RM (2007) Phytoplankton production and nutrient distributions in a subtropical estuary: Importance of freshwater flow. Estuaries and Coasts 30:390–402. doi: 10.1007/BF02819386

Murrell MC, Lores EM (2004) Phytoplankton and zooplankton seasonal dynamics in a subtropical estuary: importance of cyanobacteria. Journal of Plankton Research 26:371–382. doi: 10.1093/plankt/fbh038

Nair GB, Ramamurthy T, Bhattacharya SK, et al (2007) Global dissemination of Vibrio parahaemolyticus serotype O3:K6 and its serovariants. Clinical Microbiology Reviews 20:39–48. doi: 10.1128/CMR.00025-06

Narayanan SV, Joseph TC, Peeralil S, et al (2020) Prevalence, Virulence Characterization, AMR Pattern and Genetic Relatedness of Vibrio parahaemolyticus Isolates From Retail Seafood of Kerala, India. Frontiers in Microbiology. doi: 10.3389/fmicb.2020.00592

Nature Conservancy (2014) Pensacola Bay Community-Based Watershed Plan 2014 Report. In: The Nature Conservancy. https://www.nature.org/en-us/about-us/where-we-work/united-states/florida/stories-in-florida/florida-pensacola-east-bay/. Accessed 24 Oct 2021

Newton A, Kendall M, Vugia DJ, et al (2012) Increasing rates of vibriosis in the United States, 1996-2010: review of surveillance data from 2 systems. Clinical Infectious Diseases: An Official Publication of the Infectious Diseases Society of America 54 Suppl 5:S391-395. doi: 10.1093/cid/cis243

Nigro OD, Hou A, Vithanage G, et al (2011) Temporal and spatial variability in culturable pathogenic Vibrio spp. in Lake Pontchartrain, Louisiana, following hurricanes Katrina and Rita. Applied and Environmental Microbiology 77:5384–5393. doi: 10.1128/AEM.02509-10

Nigro OD, Steward GF (2015) Differential specificity of selective culture media for enumeration of pathogenic vibrios: advantages and limitations of multi-plating methods. Journal of Microbiological Methods 111:24–30. doi: 10.1016/j.mimet.2015.01.014

Nordstrom JL, Vickery MCL, Blackstone GM, et al (2007) Development of a Multiplex Real-Time PCR Assay with an Internal Amplification Control for the Detection of Total and Pathogenic Vibrio parahaemolyticus Bacteria in Oysters. Applied and Environmental Microbiology 73:5840–5847. doi: 10.1128/AEM.00460-07

Oliver JD (2003) Chapter 17 Culture media for the isolation and enumeration of pathogenic Vibrio species in foods and environmental samples. In: Corry JEL, Curtis GDW, Baird RM (eds) Progress in Industrial Microbiology. Elsevier, pp 249–269

Oliver JD, Bockian R (1995) In vivo resuscitation, and virulence towards mice, of viable but nonculturable cells of Vibrio vulnificus. Applied and Environmental Microbiology 61:2620–2623. doi: 10.1128/AEM.61.7.2620-2623.1995

O'Mahony J, Hill C (2002) A real time PCR assay for the detection and quantitation of Mycobacterium avium subsp. paratuberculosis using SYBR Green and the Light Cycler. Journal of Microbiological Methods 51:283–293. doi: 10.1016/s0167-7012(02)00098-2

Oren A (2004) Prokaryote diversity and taxonomy: current status and future challenges. Philosophical Transactions of the Royal Society of London. Series B, Biological Sciences 359:623–638. doi: 10.1098/rstb.2003.1458

Paczkowska J, Rowe OF, Figueroa D, Andersson A (2019) Drivers of phytoplankton production and community structure in nutrient-poor estuaries receiving terrestrial organic inflow. Marine Environmental Research 151:104778. doi: 10.1016/j.marenvres.2019.104778

Panicker G, Myers ML, Bej AK (2004) Rapid Detection of Vibrio vulnificus in Shellfish and Gulf of Mexico Water by Real-Time PCR. Applied and Environmental Microbiology 70:498–507. doi: 10.1128/AEM.70.1.498-507.2004

Park MS, Park KH, Bahk GJ (2018) Interrelationships between Multiple Climatic Factors and Incidence of Foodborne Diseases. International Journal of Environmental Research and Public Health 15:2482. doi: 10.3390/ijerph15112482

Parsons TR, Maita Y, Lalli CM (1984) A manual of chemical & biological methods for seawater analysis. Elsevier, Amsterdam

Pazhani GP, Bhowmik SK, Ghosh S, et al (2014) Trends in the Epidemiology of Pandemic and Non-pandemic Strains of Vibrio parahaemolyticus Isolated from Diarrheal Patients in Kolkata, India. PLoS Neglected Tropical Diseases 8:e2815. doi: 10.1371/journal.pntd.0002815

Pfeffer CS, Hite MF, Oliver JD (2003) Ecology of Vibrio vulnificus in Estuarine Waters of Eastern North Carolina. Applied and Environmental Microbiology 69:3526–3531. doi: 10.1128/AEM.69.6.3526-3531.2003

Potdukhe TV, Caffrey JM, Rothfus MJ, et al (2021) Viable Putative Vibrio vulnificus and parahaemolyticus in the Pensacola and Perdido Bays: Water Column, Sediments, and Invertebrate Biofilms. Frontiers in Marine Science 8:513. doi: 10.3389/fmars.2021.645755

Proctor LM, Souza AC (2001) Method for enumeration of 5-cyano-2,3-ditoyl tetrazolium chloride (CTC)-active cells and cell-specific CTC activity of benthic bacteria in riverine, estuarine and coastal sediments. Journal of Microbiological Methods 43:213–222. doi: 10.1016/S0167-7012(00)00218-9

Provasoli L, McLaughlin JJA, Droop MR (1957) The development of artificial media for marine algae. Archiv für Mikrobiologie 25:392–428. doi: 10.1007/BF00446694

Pruente VL, Jones JL, Steury TD, Walton WC (2020) Effects of tumbling, refrigeration and subsequent resubmersion on the abundance of Vibrio vulnificus and Vibrio parahaemolyticus in cultured oysters (Crassostrea virginica). International Journal of Food Microbiology 335:108858. doi: 10.1016/j.ijfoodmicro.2020.108858

Rantakokko-Jalava K, Jalava J (2001) Development of conventional and real-time PCR assays for detection of Legionella DNA in respiratory specimens. Journal of Clinical Microbiology 39:2904–2910. doi: 10.1128/JCM.39.8.2904-2910.2001

Rasmussen R (2001) Quantification on the LightCycler. In: Meuer S, Wittwer C, Nakagawara K-I (eds) Rapid Cycle Real-Time PCR: Methods and Applications. Springer, Berlin, Heidelberg, pp 21–34

Ray NE, Henning MC, Fulweiler RW (2019) Nitrogen and phosphorus cycling in the digestive system and shell biofilm of the eastern oyster Crassostrea virginica. Marine Ecology Progress Series 621:95–105. doi: 10.3354/meps13007

Reichelt JL, Baumann P, Baumann L (1976) Study of genetic relationships among marine species of the genera Beneckea and Photobacterium by means of in vitro DNA/DNA hybridization. Archives of Microbiology 110:101–120. doi: 10.1007/BF00416975

Roque A, Lopez-Joven C, Lacuesta B, et al (2009) Detection and Identification of tdh- and trh-Positive Vibrio parahaemolyticus Strains from Four Species of Cultured Bivalve Molluscs on the Spanish Mediterranean Coast. Applied and Environmental Microbiology 75:7574–7577. doi: 10.1128/AEM.00772-09

Roth PB, Twiner MJ, Mikulski CM, et al (2008) Comparative analysis of two algicidal bacteria active against the red tide dinoflagellate Karenia brevis. Harmful Algae 7:682–691. doi: 10.1016/j.hal.2008.02.002

Ruiz-Villalba A, van Pelt-Verkuil E, Gunst QD, et al (2017) Amplification of nonspecific products in quantitative polymerase chain reactions (qPCR). Biomolecular Detection and Quantification 14:7–18. doi: 10.1016/j.bdq.2017.10.001

Sakazaki R (1968) Proposal of Vibrio alginolyticus for the biotype 2 of Vibrio parahaemolyticus. Japanese Journal of Medical Science & Biology 21:359–362. doi: 10.7883/yoken1952.21.359

Schnetger B, Lehners C (2014) Determination of nitrate plus nitrite in small volume marine water samples using vanadium(III)chloride as a reduction agent. Marine Chemistry 160:91–98. doi: 10.1016/j.marchem.2014.01.010

Shaw KS, Jacobs JM, Crump BC (2014) Impact of Hurricane Irene on Vibrio vulnificus and Vibrio parahaemolyticus concentrations in surface water, sediment, and cultured oysters in the Chesapeake Bay, MD, USA. Frontiers in Microbiology. doi: 10.3389/fmicb.2014.00204

Shinde D, Lai Y, Sun F, Arnheim N (2003) Taq DNA polymerase slippage mutation rates measured by PCR and quasi-likelihood analysis: (CA/GT)n and (A/T)n microsatellites. Nucleic Acids Research 31:974–980.

Sieracki CK, Sieracki ME, Yentsch CS (1998) An imaging-in-flow system for automated analysis of marine microplankton. Marine Ecology Progress Series 168:285–296. doi: 10.3354/meps168285

Spangler R, Goddard NL, Thaler DS (2009) Optimizing Taq Polymerase Concentration for Improved Signal-to-Noise in the Broad Range Detection of Low Abundance Bacteria. PLOS ONE 4:e7010. doi: 10.1371/journal.pone.0007010

Sugimoto N, Nakano S, Yoneyama M, Honda K (1996) Improved thermodynamic parameters and helix initiation factor to predict stability of DNA duplexes. Nucleic Acids Research 24:4501–4505.

Suzuki MT, Taylor LT, DeLong EF (2000) Quantitative Analysis of Small-Subunit rRNA Genes in Mixed Microbial Populations via 5′-Nuclease Assays. Applied and Environmental Microbiology 66:4605–4614. doi: 10.1128/AEM.66.11.4605-4614.2000

Takemura A, Chien D, Polz M (2014) Associations and dynamics of Vibrionaceae in the environment, from the genus to the population level. Frontiers in Microbiology 5:38. doi: 10.3389/fmicb.2014.00038

Tall A, Teillon A, Boisset C, et al (2012) Real-time PCR optimization to identify environmental Vibrio spp. strains. Journal of Applied Microbiology 113:361–372. doi: 10.1111/j.1365-2672.2012.05350.x

Tantillo G m., Fontanarosa M, Di Pinto A, Musti M (2004) Updated perspectives on emerging vibrios associated with human infections. Letters in Applied Microbiology 39:117–126. doi: 10.1111/j.1472-765X.2004.01568.x

Theethakaew C, Feil EJ, Castillo-Ramírez S, et al (2013) Genetic Relationships of Vibrio parahaemolyticus Isolates from Clinical, Human Carrier, and Environmental Sources in Thailand, Determined by Multilocus Sequence Analysis. Applied and Environmental Microbiology 79:2358–2370. doi: 10.1128/AEM.03067-12

Thickman JD, Gobler CJ (2017) The ability of algal organic matter and surface runoff to promote the abundance of pathogenic and non-pathogenic strains of Vibrio parahaemolyticus in Long Island Sound, USA. PLOS ONE 12:e0185994. doi: 10.1371/journal.pone.0185994

Thomas F (2016) Of Life and Limb: The Failure of Florida's Water Quality Criteria to Test for Vibrio Vulnificus in Coastal Waters and the Need for Enhanced Criteria, Regulation, and Notification to Protect Public Health. Student Works

Thomas P, Mujawar MM, Sekhar AC, Upreti R (2014) Physical impaction injury effects on bacterial cells during spread plating influenced by cell characteristics of the organisms. Journal of Applied Microbiology 116:911–922. doi: 10.1111/jam.12412

Thorstenson CA, Ullrich MS (2021) Ecological Fitness of Vibrio cholerae, Vibrio parahaemolyticus, and Vibrio vulnificus in a Small-Scale Population Dynamics Study. Frontiers in Marine Science 8:285. doi: 10.3389/fmars.2021.623988

TidalCoefficient (2020) Tidal Coefficient Data. https://tides4fishing.com/tides/tidal-coefficient. Accessed 13 Nov 2020

Turner JW, Good B, Cole D, Lipp EK (2009) Plankton composition and environmental factors contribute to Vibrio seasonality. The ISME Journal 3:1082–1092. doi: 10.1038/ismej.2009.50

Urquhart EA, Jones SH, Yu JW, et al (2016) Environmental Conditions Associated with Elevated Vibrio parahaemolyticus Concentrations in Great Bay Estuary, New Hampshire. PLOS ONE 11:e0155018. doi: 10.1371/journal.pone.0155018

Van Meerssche E, Pinckney JL (2019) Nutrient Loading Impacts on Estuarine Phytoplankton Size and Community Composition: Community-Based Indicators of Eutrophication. Estuaries and Coasts 42:504–512. doi: 10.1007/s12237-018-0470-z

Vargo GA (2009) A brief summary of the physiology and ecology of Karenia brevis Davis (G. Hansen and Moestrup comb. nov.) red tides on the West Florida Shelf and of hypotheses posed for their initiation, growth, maintenance, and termination. Harmful Algae 8:573–584. doi: 10.1016/j.hal.2008.11.002

Vezzulli L, Pezzati E, Moreno M, et al (2009) Benthic ecology of Vibrio spp. and pathogenic Vibrio species in a coastal Mediterranean environment (La Spezia Gulf, Italy). Microbial Ecology 58:808–818. doi: 10.1007/s00248-009-9542-8

Waidner LA, Kirchman DL (2007) Aerobic Anoxygenic Phototrophic Bacteria Attached to Particles in Turbid Waters of the Delaware and Chesapeake Estuaries. Applied and Environmental Microbiology 73:3936–3944. doi: 10.1128/AEM.00592-07

Waidner LA, Kirchman DL (2008) Diversity and Distribution of Ecotypes of the Aerobic Anoxygenic Phototrophy Gene pufM in the Delaware Estuary. Applied and Environmental Microbiology 74:4012–4021. doi: 10.1128/AEM.02324-07

Waidner LA, Kirchman DL (2005) Aerobic anoxygenic photosynthesis genes and operons in uncultured bacteria in the Delaware River. Environmental Microbiology 7:1896–1908. doi: 10.1111/j.1462-2920.2005.00883.x

Warner EB, Oliver JD (2008) Multiplex PCR assay for detection and simultaneous differentiation of genotypes of Vibrio vulnificus biotype 1. Foodborne Pathogens and Disease 5:691–693. doi: 10.1089/fpd.2008.0120

Welschmeyer NA (1994) Fluorometric analysis of chlorophyll a in the presence of chlorophyll b and pheopigments. Limnology and Oceanography 39:1985–1992. doi: 10.4319/lo.1994.39.8.1985

Wetz JJ, Blackwood AD, Fries JS, et al (2014) Quantification of Vibrio vulnificus in an Estuarine Environment: a Multi-Year Analysis Using QPCR. Estuaries and Coasts 37:421–435. doi: 10.1007/s12237-013-9682-4

Wetz JJ, Blackwood AD, Fries JS, et al (2008) Trends in total Vibrio spp. and Vibrio vulnificus concentrations in the eutrophic Neuse River Estuary, North Carolina, during storm events. Aquatic Microbial Ecology 53:141–149. doi: 10.3354/ame01223

Wetz MS, Yoskowitz DW (2013) An ‘extreme’ future for estuaries? Effects of extreme climatic events on estuarine water quality and ecology. Marine Pollution Bulletin 69:7–18. doi: 10.1016/j.marpolbul.2013.01.020

Williams AK, Quigg A (2019) Spatiotemporal Variability in Autotrophic and Heterotrophic Microbial Plankton Abundances in a Subtropical Estuary (Galveston Bay, Texas). Journal of Coastal Research 35:434–444. doi: 10.2112/JCOASTRES-D-18-00004.1

Williams LA, LaRock PA (1985) Temporal Occurrence of Vibrio Species and Aeromonas hydrophila in Estuarine Sediments. Applied and Environmental Microbiology 50:1490–1495. doi: 10.1128/aem.50.6.1490-1495.1985

Williams TC, Froelich BA, Phippen B, et al (2017) Different abundance and correlational patterns exist between total and presumed pathogenic Vibrio vulnificus and V. parahaemolyticus in shellfish and waters along the North Carolina coast. FEMS microbiology ecology 93:

WUnderground (2020) Weather Underground Data. https://www.wunderground.com/history/daily/us/fl/pensacola/KPNS/date. Accessed 24 Oct 2021

Xu W, Gong L, Yang S, et al (2020) Spatiotemporal Dynamics of Vibrio Communities and Abundance in Dongshan Bay, South of China. Frontiers in Microbiology 11:2924. doi: 10.3389/fmicb.2020.575287

Yeung M, Thorsen T (2016) Development of a More Sensitive and Specific Chromogenic Agar Medium for the Detection of Vibrio parahaemolyticus and Other Vibrio Species. Journal of Visualized Experiments: JoVE. doi: 10.3791/54493

Zha S, Liu S, Su W, et al (2017) Laboratory simulation reveals significant impacts of ocean acidification on microbial community composition and host-pathogen interactions between the blood clam and Vibrio harveyi. Fish & Shellfish Immunology 71:393–398. doi: 10.1016/j.fsi.2017.10.034

Zhang Y, Hu L, Osei-Adjei G, et al (2018) Autoregulation of ToxR and Its Regulatory Actions on Major Virulence Gene Loci in Vibrio parahaemolyticus. Frontiers in Cellular and Infection Microbiology. doi: 10.3389/fcimb.2018.00291

Zimmerman AM, DePaola A, Bowers JC, et al (2007) Variability of Total and Pathogenic Vibrio parahaemolyticus Densities in Northern Gulf of Mexico Water and Oysters. Applied and Environmental Microbiology 73:7589–7596. doi: 10.1128/AEM.01700-07

Zou S, Zhang Q, Zhang X, et al (2020) Environmental Factors and Pollution Stresses Select Bacterial Populations in Association With Protists. Frontiers in Marine Science 7:659. doi: 10.3389/fmars.2020.00659

Appendices

Appendix A

Percent (%) match of previously-published *vvhA* (target species *Vv*) primers and newly designed primers to pathogenic and environmental sequences. Sequences in bold match the *Vv* ATCC® type strain (Reichelt et al 1976)

Reference	Primer Name	Primer Sequence	Amplicon size (bp)	Method of primer design	Match to Pathogenic Strains[A]	Match to Env. Strains[B]
(Campbell and Wright 2003)	*vvhA*-F	**TGTTTATGGTGAGAACGGTGACA**	101	Based on accession no. M34670	92%	100%
	vvhA-R	**TTCTTTATCTAGGCCCCAAACTTG**			92%	95%
(Panicker et al 2004)	L-vvh	**TTCCAACTTCAAACCGAACTATGA**	205	Based on accession no. M34670	100%	100%
	R-vvh	**ATTCCAGTCGATGCGAATACGTTG**			92%	95%
This study	vvhA-F1	**GGGYGCTTCCATCGATGTTCGCG**	199	BLASTn sequences alignment (31 total)	100%	89%
	vvhA-R1	**GTAAGTGCGGCGGTTTGCCCAACTC**			83%	63%
This study	vvhA-F1	**GGGYGCTTCCATCGATGTTCGCG**	203	BLASTn sequences alignment (31 total)	100%	89%
	vvhA-R2	**CAATGTAAGTGCGGCGGTTTGCCC**			100%	84%

[A] Known-pathogenic strains of *Vv* (12 sequences) isolated from human vibriosis-related cases used for multiple sequence alignment analysis of *vvhA* in *Vv*

[B] "Other" (yet-unknown pathogenicity) strains of *Vv* (19 sequences) used for multiple sequence alignment analysis of *vvhA* in *Vv*

Appendix B

Percent (%) match of previously-published *tdh* (target species *Vv*) primers and newly designed primers to pathogenic and environmental sequences. Sequences in bold match the *Vv* ATCC® type strain (Reichelt et al 1976)

Reference	Primer Name	Primer Sequence	Amplicon size (bp)	Method of primer design	Match to Pathogenic Strains[A]	Match to Env. Strains[B]
(Bej et al 1999)	*tdh*-F	TGGAATAGAACCTTCACTTTCACC	622	Subcloning and sequencing	0%	0%
	tdh-R	GATGTCAGCCATTTAGTACC			0%	0%
(Nordstrom et al 2007)	*tdh* forward	TCCCTTTTCCTGCCCCC	164	GeneBank sequences (unknown number)	0%	0%
	tdh reverse	CGCTGCCATTGTATAGTCTTTATC			0%	0%
(Gutierrez West et al 2013)	*tdh*86F	CTGTCCCTTTTCCTGCCCCCG	292	Subcloning and sequencing	0%	0%
	*tdh*331R	AGCCAGACACCGCTGCCATTG			0%	0%
This study	tdhVv-F1	**CGGTYGCGAAGCAYGTTGGTG**	240	BLASTn sequences alignment (28 total)	92%	67%
	tdhVv-R1	**GTGCAATRCGGCCACCGTGGTTC**			92%	80%
This study	tdhVv-F2	**CCCTGCAAACATCTCTGATGATCTTG**	179	BLASTn sequences alignment (28 total)	100%	87%
	tdhVv-R2	**CGGTGATCACGACGTGRCGC**			92%	93%

[A] Known pathogenic strains of *Vv* (13 sequences) isolated from human vibriosis-related cases used for multiple sequence alignment analysis of *tdh* in *Vv*

[B] "Other" (yet-unknown pathogenicity) strains of *Vv* (15 sequences) used for multiple sequence alignment analysis of *tdh* in *Vv*

Appendix C

Percent (%) match of previously-published *trh* (target species *Vp*) primers and newly designed primers to pathogenic and environmental sequences. Sequences in bold match the *Vp* ATCC® type strain (Fujino et al 1965; Sakazaki 1968)

Reference	Primer Name	Primer Sequence	Amplicon size (bp)	Method of primer design	Pathogenic % Match[A]	Env. % Match[B]
(Bej et al 1999)	L-*trh*	TTGGCTTCGATATTTTCAGTATCT	486	Subcloning and sequencing	0%	0%
	R-*trh*	CATAACAAACATATGCCCATTTCCG			0%	0%
(Nordstrom et al 2007)	*trh* forward	TTGCTTTCAGTTTGCTATTGGCT	273	GeneBank Sequences (unknown number)	0%	0%
	trh reverse	TGTTTACCGTCATATAGGCGCTT			0%	0%
(Gutierrez West et al 2013)	*trh*90F	**ACCTTTTCCTTCTCCWGGKTCSG**	411	Type strain ATCC® #17802	100%	100%
	*trh*500R	**CCGCTCTCATATGCYTCGACAKT**			100%	100%
This study	trh-F1	**GTAAACATCAATGGTCATAACTATAC GATGGCAG**	210	BLASTn sequences (37 total)	50%	31%
	trh-R1	**CTCATATGCCTCGACAGTAACAAAG**			100%	100%
This study	trh-F2	**GCCTATATGACAGTAAACATCAATGG TCAYAAC**	214	BLASTn sequences (37 total)	63%	31%
	trh-R2	**CCTCGACAGTAACAAAGTATTCTGAT GTTTC**			46%	15%

[A] Known pathogenic strains of *Vp* (24 sequences) isolated from human vibriosis-related cases used for multiple sequence alignment analysis of *trh* in *Vp*

[B] "Other" (yet-unknown pathogenicity) strains of *Vp* (13 sequences) used for multiple sequence alignment analysis of *trh* in *Vp*

Appendix D

Percent (%) match of previously-published *tdh* (target species *Vp*) primers and newly designed primers to pathogenic and environmental sequences. Sequences in bold match the *Vp* ATCC® type strain (Fujino et al 1965; Sakazaki 1968)

Reference	Primer Name	Primer Sequence	Amplicon size (bp)	Method of primer design	Match to Pathogenic Strains[A]	Match to Env. Strains[B]
(Panicker et al 2004)	*tdh*-F	CCACTACCACTCTCATATGC	78	referenced from (Nishibuchi and Kaper, 1985)	0%	0%
	tdh-R	GATGTCAGCCATTTAGTACC			0%	0%
(Nordstrom et al 2007)	*tdh* forward	GATAAAGACTATACAATGGCAGCG	342	BLASTn sequences alignment (unknown)	0%	0%
	tdh reverse	GGGGGCAGGAAAAGGGA			0%	0%
(Gutierrez West et al 2013)	*tdh*86F	CTGTCCCTTTTCCTGCCCCCG	470	BLASTn sequences alignment (unknown)	0%	0%
	*tdh*331R	AGCCAGACACCGCTGCCATTG			0%	0%
This study	tdhVp-F1	**GCTCGCCATGTRGTTATCACAGACGTAAACG**	195	BLASTn sequences alignment (136 total)	88%	81%
	tdhVp-R1	GTTGTTAGCATTGAGTTGAATGCHGCTG			82%	84%
This study	tdhVp-F2	**GGGCGTAACWCGTGCAGTAACGTGG**	234	BLASTn sequences alignment (136 total)	100%	93%
	tdhVp-R2	**CCTTTGATAACCARACCTTTGAAGATCACTTG**			97%	93%

[A] Known pathogenic strains of *Vp* (33 sequences) isolated from human vibriosis-related cases used for multiple sequence alignment analysis of *tdh* in *Vp*

[B] "Other" (yet-unknown pathogenicity) strains of *Vp* (103 sequences) used for multiple sequence alignment analysis of *tdh* in *Vp*